AD_____

Award Number: DAMD17-98-1-8479

TITLE: Angiogenesis Regulates Prostate Cancer Metastasis

PRINCIPAL INVESTIGATOR: Curtis A. Pettaway, Ph.D.

CONTRACTING ORGANIZATION: University of Texas
M.D. Anderson Cancer Center
Houston, Texas 77030

REPORT DATE: March 2001

TYPE OF REPORT: Final

PREPARED FOR: U.S. Army Medical Research and Materiel Command
Fort Detrick, Maryland 21702-5012

REPORT DOCUMENTATION PAGE

Form Approved
OMB No. 074-0188

1. AGENCY USE ONLY (Leave blank)	2. REPORT DATE	3. REPORT TYPE AND DATES COVERED
	March 2001	Final (1 Sep 98 - 28 Feb 01)

4. TITLE AND SUBTITLE
Angiogenesis Regulates Prostate Cancer Metastasis

5. FUNDING NUMBERS
DAMD17-98-1-8479

6. AUTHOR(S)
Curtis A. Pettaway, Ph.D.

7. PERFORMING ORGANIZATION NAME(S) AND ADDRESS(ES)
University of Texas M.D. Anderson Cancer Center
Houston, Texas 77030

E-Mail: cpettawa@mdanderson.org

8. PERFORMING ORGANIZATION REPORT NUMBER

9. SPONSORING / MONITORING AGENCY NAME(S) AND ADDRESS(ES)
U.S. Army Medical Research and Materiel Command
Fort Detrick, Maryland 21702-5012

10. SPONSORING / MONITORING AGENCY REPORT NUMBER

11. SUPPLEMENTARY NOTES
Report contains color graphics

12a. DISTRIBUTION / AVAILABILITY STATEMENT
Approved for Public Release; Distribution Unlimited

12b. DISTRIBUTION CODE

13. ABSTRACT *(Maximum 200 Words)*

14. SUBJECT TERMS
Prostate Cancer, Metastasis, Angiogenesis

15. NUMBER OF PAGES
46

16. PRICE CODE

17. SECURITY CLASSIFICATION OF REPORT	18. SECURITY CLASSIFICATION OF THIS PAGE	19. SECURITY CLASSIFICATION OF ABSTRACT	20. LIMITATION OF ABSTRACT
Unclassified	Unclassified	Unclassified	Unlimited

Table of Contents

Final Report- 5/2001

ANGIOGENESIS REGULATES PROSTATE CANCER METASTASIS

PCRP-97; New Investigator; Carcinogenesis, Etiology, and Tumor Biology

Curtis A. Pettaway, M.D.
(713) 792-3250
(713) 794-4824 (fax)
cpettawa@mdanderson.org
The University of Texas M. D. Anderson Cancer Center
1515 Holcombe Boulevard, Urology Box 446
Houston, Texas 77030

Introduction

Cancer progression depends upon the establishment of an adequate blood supply. The purpose of our studies has been to evaluate the relevance of angiogenesis in the progression of prostate cancer by evaluating the roles of three different angiogenic molecules (vascular endothelial growth factor [VEGF], interleukin 8 [IL-8], and basic fibroblast growth factor [bFGF]).

Hypothesis

The expression of the angiogenic molecules regulate the metastasis of prostate cancer

Specific Aims and Study Design

1) We determined the *in vitro* expression of angiogenesis factors by human prostate cancer cell lines PC-3, LNCaP and their *in vivo* derived variant cells via northern analysis and protein levels via ELISA. LNCaP cells with metastatic potential overexpressed VEGF while PC-3M-LN4 cells (highly metastatic) overexpressed IL-8.
2) To determine *in vivo* expression of angiogenesis factors, prostate cancer cells implanted into the prostate of athymic mice were analyzed and *in vivo* angiogenic factor expression and angiogenesis (microvessel density, MVD) was performed. *In vivo* mRNA and protein expression directly correlated with *in vitro* results. Further, MVD correlated with metastatic potential. Sense and antisense IL-8 transfections in PC-3 cells of low and high metastatic potential (respectively) resulted in enhanced angiogenesis, tumorigenicity, and metastasis for sense IL-8 transfectants with the opposite results for antisense IL-8 transfectants.

3&4) To develop and test sense and antisense viral vectors for bFGF, VEGF, and IL-8 and to infect human prostate cancer cells antisense adenoviral vectors for bFGF, VEGF, and IL-8 were constructed using the AD5 PCA-14 replication deficient Adenovirus. Gene expression in this vector is driven via a CMV promoter. Multiplicity of infection parameters were established for each cell line with respect to bFGF, IL-8, and VEGF production with the specific adenoviral vector.

5) To determine whether altered expression of bFGF, IL-8 and VEGF via adenoviral vector mediated modulation affects growth, vascularity, and metastasis of human prostate cancer growing in nude mice. LNCaP- LN3 cells that overexpress VEGF were infected with the adenoviral VEGF-AS construct or control virus. Tumor growth in the VEGF antisense adenoviral group was abolished.
6) Gene therapy with antisense virus has been performed. Treatment of established PC-3M-LN4 tumors in nude mice with an adenoviral IL-8 vector injected intratumorally resulted in a significant reduction in tumorigenicity, MVD, and matrixmetalloproteinase expression. Similar *in vivo* studies with the VEGF adenoviral antisense construct are pending. Studies utilizing the bFGF adenoviral antisense will not be performed due to limited bFGF expression in human specimens studied, thus far, and time limitations.
7) Angiogenesis factor expression in human prostate cancer specimens revealed that VEGF expression did not differ significantly within a given tumor but was significantly higher in tumors of higher Gleason score and pathologic stage. Preliminary data reveals that Il-8 expression (but not bFGF expression) is also associated with increasing Gleason score and pathologic stage.

Study Relevance

The above studies help to establish the functional relevance of VEGF and IL-8 induced angiogenesis as important regulators of prostate cancer progression, in both animal models and patients, and confirm relevance of angiogenesis as a therapeutic target.

Title: Angiogenesis Regulates Prostate Metastasis- DAMD17-98-1-8479
Principal Investigator: Curtis A. Pettaway, M.D.
Report Body

I. Progress

Task 1 - Determine *in vitro* and expression of angiogenesis factors by human prostate cancer cell lines (months 1-6) - Completed

Task 1 evaluated the *in vitro* expression of the angiogenic factors vascular endothelial growth factor (VEGF), interleukin 8 (IL-8), and basic fibroblast growth factor (bFGF) by prostate cancer cells from the same lineage that have differing metastatic properties. Clin. Cancer Res. 2:1627, (1996). The hypothesis was that the expression of these factors would correlate with *in vivo* growth. We confirmed that the highly metastatic line LNCaP-LN3 overexpressed VEGF by northern analysis and protein by ELISA compared to either the parental LNCaP, or the line selected for growth within the prostate, LNCaP-Pro 5 (lowest levels of VEGF at both the mRNA and protein level). Expression levels of bFGF and IL-8 *in vitro* were negligible in all three lines. Clin. Cancer Res. 5:783, (1999).

We also evaluated the expression of VEGF, bFGF, and IL-8 by PC-3 and the highly metastatic PCM-LN4 cell line. In contrast to LNCaP cell lines, we observed that PC-3M-LN4 overexpressed IL-8 mRNA and protein relative to PC3-P by northern analysis and Elisa. However, significantly smaller amounts of bFGF and VEGF were produced by the two cell lines. Clin. Cancer Res. 6:2104 (2000).

Task 2 - Determine the *in vivo* expression of angiogenesis factors of human prostate cancer cells implanted into the prostate of athymic mice (months 1-12) - Completed

The highly metastatic LNCaP-LN3 cell line growing within the prostate of athymic nude mice overexpressed VEGF mRNA and protein compared with either LNCaP which had intermediate expression, and LNCaP-Pro 5, which expressed the lowest levels of VEGF. Clin. Cancer Res. 5:783 (1999). Furthermore, by anti-CD31 immunostaining the LNCaP-LN3 tumors were more vascular than either LNCaP (intermediate) or LNCaP-Pro5 (least vascular). Virtually no differences were noted for the three LNCaP cell lines with respect to bFGF and IL-8 mRNA or protein *in vivo*. Thus, the *in vivo* expression of these factors correlated with *in vitro* expression and tumor induced angiogenesis and metastasis. Serum levels of VEGF were consistent with gene and protein expression. We evaluated the *in vivo* expression of IL-8, bFGF, and VEGF mRNA and protein by PC3-P and PC-3M-LN4 growing within the prostate of athymic nude mice. Clin. Cancer Res. 6: 2104(2000). The highly metastatic PC-3M-LN4 cell line overexpressed IL-8 mRNA and protein relative to the poorly metastatic PC3P cell line. By anti-CD31 immunostaining, the PC3P-LN4 tumors were more vascular (as judged by microvessel density counts [MVD]) than the PC3P tumors. These studies confirm that the *in vivo* expression of these angiogenic factors mirrors their *in vitro* expression, and that the overexpression of these factors correlates with enhanced tumor induced neovascularization and metastatic potential.

As an extension of this task, we demonstrated the causality between IL-8 expression and the tumorigenicity and metastatic potential of human prostate cancer. We transfected the poorly metastatic prostate cancer cell line PC3-P with sense IL-8 vectors and the highly metastatic PC-3M-LN4 cell line with antisense IL-8 constructs. Clin. Cancer Res. 6:2104 (2000). After determining that the IL-8 expression by PC3-P was increased and the expression by PC-3M-LN4 was decreased, these cells were implanted into the prostates of athymic nude mice. Sense transfected PC3-P cells demonstrated increased IL-8 expression, and enhanced tumorigenicity, tumor induced neovascularization, and metastasis compared with Neo transfected controls and PC3-P. Conversely, antisense transfected PC-3M-LN4 demonstrated decreased IL-8 expression and decreased tumorigenicity, tumor induced angiogenesis, and metastasis compared with Neo controls or PC-3M-LN4. Moreover, we also demonstrated that IL-8 regulates MMP-9 expression by human prostate cancer and leads to enhanced invasive capacity. Clin. Cancer Res. 6:2104 (2000) Total mice utilized = approximately 150 mice.

Task 3 & 4 - To develop and test sense and antisense viral vectors for bFGF, VEGF, and IL-8 and to infect human prostate cancer cells (months 1-18)

The sense and antisense adenoviral vectors for bFGF, VEGF, and IL-8 were constructed using the AD5 PCA-14 replication deficient Adenovirus (see Sept. 1999 annual progress report for map). Gene expression in this vector is driven via a CMV promoter. The bFGF & IL-8 sense and antisense vectors were tested in PC-3M and *in vivo* selected variant lines. The VEGF sense and antisense adenoviral vectors were tested with LNCaP and *in vivo* selected variant cell lines. Clin. Cancer Res. 2:1627, (1996). Both cytotoxicity and either increases or decreases in angiogenic factor expression were correlated with the multiplicity of infection (MOI) at MOI's of 1:1, 1:3, 1:5, 1:10, 1:20, 1:50, and 1:100. A β-galactosidase adenovirus was used as a control for these experiments (vector construction maps available upon request). Cytotoxicity was assessed through cell counting 48-72 hours after infection. Expression of cell associated and secreted bFGF, IL-8, and VEGF was determined by ELISA assay of cell lysates and conditioned media from each MOI. An MOI of 10:1 produced increases in bFGF & Il-8 protein production of 800 and 1100% of control (respectively) in PC-3M cells. Similarly in LNCaP cells an MOI of 10:1 produced a 1000% increase in VEGF production. Antisense adenoviral infection at an MOI of 10:1 reduced bFGF and IL-8 production to 25 and 55% of control respectively in PC-3M cells and to 20% of control for LNCaP-LN3 cells infected with the adenoviral VEGF antisense virus. Recently upon repeat testing we have discovered difficulty with the VEGF adenoviral antisense in that VEGF levels by ELISA have not shown dramatic decreases previously shown. This is currently under investigation. By PCR the DNA construct is present however the orientation of the DNA and the presence of the CMV promoter must be confirmed.

Task 5 - To determine whether altered expression of bFGF, IL-8 and VEGF affects growth, vascularity, and metastasis of human prostate cancer growing in nude mice. (months 8-24, revised to 36 months

Preliminary Studies to determine the *in vivo* effect of adenoviral mediated modulation of VEGF on LNCaP cell lines have been completed. Subsequent to infection of LNCaP-LN3 cells (high VEGF production) with adenoviral VEGF-AS and intraprostatic injection of parental, VEGF-AS, or control virus treated cells, tumor growth and metastasis were evaluated. Tumors readily formed in mice injected with parental LN3 as well as control virus LN3 inoculated mice but were totally absent among the mice injected with LNCaP-LN3 VEGF-AS treated cells. If confirmed, these data suggest that VEGF expression is essential for growth of LNCaP cells *in vivo*. Data from the above transfection studies (Task # 2) strongly suggested that IL-8 is directly involved in the regulation of metastasis. Clin. Cancer Res. 6:2104 (2000) Thus, the principal of IL-8 modulation in prostate cancer cells affecting angiogenesis, growth, and metastasis has been shown. Therefore, we will not pursue modulating IL-8 expression via adenoviral mechanisms as originally proposed. Our existing data from human prostate cancer cell lines and patient specimens suggests that bFGF expression is not prominent when compared with VEGF and IL-8 expression (see also Task #7). Therefore, we will not pursue functional studies to modulate its expression as originally proposed. Total number of mice = 50

Task 6 - Gene therapy with antisense virus to bFGF, IL - 8, and VEGF (months 12-30, revised to 40 months)

PC-3M-LN4 cells were injected subcutaneously (2 x 10^6 cells/mouse). Treatment using the adenoviral antisense (Adv-ASIL-8) or control vector (Adv-PolyA) was begun on day 21 when tumors were established (3-6mm size). Mice received 5 x 10^9 viral particles via two separate intratumoral injections 10 days apart. Six weeks post inoculation tumor weights were significantly decreased in mice receiving Adv-AS-IL-8 (median = 92 mg, versus saline = 223mg or Adv-PolyA = 173, $p = <0.05$) therapy. ISH mRNA analysis revealed decreased IL-8 and MMP-9 expression (65 ± 13 and 45 ± 15 respectively in the Adv-AS-IL-8 treated tumors compared with Adv-PolyA or saline controls (95 ± 20 & 105 ± 16, 100 ± 17 & 100 ± 20 respectively). Further, MVD as judged by CD-31 immunohistochemistry was reduced in the Adv-AS-IL-8 treated tumors (42 ± 8)

compared with Adv-PolyA or saline controls (56 ± 12 & 61 ± 10 respectively). Thus, proof of principal was established. Studies utilizing VEGF adenoviral vectors are to follow as soon as technical issues are settled. Recently we obtained the DC101 anti-VEGF receptor antibody virus (rat anti-mouse VEGF receptor 2 [flk-1] antibody to modulate inhibit VEGF binding to its receptor. We treated mice with established PC-3M-MM2 tumors (androgen insensitive prostate cancer) with DC101 for a total of 7 doses bi-weekly for 4 weeks. This therapy inhibited tumor-induced angiogenesis, growth and metastasis. Further the anti-tumoral effect could be enhanced with paclitaxel chemotherapy (Sweeney et. al.) Proc. Am. Assoc. Cancer Res. 42: #4418 (2001) Similar studies are planned utilizing LNCaP cells. Total mice to be used. = 220 mice.

Task 7 - Angiogenesis factor expression in Human Prostate Cancer (months 1-30, revised to 36months)

We completed and published an evaluation of the expression of VEGF by *in situ* hybridization (ISH) in 59 tumors from 40 radical prostatectomy specimens to determine the relationship of VEGF expression to tumor location, Gleason score, and pathological stage (Clin. Cancer Res. 6:2295[2000]). VEGF expression did not differ significantly within a given tumor but was significantly higher in tumors of higher Gleason score and pathologic stage. In fact, VEGF expression by ISH was highly associated with seminal vesicle involvement and lymph node metastasis in radical prostatectomy specimens and this was independent of the Gleason score. We have also performed mRNA ISH for the angiogenesis factors IL-8, bFGF, and the negative angiogenesis regulator interferon beta. Our preliminary analysis reveals that IL-8 expression is associated with increasing Gleason score and pathologic stage. However, bFGF expression was weak and did not have the same association. Analysis of interferon beta expression is in progress. Total specimens =40

Conclusion

The above studies help to establish the functional relevance of VEGF and IL-8 induced angiogenesis as important regulators of prostate cancer progression in both animal models and patients and confirm relevance of angiogenesis as a therapeutic target.

Reportable Outcomes:

1. Manuscripts

1. Balbay MD, **Pettaway CA**, Kuniyasu H, Inoue K, Ramirez E, Li E, Fidler IJ, Dinney CP. Clin. Cancer Res., 5:783-9, 1999.

2. Inoue K, Eve BE, Slaton JW, Kim SJ, Perrotte P, Balbay MD, Yano S, Bar-Eli M, Radinsky R, **Pettaway CA** and Dinney CPN. Clin. Cancer Res., 6:2104-2119,2000.

3. Kuniyasu H, Troncoso P, Johnston D, Bucana CD, Tahara E, Fidler IJ, and **Pettaway CA**. Clin. Cancer Res., 6: 2295-2308,2000.

2. Presentations

Sweeney JP, Kedar D, Karashima T, Kim SJ, Mian B, Huang SF, Fan Z, Hicklin D, **Pettaway CA,** Dinney CPN: Treatment of Human Prostate Cancer in a Orthotopic Murine Model with the Anti-vascular Endothelial Growth Factor Receptor Monoclonal Antibody DC101. Pro. Am. Assoc. Cancer Res., 42: #4418, 2000.

Uehara, H, Troncoso, P, Johnston, D, Fidler, IJ, Dinney, CPN, **Pettaway, CA**: Interleukin-8 Expression in Radical Prostatectomy Specimens is Associated with Gleason Score and Pathologic Stage. Proc. American Urologic Association Meeting, June 2001

3.New Grant Support

Grant Number: P50 CA90270, NIH, 05/01/01 - 01/01/06.
Grant Title: "University of Texas M. D. Anderson SPORE in Prostate Cancer"
Project 1 (Fidler/Dinney) "The Biology of Human Prostate Cancer Metastasis" ($1,056,518)- Dr. Colin Dinney (co investigator) has written a clinical trial based upon neoadjuvant downmodulation of angiogenic factor expression in the prostate prior to radical prostatectomy utilizing adenoviral vector containing interferon beta.

Project 5 (Strom/Pettaway) "Clinical, Epidemiological, and Molecular Markers of Prostate Cancer Progression" ($1,080,688) Dr. Pettaway is Co-leader on this project that will explore racial variation in molecular markers of angiogenesis and invasion.

4. Promotion

Dr Curtis Pettaway was promoted to the rank of Associate Professor of Urology and Cancer Biology of The University of Texas M. D. Anderson Cancer based in part on his ability to receive peer reviewed (current DOD grant) funding to carry out basic and translational research.

Highly Metastatic Human Prostate Cancer Growing within the Prostate of Athymic Mice Overexpresses Vascular Endothelial Growth Factor[1]

M. Derya Balbay, Curtis A. Pettaway, Hiroki Kuniyasu, Keiji Inoue, Edilberto Ramirez, Emily Li, Isaiah J. Fidler, and Colin P. N. Dinney[2]

Departments of Urology [M. D. B., C. A. P., C. P. N. D.], Cancer Biology [H. K., K. I., E. L., I. J. F., C. P. N. D.], and Epidemiology [E. R.], The University of Texas M. D. Anderson Cancer Center, Houston, Texas 77030

ABSTRACT

Angiogenesis is essential for tumor progression and metastasis. It is mediated by the release of angiogenic factors by the tumor or host. We analyzed the expression of angiogenic factors by the prostate cancer cell line LNCaP and two derived variants, *in vitro* and *in vivo*, to determine whether metastatic cell lines express higher levels of these factors. The production of three angiogenic factors, vascular endothelial growth factor (VEGF), basic fibroblast growth factor (bFGF), and interleukin 8 (IL-8), by LNCaP and its variants, LNCaP-LN3 (highly metastatic) and LNCaP-Pro5 (slightly metastatic), was measured by ELISA. VEGF, bFGF, and IL-8 mRNA expression was determined *in vitro* by Northern blot analysis. VEGF mRNA expression was determined *in vivo* by *in situ* hybridization. VEGF and flk-1 protein expression and microvessel density of LNCaP cell tumors were quantified by immunohistochemistry. *In vitro*, VEGF production by LNCaP-LN3 (3.15 ± 0.04 pg/ml/10^3 cells) was significantly higher than those of both LNCaP (2.38 ± 0.34 pg/ml/10^3 cells) and LNCaP-Pro5 (1.67 ± 0.37 pg/ml/10^3 cells; $P = 0.049$ and 0.001, respectively). None of the three cell lines produced detectable levels of bFGF or IL-8 *in vitro*. *In vivo*, LNCaP-LN3 tumors exhibited higher levels of VEGF mRNA and protein (152.2 ± 28.5 and 200.5 ± 28.3) and of flk-1 protein (156.5 ± 20.6) and had higher microvessel density (16.4 ± 4.2) than either LNCaP tumors (89 ± 17.5, 173.3 ± 23.0, 124.6 ± 21.6, and 12.4 ± 3.5, respectively) or LNCaP-Pro5 tumors (63 ± 14.7, 141.2 ± 38.1, 126.1 ± 20, and 5.8 ± 2.2, respectively). In conclusion, metastatic human prostate cancer cells exhibited enhanced VEGF production and tumor vascularity compared with prostate cancer cells of lower metastatic potential. Thus, VEGF may play an important role in prostate cancer metastasis.

INTRODUCTION

Tumor growth and metastasis depend upon the induction of a blood supply (1, 2). This process, angiogenesis, is regulated by a diverse group of molecules, including VEGF[3] (2, 3), bFGF (4, 5), and IL-8 (6). The prevascular phase of a tumor is usually associated with local, nonmetastatic tumors; a vascular phase precedes invasion and metastasis (7). The vascular density of prostate cancer, a histological indicator of angiogenesis, correlates with invasion and metastasis (8, 9).

The acquisition of an angiogenic phenotype is mediated by angiogenic factors released by the tumor or host cells and depends upon the balance between stimulatory and inhibitory factors released by the tumor and its microenvironment (10). Following the induction of vascularization, the rate of tumor growth increases exponentially (11, 12).

The specific angiogenic factors regulating prostate cancer growth and metastasis have not been elucidated. It is highly unlikely that any one factor will be solely responsible for angiogenesis in all prostate cancers, and furthermore, multiple factors may be necessary for angiogenesis to occur in a single tumor.

VEGF is expressed by both benign and malignant prostate cells as well as by neuroendocrine cells (13). The level of expression by malignant cells is greater than that by benign prostate cells (14, 15). VEGF expression enhances the tumorigenicity of human prostate cancer. Administration of VEGF to mice receiving whole-body irradiation increased the growth of human prostate cancer xenografts and led to rapid tumor progression (16). In addition, administration of an anti-VEGF antibody to nude mice that were growing the human prostate cancer cell line DU145 completely inhibited neovascularization within the tumor (17). In androgen-responsive cells, VEGF expression seems to be androgen dependent. For instance, VEGF expression by the androgen-responsive PC-82 and A-2 human prostate lines growing s.c. in severe combined immunodeficient mice was inhibited by castration (18). Androgen withdrawal also down-regulates VEGF production by human prostate cancer (19, 20).

Received 6/19/98; revised 1/25/99; accepted 2/3/99.

The costs of publication of this article were defrayed in part by the payment of page charges. This article must therefore be hereby marked *advertisement* in accordance with 18 U.S.C. Section 1734 solely to indicate this fact.

[1] Supported in part by Cancer Center Core Grant CA 16672, NIH Grant CA 67914, Robert Wood Johnson Foundation, and the Department of Defense.

[2] To whom requests for reprints should be addressed at The University of Texas M. D. Anderson Cancer Center, Urology, Box 110, 1515 Holcombe Boulevard; Phone: (713) 792-3250; Fax: (713) 794-4824.

[3] The abbreviations used are: VEGF, vascular endothelial growth factor; bFGF, basic fibroblast growth factor; IL-8, interleukin 8; GAPDH, glyceraldehyde phosphate dehydrogenase; IHC, immunohistochemistry; ISH, *in situ* hybridization.

Table 1 Tumorigenicity and production of metastasis by LNCaP cells and two variants subsequent to orthotopic implantation in atymic nude mice

LNCaP cell line	Tumorigenicity	Prostate weight, g (mean ± SD)	Para-aortic lymph node metastases
LNCaP	24/43	1.2 ± 1.0	12/43
LNCaP-Pro5	10/17	3.3 ± 1.7[a]	2/17
LNCaP-LN3	19/19[b]	1.2 ± 0.9	13/19[c]

[a] $P < 0.05$, compared with LNCaP and LNCaP-LN3.

[b] $P < 0.001$, compared with LNCaP; $P = 0.002$, compared with LNCaP-Pr05.

[c] $P < 0.003$, compared with LNCaP; $P < 0.001$, compared with LNCaP-Pr05. Adapted from Pettaway *et al.* (21).

Here, we evaluated the expression of angiogenic factors in an orthotopic model of human prostate cancer. We previously established this model by directly implanting the human prostate cancer cell line LNCaP into the prostates of athymic nude mice. We selected from the parental LNCaP cell line distinct subpopulations that either were more tumorigenic within the prostate (LNCaP-Pro5) or had a greater propensity to metastasize (LNCaP-LN3; Ref. 21). The purpose of the study described herein was to evaluate whether the expression of the angiogenic factors VEGF, bFGF, and IL-8 by LNCaP and its variants, LNCaP-Pro5 and LNCaP-LN3, correlated with enhanced angiogenesis and metastasis.

MATERIALS AND METHODS

Tumor Cell Lines. The three cancer cell lines were maintained as monolayers in RPMI 1640 supplemented with 10% fetal bovine serum, vitamins, sodium pyruvate, L-glutamine, nonessential amino acids, and penicillin-streptomycin. The low metastatic LNCaP-Pro5 and high metastatic LNCaP-LN3 variants were isolated by intraprostatic injection of LNCaP and sequential selection for nonmetastatic and metastatic variants as described previously. The LNCaP cell line is intermediate in its metastatic potential compared with these variant lines (Table 1; Ref. 21).

Animals. Male athymic BALB/c nude mice were obtained from the Animal Production Area of the National Cancer Institute-Frederick Cancer Research Facility (Frederick, MD). The mice were maintained in a laminar air flow cabinet under specific pathogen-free conditions and used at 8–12 weeks of age. Animal facilities were approved by the American Association for Accreditation of Laboratory Animal Care in accordance with the standards of the United States Department of Agriculture, Department of Health and Human Services, and IH.

ELISA. Fifty thousand viable cells from the LNCaP, LNCaP-Pro5, and LNCaP-LN3 cell lines were seeded onto 35-mm Petri dishes. Conditioned medium was removed after 9 h of incubation and centrifuged at 5000 rpm for 5 min before washing with 1 ml of HBSS. Both conditioned medium and cell suspensions were stored at −20°C prior to assay. The levels of cell-associated and supernatant VEGF, bFGF, and IL-8 were measured using commercially available ELISA kits (Quantikine; R&D Systems, Minneapolis, MN). The protein level for each angiogenic factor was quantified by comparing its optical density to the standard curve for each factor and normalizing for cell number.

Northern Blot Analysis. Polyadenylated mRNA was extracted from 50–70% confluent monolayer cultures of cells growing in culture using the Fast Track mRNA isolation kit (Invitrogen, San Diego, CA). The mRNA was electrophoresed on a 1% denaturing formaldehyde/agarose gel and electrotransferred to a GeneScreen nylon membrane (DuPont, Boston, MA) using a UV cross-linker (Stratalinker, model 1800; Stratagene, La Jolla, CA) cross-linked with 120,000 μJ/cm^2. Filters were washed at 55°C with 30 mM sodium citrate and 0.1% sodium dodecyl sulfate (w/v). The membranes were then hybridized and probed for VEGF, bFGF, and IL-8; GAPDH was used as a control for loading. The cDNA probes used were (*a*) a 1.3-kb *Pst*I cDNA for GAPDH (22); (*b*) a 1.4-kb cDNA fragment of bovine bFGF (23); (*c*) a 204-bp *Bam*HI-*Eco*RI fragment of the human VEGF cDNA (a gift of Dr. Brygida Berse, Harvard Medical School, Boston, MA; Ref. 24); and (*d*) a 0.5-kb *Eco*RI cDNA fragment corresponding to human IL-8 (a gift of Dr. K. Matsushima, Kanazawa, Japan; Ref. 25). The probes were radiolabeled by a random primer technique and [α-^{32}P]dCTP (Amersham Corp.). Autoradiography of the membrane was performed after washing. Densitometry scanning permitted quantification of the bands.

Orthotopic Implantation of the Tumor Cells. For the *in vivo* portion of the study, cultured LNCaP, LNCaP-Pro5, and LNCaP-LN3 cells (70% confluent) were prepared for injection as described previously (21). Mice were anesthetized with methoxyflurane, a lower midline incision was made, and the prostate was exposed. Viable tumor cells (2×10^6 cells in 40 μl of HBSS) were injected into one of the dorsal lobes of the prostate. The formation of a "bleb" was the sign of a satisfactory injection. Organs were returned to their proper locations, and the abdominal wall was closed in a single layer with metal clips.

Necropsy. The mice were killed 5 weeks after injection. Prostate tumors were harvested, weighed, and either embedded in OCT solution (Sokera Inc., Torrence, CA) for frozen sections or fixed in formalin for paraffin sections.

Immunohistochemical Determination of VEGF, bFGF, IL-8, and flk-1. The expression of VEGF, bFGF, IL-8, and VEGF receptor flk-1 was detected in paraffin sections of tumors using rabbit polyclonal IgG antihuman antibodies for VEGF, bFGF, and IL-8 diluted to 1:500, 1:500, and 1:50, respectively. An antimouse polyclonal antibody to flk-1 (Santa Cruz Biotechnology, Santa Cruz, CA) was used at 1:100 dilution. The α-immunoperoxidase technique for IHC staining was performed with a second peroxidase-conjugated goat antirabbit antibody (IgG, F[ab]$_2$ fragment; Jackson ImmunoResearch Laboratory, West Grove, PA) at a 1:500 dilution. We confirmed the specificity of the VEGF and flk-1 staining by the absorption test using the control peptides SC 152P and SC 315P. Briefly, primary antibodies were pretreated with control peptide overnight at 4°C, and this pretreated antibody was used for IHC analysis, as described above. No immunostaining was observed using the pretreated antibodies (data not shown).

Quantification of Microvessel Density. Cryostat sections of tumors were fixed with 2% paraformaldehyde in PBS (pH 7.5) for 10 min and then washed twice with PBS. The sections were then treated for 5 min with 1% Triton X-100 and

Table 2 In vitro production of bFGF, IL-8, and VEGF in LNCaP cells and selected variants

bFGF, IL-8, and VEGF concentrations (pg/ml/10^3 cells) were measured in both cell-associated and culture supernatants of LNCaP, LNCaP-Pro5, and LNCaP-LN3 cells after 96 h. Values are means ± SD of four separate experiments.

	Culture supernatants			Cell-associated supernatants		
Cell line	bFGF	IL-8	VEGF[a]	bFGF	IL-8	VEGF
LNCaP	0	0	2.38 ± 0.34	0	0	0
LNCaP-Pro5	0	0	1.67 ± 0.37	0	0	0
LNCaP-LN3	0	0	3.15 ± 0.04	0	0	0.25 ± 0.02
253JB-V	0	8.50 ± 3.24	2.87 ± 0.05	2.77 ± 0.87	1.76 ± 0.06	0

[a] Tukey's honestly significant difference test *P*s: LNCaP *vs.* LNCaP-Pro5, $P = 0.064$; LNCaP-LN3 *vs.* LNCaP, $P = 0.049$; LNCaP-LN3 *vs.* LNCaP-Pro5, $P = 0.001$.

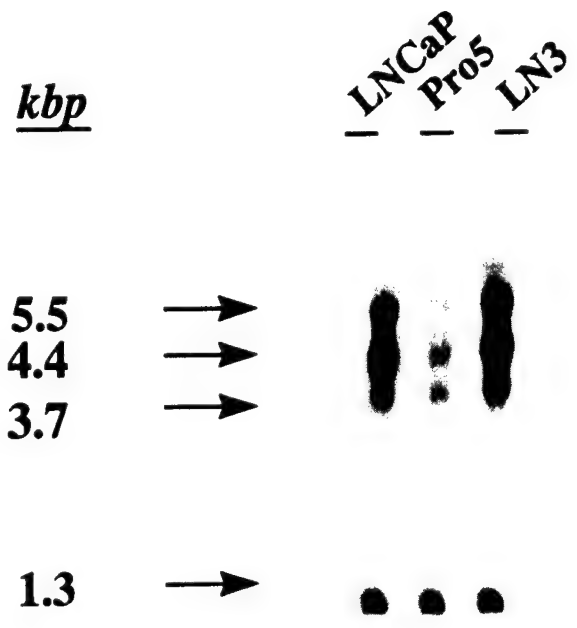

Fig. 1 In vitro VEGF expression in LNCaP, LNCaP-Pro5, and LNCaP-LN3 cells, as shown by Northern blot analysis. Relative VEGF mRNA expression was highest in LNCaP-LN3 (1.64) compared with LNCaP-Pro5 (0.41) and LNCaP (1.09) after normalization to GADPH. Four distinct mRNA transcripts were identified in the LNCaP cell lines.

washed three times with PBS. Endogenous peroxidase was blocked with 3% hydrogen peroxide in methanol, and the sections were washed with PBS and incubated overnight in protein-blocking solution. The excess blocking solution was removed, and the samples were incubated with rat antimouse CD31 antibody that stains endothelial cells (PharMingen, San Diego, CA). Swine peroxidase-conjugated anti-rabbit antibody was applied for 30 min after the primary antibody was removed. The samples were rinsed with PBS and developed with 3-amino-9-ethylcarbazole at room temperature for 20 min. The sections were counterstained with aqueous hematoxylin. A positive reaction was indicated by a brownish precipitate.

The tissues were examined at low power (×40), and five high-power fields of viable tumor at the periphery of the tumor were selected for vessel counts. Selected fields (high-power field, ×20 objective and ×10 ocular, 0.739 mm^2 per field) were recorded using a computer-linked cooled CCD Optronics Tec 470 camera (Optronics Engineering, Goletha, CA). Microvessels were quantified according to the method described by Weidner *et al.* (26). Clusters of stained endothelial cells distinct from adjacent microvessels, tumor cells, or other stromal cells were counted as one microvessel. The results were expressed as the number of microvessels identified within a single ×200 field.

Oligonucleotide Probes. Specific antisense oligonucleotide DNA probes were designed complementary to the mRNA transcripts of the three angiogenesis-related genes based on the published reports of the DNA sequence: VEGF/vascular permeability factor, TGG'TGA'TGT'TGG'ACT'CCT'CAG'TGG'GCU, 57.7% guanosine-cytosine content (24); bFGF, CGG'GAA'GGC'GCC'GCT'GCC'GCC', 85.7% guanosine-cytosine content (23); IL-8, CTC'CAC'CCA'CCT'CTG'CAC'CC), 65% guanosine-cytosine content (25). The specificity of the oligonucleotide sequence was initially determined by a Gene Bank European Molecular Biology Library database search with the use of the Genetics Computer Group sequence analysis program (GCG; Madison, WI) based on the FastA algorithm (27). These sequences showed 100% homology with the target gene and minimal homology with nonspecific mammalian gene sequences. The specificity of each of the sequences was also confirmed by Northern blot analysis. A poly$(dT)_{20}$ oligonucleotide was used to verify the integrity and lack of degradation of mRNA in each sample. All DNA probes were synthesized with six biotin molecules (hyperbiotinylated) at the 3′ end via direct coupling using standard phosphoramidile chemistry (Research Genetics, Huntsville, AL; Ref. 28). The lyophilized probes were reconstituted to a stock solution at 1 μg/μl in 10 mM Tris (pH 7.6) and 1 mM EDTA. The stock solution was diluted with Probe Diluent (Research Genetics) immediately before use.

***In Situ* mRNA Hybridization.** Paraffin-embedded sections of fixed tissue (3–5 μm) were mounted on ProbOn slides (Fisher Scientific, Pittsburgh, PA). The slides were dewaxed and prepared, and ISH was performed using the MicroProbe system (Fisher Scientific) as described previously (29, 30). Slides were rinsed three times in Tris buffer for 30 s; the probes were then hybridized at 45°C for 45 min. The slides were washed three times for 2 min each time with 2× SSC at 45°C. The samples were then incubated with alkaline phosphatase-labeled avidin for 30 min at 45°C, rinsed in 50 mM Tris buffer (pH 7.6), and then briefly (1 min) rinsed in alkaline phosphatase enhancer.

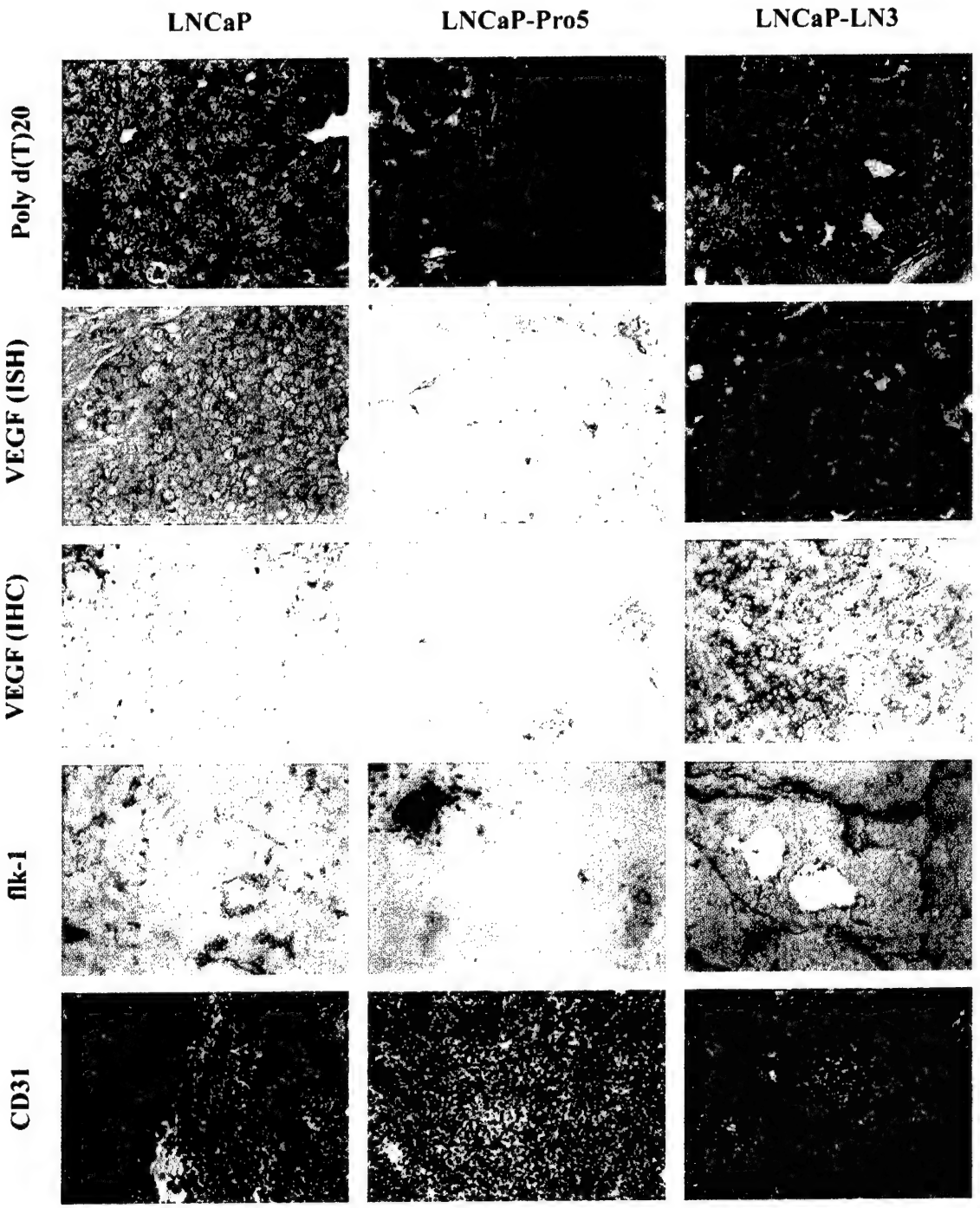

Fig. 2 ISH and immunohistochemical staining of LNCaP, LNCaP-Pro5, and LNCaP-LN3 growing in the prostates of athymic nude mice. Note the increased expression of both VEGF mRNA and protein in the highly metastatic LNCaP-LN3 tumors. Poly(dT) staining served as the control for mRNA integrity. Microvessel density by anti-CD31 staining of endothelial cells and flk-1 expression on tumoral vessels were also greater in LNCaP-LN3 cell tumors.

The samples were then incubated with chromogen substrate for 20 min at 45°C. If necessary, an additional incubation was performed with fresh chromogen to enhance a weak reaction. The samples were then covered with Universal Mount mounting medium (Research Genetics), heat-dried, and examined. Red staining indicated a positive reaction in this assay. Appropriate controls for endogenous alkaline phosphatase were included by treating the samples in the absence of biotinylated probe, using chromogen alone. No immunoreactivity was observed in the controls.

Table 3 *In situ* mRNA and immunohistochemical analysis of VEGF, VEGF receptor flk-1, and microvessel density in LNCaP and selected variants

Mice were injected with 2×10^6 cells and necropsied 5 weeks after injection. Five different areas of three separate tumors were analyzed. Values are means ± SD of 15 determinations of each cell line. Statistical comparisons were performed using Tukey's honestly significant difference test.

Cell line	VEGF (ISH)[a]	VEGF (IHC)[b]	flk-1[c]	CD31[d]
LNCaP	89 ± 17.5	173.3 ± 23.0	124.6 ± 21.6	12.4 ± 3.5
LNCaP-Pro5	63 ± 14.7	141.2 ± 38.1	126.1 ± 20.0	5.8 ± 2.2
LNCaP-LN3	152.2 ± 28.5	200.5 ± 28.3	156.5 ± 20.6	16.4 ± 4.2
Tukey's honestly significant difference test *P*s				
LNCaP *vs.* LNCaP-Pro5	0.117	0.011	0.973	0.001
LNCaP *vs.* LNCaP-LN3	0.001	0.023	0.001	0.001
LNCaP-LN3 *vs.* LNCaP-Pro5	0.001	0.001	0.001	0.001

[a] VEGF mRNA density was evaluated by computer-assisted image analysis and is expressed as the ratio of the intensity of tumor ISH to that of the normal glandular epithelium, normalized to poly(dT) expression. The differences between LNCaP and LNCaP-LN3 ($P = 0.001$) and between LNCaP-LN3 and LNCaP-Pro5 ($P = 0.001$) were significant.

[b] VEGF cytoplasmic staining was evaluated by computer-assisted image analysis and is expressed as a ratio of the tumor expression to normal prostatic glandular epithelial cell expression. The differences between LNCaP and LNCaP-Pro5 ($P = 0.011$), between LNCaP and LNCaP-LN3 ($P = 0.023$), and between LNCaP-LN3 and LNCaP-Pro5 ($P = 0.001$) were significant.

[c] flk-1 cytoplasmic staining in endothelial cells was evaluated by computer-assisted image analysis and is expressed as a ratio of tumor vascular endothelium expression to normal glandular vascular endothelium expression. The differences between LNCaP and LNCaP-LN3 and between LNCaP-LN3 and LNCaP-Pro5 were significant ($P = 0.0001$ for both comparisons).

[d] CD31 staining reflecting microvessel density was counted under ×200 magnification in 0.739-mm^2 fields. The differences between LNCaP and LNCaP-Pro5, between LNCaP and LNCaP-LN3, and between LNCaP-LN3 and LNCaP-Pro5 were significant ($P = 0.0001$ for each comparison).

To check the specificity of the hybridization signal, the following controls were used: (*a*) RNase pretreatment of tissue sections, (*b*) substitution of the antisense probe with a biotinylated sense probe, and (*c*) competition assay with unlabeled antisense probes. Markedly decreased or no signal was obtained after all of these treatments (31).

Densitometry Quantification of IHC and ISH. The intensity of IHC staining and ISH was evaluated in five fields at the periphery of the tumors representing areas of most intense staining. Each field was evaluated using the ImageQuant analyzer and Optimas software program (Bioscan, Edmonds, WA). IHC staining intensity of each sample was compared with the staining intensity of the normal prostate glands in the sample and expressed as a ratio (tumor cells:normal glandular cells). ISH was quantified in a similar manner using serial sections of the same tumor block. Normal prostate glands served as the internal control for mRNA expression, and poly(dT) staining controlled for mRNA preservation. Results were expressed as the ratio of the intensity of tumor ISH staining to that of normal glandular cell staining and normalized for poly(dT) expression.

Statistical Analysis. One-way ANOVA was used to examine group differences in VEGF production by the cell lines *in vitro* and in VEGF mRNA and protein expression as well as flk-1 protein expression on tumor sections *in vivo*. When ANOVA indicated a significant ($P < 0.05$) difference, a post hoc test was performed using Tukey's honestly significant difference multiple comparison test.

RESULTS

***In Vitro* Expression of VEGF, bFGF, and IL-8.** The *in vitro* production of cell-associated and secreted VEGF, IL-8, and bFGF protein by the parental LNCaP cell line and the variant LNCaP-Pro5 and LNCaP-LN3 cell lines is shown in Table 2. The 253J B-V cell line served as a positive control for bFGF and IL-8 production (32). By ELISA, VEGF was the only angiogenic peptide detected among the LNCaP cell lines. The highly metastatic LNCaP-LN3 cell line secreted significantly more VEGF (3.15 ± 0.04 pg/ml/10^3 cells) than the LNCaP cell line (2.38 ± 0.34 pg/ml/10^3 cells) or the LNCaP-Pro5 line (1.67 ± 0.37 pg/ml/10^3 cells; $P = 0.049$ and 0.001, respectively).

Northern blot analysis confirmed the results of ELISA. Densitometric analysis indicated that the relative steady-state gene expression of VEGF by LNCaP-LN3 was 4-fold greater than that by LNCaP-Pro5 and 1.5-fold greater than that by LNCaP (Fig. 1). Four VEGF transcripts were identified by Northern blot analysis. We did not identify bFGF or IL-8 mRNA transcripts in the three LNCaP cell lines (data not shown).

***In Vivo* Expression of VEGF, bFGF, IL-8, flk-1, and Microvessel Density.** We used IHC and ISH to compare the expressions of VEGF, bFGF, IL-8, and flk-1 and the microvessel densities of the LNCaP, LNCaP-Pro5, and LNCaP-LN3 cell lines growing in the prostates of nude mice. Representative tumor sections analyzed for immunoreactivity of VEGF are shown in Fig. 2. The immunoreactivity of VEGF was highest in the LNCaP-LN3 tumors, intermediate in LNCaP tumors, and lowest in LNCaP-Pro5 tumors, which is in accordance with our *in vitro* findings. Computer-assisted analysis of representative sections confirmed these results (Table 3). Using ISH, we observed that steady-state mRNA expression of VEGF was also greatest in the LNCaP-LN3 tumors, intermediate in the LNCaP tumors, and least in the LNCaP-Pro5 tumors (Fig. 2). Relative expressions of VEGF mRNA and protein were 2.4-fold higher in the LNCaP-LN3 tumors than in the LNCaP-Pro5 tumors (Fig. 2 and Table 3). *In vivo* bFGF and IL-8 protein (by IHC) and mRNA (by ISH) were expressed at similar low levels in all three tumors (data not shown).

By anti-CD31 immunostaining, microvessel density was significantly greater in the LNCaP-LN3 tumors than in either LNCaP or LNCaP-Pro5 tumor tissue ($P = 0.001$; Fig. 2 and Table 3). By image analysis, the VEGF receptor flk-1 was also significantly overexpressed on endothelial cells within the

LNCaP-LN3 tumors compared with either LNCaP or LNCaP-Pro5 tumors (Fig. 2 and Table 3).

DISCUSSION

Tumor growth and metastasis depend upon the induction of a blood supply. This process of angiogenesis is mediated, in part, by the secretion of angiogenic factors such as VEGF by tumors growing in their relevant microenvironment. VEGF is secreted by a wide variety of tumor cells, and its secretion correlates with the metastatic potential of these tumor cells (33–35). Our data indicate that the malignant potential of the human prostate carcinoma cell line LNCaP and its variant lines, LNCaP-LN3 and LNCaP-Pro5, correlated with their VEGF expression. *In vitro* evaluation revealed that the highly metastatic cell line LNCaP-LN3, which we selected for its ability to metastasize to regional lymph nodes, overexpressed VEGF protein compared with the poorly metastatic cell line LNCaP-Pro5, which was selected for its growth within the prostate. Increased steady-state gene expression of VEGF mRNA was also observed in the LNCaP-LN3 cell line. By Northern blot analysis, we observed four mRNA transcripts. The relative expressions of these four VEGF mRNA transcripts by the three cell lines were compared following normalization to GADPH. These transcripts represent both secreted and freely soluble VEGF (36). The increased expression of VEGF by LNCaP-LN3 was confirmed *in vivo* using IHC and ISH. Assessment of VEGF mRNA and protein was performed at the invasive edge of each tumor because the centers of the tumors were often necrotic (and potentially hypoxic and acidotic), making VEGF expression within these regions difficult to interpret because of artifacts (37, 38). Using antibodies directed against murine CD31, we also identified increased microvessel density in the periphery of the LNCaP-LN3 prostate tumor, which corresponded to the area of greatest VEGF expression. This suggests that the local production of VEGF by metastatic prostate cancer cells induced the increase in neovascularization, which presumably resulted in enhanced metastasis. VEGF is likely an important angiogenic factor secreted by LNCaP cells because we did not detect significant expression of either bFGF or IL-8 by these cells *in vitro* or *in vivo*. However, other angiogenic molecules, such as platelet-derived endothelial cell growth factor, transforming growth factor-β, and angiogenin, were not measured in this study.

VEGF promotes the formation of new capillaries by stimulating endothelial cell division and migration and by increasing capillary permeability following ligand binding to the endothelial cell surface membrane (39–41). We observed that the VEGF receptor protein flk was overexpressed within all LNCaP tumors compared with normal prostate epithelium (data not shown). In addition, the intensity of immunoreactivity to anti-flk-1 was increased on the cell membrane of the endothelial cells within LNCaP-LN3 tumors compared with either LNCaP or LNCaP-Pro5, suggesting that VEGF up-regulates its own receptors on the endothelial cells within the tumor. These observations are consistent with previous reports in which the VEGF receptor protein flk was up-regulated in gastrointestinal tract adenocarcinomas (33), renal cell carcinoma (34, 42), and transitional cell carcinoma of the bladder (42).

In conclusion, these results indicate that the metastatic potential of a human prostate cancer cell line correlates with its VEGF expression. We further speculate that VEGF plays a role in spontaneous metastasis subsequent to orthotopic implantation of LNCaP cells. Studies are currently in progress to directly test this hypothesis.

REFERENCES

1. Folkman, J. What is the evidence that tumors are angiogenesis dependent? J. Natl. Cancer Inst. (Bethesda), *82:* 4–6, 1989.

2. Folkman, J. How is blood vessel growth regulated in normal and neoplastic tissue? G.H.A. Clowes Memorial Award Lecture. Cancer Res., *46:* 467–473, 1986.

3. Folkman, J., and Klagsbrun, M. Angiogenic factors. Science (Washington DC), *235:* 442–447, 1992.

4. New, B., and Yeoman, L. Identification of basic fibroblast growth factor sensitivity and receptor and ligand expression in human colon tumor cell lines. J. Cell. Physiol., *150:* 320–326, 1992.

5. Kim, K., Li, B., Winer, J., Armanini, M., Gillett, N., Philips, H., and Ferrara, N. Inhibition of vascular endothelial growth factor-induced angiogenesis suppresses tumor growth *in vivo*. Nature (Lond.), *362:* 841–844, 1993.

6. Koch, A. E., Polverini, P. J., Kunkel, S. L., Harlow, L. A., DiPietro, L. A., Elner, V. M., Elner, S. G., and Strieter, R. M. Interleukin-8 as a macrophage-derived mediator of angiogenesis suppresses tumor growth *in vivo*. Science (Washington DC), *258:* 1798–1801, 1992.

7. Chodak, G. W., Haundenschild, C., Gittes, R. F., and Folkman, J. Angiogenic activity as a marker of neoplastic and preneoplastic of the human bladder. Ann. Surg., *192:* 762–771, 1980.

8. Weidner, N., Carroll, P. R., Flax, J., Blumfeld, W., and Folkman, J. Tumor angiogenesis correlates with metastasis in invasive prostate carcinoma. Am. J. Pathol., *143:* 401–409, 1993.

9. Bigler, S. A., Deering, R. E., and Brawer, M. A. Comparison of microscopic vascularity in benign and malignant prostate tissue. Hum. Pathol., *24:* 220–226, 1993.

10. Liotta, L. A., Steeg, P. S., and Stetler-Stevenson, W. G. Cancer metastasis and angiogenesis: an imbalance of positive and negative regulation. Cell, *64:* 327–336, 1991.

11. Folkman, J., and Sing, Y. Angiogenesis. J. Biol. Chem., *267:* 10931–10934, 1992.

12. Blood, C. H., and Zetter, B. R. Tumor interactions with vasculature: angiogenesis and tumor metastasis. Biochim. Biophys. Acta, *1032:* 89–118, 1990.

13. Harper, M. E., Glynne-Jones, E., Goddard, L., Thurston, V. J., and Griffiths, K. Vascular endothelial growth factor (VEGF) expression in prostatic tumours and its relationship to neuroendocrine cells. Br. J. Cancer, *74:* 910–916, 1996.

14. Jackson, W. M., Bentel, J. M., and Tilley, W. D. Vascular endothelial growth factor (VEGF) in prostate cancer and benign prostatic hyperplasia. J. Urol., *157:* 2323–2328, 1997.

15. Ferrer, F. A., Miller, L. J., Andrawis, R. I., Kurtzman, S. H., Albertsen, P. C., Laudone, V. P., and Kreutzer, D. L. Vascular endothelial growth factor (VEGF) expression in human prostate cancer: *in situ* and *in vitro* expression of VEGF by human prostate cancer cells. J. Urol., *157:* 2329–2333, 1997.

16. Gridley, D. S., Andres, M. L., and Slater, J. M. Enhancement of prostate cancer xenograft growth with whole-body radiation and vascular endothelial growth factor. Anticancer Res., *17:* 923–928, 1997.

17. Borgstrom, P., Bourdon, M. A., Hillan, K. J., Sriramarao, P., and Ferrara, N. Neutralizing anti-vascular endothelial growth factor antibody completely inhibits angiogenesis and growth of human prostate carcinoma micro tumors *in vivo*. Prostate, *35:* 1–10, 1998.

18. Joseph, I. B., and Isaacs, J. T. Potentiation of the antiangiogenic ability of Ilinomide by androgen ablation involves down-regulation of vascular endothelial growth factor in human androgen-responsive prostatic cancers. Cancer Res., *57:* 1054–1057, 1997.

19. Stewart, R. J., and Folkman, J. Vascular endothelial growth factor is regulated by androgens in hormone-responsive human prostate carcinoma. J. Urol., *157* (Suppl. 4)*:* 4, 1997.

20. Moon, W. C., Choi, H. R., and Moon, S. Y. Endocrine therapy inhibits expression of vascular endothelial growth factor and angiogenesis in prostate cancer. J. Urol., *157* (Suppl. 4)*:* 223, 1997.

21. Pettaway, C. A., Pathak, S., Greene, G., Ramirez, E., Wilson, M. R., Killion, J. J., and Fidler, I. J. Selection of highly metastatic variants of different human prostatic carcinomas using orthotopic implantation in nude mice. Clin. Cancer Res., *2:* 1627–1636, 1996.

22. Fort, P., Marty, L., Liechaczyk, M., Sabrouty, S. E., Dani, C., and Blanchard, J. M. Various rat adult tissues express only one major mRNA species from the glyceraldehyde-3-phosphate dehydrogenase multigene family. Nucleic Acids Res., *13:* 1431–1442, 1985.

23. Rogelj, S., Weinberg, R. A., Fanning, P., and Klagsbrun, M. Basic fibroblast growth factor fused to a signal peptide transformed cells. Nature (Lond.), *331:* 173–175, 1988.

24. Berse, B., Brown, L. F., Van der Walter, L., Dvorak, H. F., and Singer, D. R. Vascular permeability factor (vascular endothelial growth factor) gene is expressed differentially in normal tissues, macrophages and tumors. Mol. Biol. Cell, *3:* 211–220, 1992.

25. Matsushima, K., Morishita, K., Yoshimura, T., Lavu, S., Kobayashi, Y., Lew, W., Appela, E., Kung, H. F., Leonard, E. J., and Oppenheim, J. J. Molecular cloning of human monocyte-derived neutrophil chemotactic factor (MCNCF) and the induction of MDNCF mRNA by interleukin-1 and tumor necrosis factor. J. Exp. Med., *167:* 1883–1893, 1988.

26. Weidner, N., Semple, J. P., Welch, W. R., and Folkman, J. Tumor angiogenesis and metastasis-correlation in invasive breast carcinoma. N. Engl. J. Med., *324:* 1–8, 1991.

27. Pearson, W. R., and Lipman, D. J. Improved tools for biological sequence comparison. Proc. Natl. Acad. Sci. USA, *85:* 2444–2448, 1988.

28. Caruthers, M. H., Beaucage, S. L., Efcavitch, J. W., Fisher, E. F., Goldman, R. A., DeHaseth, P. L., Mandecki, W., Matteucci, M. D., Rosendahl, M. S., and Sabintsky, Y. Chemical synthesis and biological studies on mutated gene-control regions. Cold Spring Harbor Symp. Quant. Biol., *47:* 411–418, 1982.

29. Parks, C. S., Brigati, D. J., and Manahan, L. J. Automated molecular pathology: one-hour *in situ* DNA hybridization. J. Histotechnol., *14:* 219–229, 1991.

30. Reed, J. A., Manahan, L. J., Park, C. S., and Brigati, D. J. Complete one-hour immunohistochemistry based on capillary action. BioTechniques, *13:* 434–443, 1992.

31. Kitadai, Y., Ellis, L. M., Takahashi, Y., Bucana, C. D., Anzai, H., Tahara, E., and Fidler, I. J. Multiparametric *in situ* messenger RNA hybridization analysis to detect metastasis-related genes in surgical specimens of human colon carcinomas. Clin. Cancer Res., *1:* 1095–1102, 1995.

32. Perrotte, P., Bielenberg, D. R., Eve, B. Y., and Dinney, C. P. Organ-specific angiogenesis and metastasis of human bladder carcinoma growing in athymic mice. Mol. Urol., *1:* 299–307, 1997.

33. Brown, L. F., Berse, B., Jackmon, R. W., Tognazzi, K., Manseau, E. J., Senger, D. R., and Dvorak, H. F. Expression of vascular permeability factor (vascular endothelial growth factor) and its receptors in adenocarcinoma of the gastrointestinal tract. Cancer Res., *53:* 4727–4735, 1993.

34. Takahashi, A., Sasaki, H., Kim, S. J., Tobisu, K., Kakizoe, T., Tsukamoto, T., Kumamoto, Y., Sugimura, T., and Terada, M. Markedly increased amount of mRNAs for vascular endothelial growth factor and placental growth factor in renal cell carcinoma associated with angiogenesis. Cancer Res., *54:* 4233–4237, 1994.

35. Takahashi, Y., Cleary, K. R., Mai, M., Kitadai, Y., Bucana, C. D., and Ellis, L. M. Significance of vessel count and vascular endothelial growth factor and its receptor (KDR) in intestinal-type gastric cancer. Clin. Cancer Res., *2:* 1679–1684, 1996.

36. Houck, K. A., Leung, D. W., Rowland, A. M., Winer, J., and Ferrara, N. Dual regulation of vascular endothelial growth factor bioavailability by genetic and proteolytic mechanisms. J. Biol. Chem., *267:* 26031–26037, 1992.

37. Shweili, D., Itin, A., Soffer, D., and Keshet, E. Vascular endothelial growth factor induced by hypoxia may mediate hypoxia-initiated angiogenesis. Nature (Lond.), *359:* 843–845, 1992.

38. Takano, S., Yoshii, Y., Kondo, S., Suzuki, H., Maruno, T., Shirai, S., and Nose, T. Concentration of vascular endothelial growth factor in the serum and tumor tissue of brain tumor patients. Cancer Res., *56:* 2185–2190, 1996.

39. Senger, D. R., Ledbetter, S. R., Claffey, K. P., Papadopoulos-Sergiou, A., Perruzi, C. A., and Detmar, M. Stimulation of endothelial cell migration by vascular permeability factor/vascular endothelial growth factor through cooperative mechanisms involving the $\alpha_v\beta_3$ integrin, osteopontin and thrombin. Am. J. Pathol., *149:* 293–305, 1996.

40. Bikfalvi, A., Sauzeau, C., Moukadiri, H., Maclouf, J., Busso, N., Bryckaert, M., Plouet, J., and Tobelem, G. Interaction of vasculotropin/vascular endothelial growth factor with human umbilical vein endothelial cells: binding, internalization, degradation and biological effects. J. Cell. Physiol., *149:* 50–59, 1991.

41. Senger, D. R., van de Water, L., Brown, L. F., Nagy, J. A., Yeo, K. T., Berse, B., Jackman, R. W., Dvorak, A. M., and Dvorak, H. F. Vascular permeability factor (VPF, VEGF) in tumor biology. Cancer Metastasis Rev., *12:* 303–324, 1993.

42. Brown, L. F., Berse, B., Jackman, R. W., Tognazzi, K., Manseau, E. J., Dvorak, H. F., and Senger, D. R. Increased expression of vascular permeability factor (vascular endothelial growth factor) and its receptors in kidney and bladder carcinomas. Am. J. Pathol., *143:* 1255–1262, 1993.

Interleukin 8 Expression Regulates Tumorigenicity and Metastases in Androgen-independent Prostate Cancer[1]

Keiji Inoue, Joel W. Slaton, Beryl Y. Eve, Sun Jin Kim, Paul Perrotte, M. Derya Balbay, Seiji Yano, Menashe Bar-Eli, Robert Radinsky, Curtis A. Pettaway, and Colin P. N. Dinney[2]

Departments of Cancer Biology [K. I., B. Y. E., J. W. S., S. J. K., S. Y., M. B-E., R. R., C. A. P., C. P. N. D.] and Urology [P. P., J. W. S., M. D. B., C. A. P., C. P. N. D.], The University of Texas M. D. Anderson Cancer Center, Houston, Texas 77030

ABSTRACT

Interleukin 8 (IL-8) is mitogenic and chemotactic for endothelial cells. Within a neoplasm, IL-8 is secreted by inflammatory and neoplastic cells. The highly metastatic PC-3M-LN4 cell line overexpresses IL-8 relative to the poorly metastatic PC-3P cell line. We evaluated whether IL-8 expression by human prostate cancer growing within the prostate of athymic nude mice regulates tumor angiogenesis, growth, and metastasis. PC-3P cells were transfected with the full-length sense IL-8 cDNA, whereas PC-3M-LN4 cells were transfected with the full-sequence antisense IL-8 cDNA. Control cells were transfected with the neomycin resistance gene (*Neo*). *In vitro*, sense-transfected PC-3P cells overexpressed IL-8-specific mRNA and protein, which resulted in up-regulation of matrix metalloproteinase 9 (MMP-9) mRNA, and collagenase activity, resulting in increased invasion through Matrigel. After antisense transfection of the PC-3M-LN4 cells, IL-8 and MMP-9 expression, collagenase activity, and invasion were markedly reduced relative to controls. After orthotopic implantation, the sense-transfected PC-3P cells were highly tumorigenic and metastatic, with significantly increased neovascularity and IL-8 expression compared with either PC-3P cells or controls. Antisense transfection significantly reduced the expression of IL-8 and MMP-9 and tumor-induced neovascularity, resulting in inhibition of tumorigenicity and metastasis. These results demonstrate that IL-8 expression regulates angiogenesis in prostate cancer, in part by induction of MMP-9 expression, and subsequently regulates the growth and metastasis of human prostate cancer.

INTRODUCTION

Prostate cancer is the most common malignancy and the second leading cause of cancer-related deaths among men in the United States (1). Although modest improvements in early detection and therapy have occurred (2, 3), most deaths from prostate cancer are caused by metastases that resist conventional androgen-deprivation therapy (4–6). Continued empiricism in the treatment of advanced prostate cancer is unlikely to produce significant improvement over current therapy. Rather, knowledge of the cellular and molecular properties of prostate cancer and of the tumor-host interactions that influence the dissemination of metastatic disease is essential for the design of more effective treatment.

Metastasis is a highly selective process involving multiple tumor-host interactions (7–11). A crucial step in metastasis is vascularization in and around the tumor (12, 13). The balance between stimulatory and inhibitory factors released by the tumor and the microenvironment regulates this process of angiogenesis (14–16). Human prostate cancer produces a number of proangiogenic factors, including VEGF[3] (17, 18), bFGF, (19, 20), and IL-8 (18, 21, 22). MVD, a pathological surrogate for angiogenesis, correlates with stage and prognosis for patients with prostate cancer (23).

IL-8 was originally identified as a leukocyte chemoattractant (24, 25) but is now also known to be an autocrine growth factor for malignant melanoma (26) and keratinocytes (27). In addition, IL-8 displays mitogenic and morphogenic activity for endothelial cells (28) and regulates angiogenesis in lung cancer (29, 30) and melanoma (31, 32). IL-8 is expressed by prostate cancer (18, 21, 22), and this expression correlates with metastatic potential (21). Moreover, Moore *et al.* (33) reported recently that neutralizing antibodies to IL-8 inhibited the angiogenic activity of PC-3 prostate cancer homogenates and reduced tumorigenicity *in vivo*, implicating IL-8 as an important modulator of prostate cancer growth.

Therefore, in the present study we forced the expression of IL-8 by human prostate cancer cells to determine whether IL-8 is associated with angiogenesis *in vivo* and to confirm the relationship between IL-8 expression and the subsequent tumorigenicity of human prostate cancer growing within the prostate of athymic nude mice. Overexpression of MMP-2 and MMP-9, which are regulated by transforming growth factor-β, correlated with progression and poor survival of patients with prostate cancer (34–38). Because IL-8 regulated the expression of

Received 12/8/99; revised 2/22/00; accepted 2/23/00.

The costs of publication of this article were defrayed in part by the payment of page charges. This article must therefore be hereby marked *advertisement* in accordance with 18 U.S.C. Section 1734 solely to indicate this fact.

[1] Supported in part by NIH Grants CA67914, CA56973, and Core Grant CA-16672, a grant from the Department of Defense, and a grant from the Robert Wood Johnson Foundation.

[2] To whom requests for reprints should be addressed, Department of Urology, Box 173, The University of Texas M. D. Anderson Cancer Center, 1515 Holcombe Boulevard, Houston, TX 77030. Phone: (713) 792-3250; Fax: (713) 794-4824; E-mail: cdinney@mdanerson.org.

[3] The abbreviations used are: VEGF, vascular endothelial cell growth factor; bFGF, basic fibroblast growth factor; IL, interleukin; rIL, recombinant IL; MMP, matrix metalloproteinase; MVD, microvessel density; GAPDH, glyceraldehyde-3-phosphate dehydrogenase; CMEM, complete Eagle's minimum essential medium; ISH, *in situ* hybridization; IHC, immunohistochemical staining; ActD, actinomycin D; CAT, chloramphenicol acetyltransferase; RT-PCR, reverse transcription-PCR.

MMP-2 by human melanoma (32), we determined whether IL-8 also regulated MMP-9 expression by human prostate cancer.

MATERIALS AND METHODS

Cell Lines and Culture Conditions. Cells of the highly metastatic human prostate carcinoma cells line PC-3M-LN4 (39) and the poorly metastatic cell line PC-3P (40) were grown as monolayer cultures in RPMI 1640 supplemented with 10% fetal bovine serum, vitamins, sodium pyruvate, L-glutamine, nonessential amino acids, and penicillin-streptomycin [complete RPMI (CRPMI); Ref. 39].

Transfection and Selection of PC-3P and PC-3M-LN4 Cells Expressing IL-8. Tumor cells were plated onto 100-mm dishes at a density of 1×10^6/dish. The monolayers (60–70% confluent) were transfected with pcDNA3/sense IL-8, pcDNA3/antisense IL-8 [a gift from Dr. K. Matsushima (24)], or control pcDNA3/neo plasmids using a stable mammalian transfection kit from Stratagene (La Jolla, CA). The cultures were placed in a 37°C incubator for 12 h and then washed and fed with modified complete MEM (CMEM). After 24 h, 500-1000 μg/ml G418 sulfate (Life Technologies, Inc., Gaithersburg, MD) were added. The CMEM/G418 medium was replaced every 3 days until individual resistant colonies were isolated and established in culture as individual lines. All of the lines were maintained in CMEM/G418 and frozen after one to three *in vitro* passages. To avoid clonal variations, six positive clones were then pooled for the *in vitro* and *in vivo* studies.

The less tumorigenic and metastatic PC-3P cells and the highly tumorigenic, highly metastatic PC-3M-LN4 cells were transfected with pcDNA3/sense IL-8 or pcDNA3/antisense IL-8, respectively, or with control pcDNA3/neo. Individual G418-resistant (500–1000 μg/ml) colonies were established as separate adherent cultures. We selected pooled sense IL-8 transfected PC-3P cells [PC-3P(IL-8)], the highest IL-8-expressing clone [PC-3P(IL-8 High)], and the lowest IL-8-expressing clone [PC-3P(IL-8 Low)], and we selected pooled antisense IL-8 transfected PC-3LN4 cells [PC-3M-LN4(AS IL-8)], the highest IL-8 expressing clone [PC-3M-LN4(AS IL-8 High)], and the lowest IL-8 expressing clone [PC-3M-LN4(AS IL-8 Low)], according to the expression level of IL-8 mRNA and protein as determined by Northern blot analysis and ELISA, respectively.

Northern Blot Analysis. Polyadenylated mRNA was extracted directly from the tumors or from 10^8 cultured cells using the Fasttrack mRNA isolation kit (Invitrogen, San Diego, CA). The mRNA was electrophoresed onto 1% denatured formaldehyde agarose gel, electrotransferred to Genescreen nylon membrane (DuPont, Boston, MA), and cross-linked with a UV Stratalinker 1800 (Stratagene) at 120,000 mJ/cm^2. Filters were washed twice at 65°C with 30 mM NaCl/3 mM sodium citrate-0.1% SDS (w/v). The membranes were then hybridized and probed for IL-8, bFGF, VEGF, and MMP-9; the presence of GAPDH was used to control for loading. The cDNA probes used were: (*a*) a 0.5-kb *Eco*RI cDNA fragment corresponding to human IL-8 (a gift of Dr. K. Matsushima, Kanazawa, Japan; Ref. 24); (*b*) a 1.4-kb cDNA fragment of bovine bFGF (41); (*c*) a 204-kb fragment of human VEGF cDNA inserted in a pGEM-based construct (a gift Dr. B. Berse, Harvard Medical School, Boston, MA; Ref. 42); (*d*) a 1.0-kb cDNA fragment corresponding to human MMP-9, (21); and (*e*) a 1.28-kb fragment from pR GAPDH cut with *Pst*I (43). The insert was excised with *Bam*HI and *Eco*RI. Each cDNA fragment was purified by agarose gel electrophoresis, recovered using GeneClean (BIO 101, Inc., La Jolla, CA), and radiolabeled by a random primer technique using a commercial kit (Boehringer Mannheim Corp., Indianapolis, IN) and [α-^{32}P]dCTP (Amersham Corp., Arlington Heights, IL; Ref. 44). The steady-state expression of IL-8, bFGF, VEGF, and MMP-9 mRNA transcripts was quantified by densitometry of autoradiographs using the Image Quant software program (Molecular Dynamics, Sunnyvale, CA); each sample measurement was calculated as the ratio of the average areas of the specific mRNA transcripts to the 1.3-kb GAPDH mRNA transcript in the linear range of the film.

ELISA for IL-8, bFGF, and VEGF. Viable cells (5×10^3) were seeded in a 96-well plate. Conditioned medium was removed after 24 h; the cells were washed with 200 μl of HBSS, and 200 μl of 10% bovine serum supplemented by fresh MEM were added. Twenty-four h later, IL-8 and VEGF in cell-free culture supernatants and cell-associated bFGF in freeze-thaw cell lysates were determined using the commercial Quantine ELISA kit (R&D System, Minneapolis, MN). The protein concentration for each factor was then determined by absorbance comparison to the standard curve. Results were expressed as numbers of cells (45).

Growth Curve. Viable cells (1×10^3) were seeded in a 96-well plate. Conditioned medium was removed after 24 h, and the cells were washed with 200 μl of HBSS. Either 200 μl of fresh CRPMI medium or CMEM/G418 conditioned medium were added. Every 24 h, the numbers of viable cells in each cell line were determined by absorbance comparison. The doubling time of each cell line was determined by plotting the absorbance on a semilogarithmic axis *versus* time (Cricket Software, Malvern, PA). The doubling times of the PC-3P sense IL-8 transfectants (IL-8, 40.1 h; IL-8 Low, 38.1 h; IL-8 High, 41.2 h) were similar to those of PC-3P (38.6 h) and PC-3P(Neo) (39.1 h). The doubling times of the PC-3M-LN4 antisense IL-8 transfectants (AS IL-8, 22.0 h; AS IL-8 Low, 21.5 h; AS IL-8 High, 21.7 h) were similar to those of PC-3M-LN4 (22.0 h) and PC-3M-LN4(Neo) (22.6 h).

Collagenase Activity. To determine collagenase activity, electrophoresis of serum-free conditioned medium was performed as described previously (46). Cells (5×10^3) were seeded in six-well plates and grown to 60–70% confluence. The cells were washed with HBSS and grown for 24 h in serum-free medium. The supernatant fluid was collected to determine collagenase activity, and the remaining cells were counted to confirm the cell number. Collected samples were centrifuged to concentrate using MICROCON microconcentrators (Amicon, Inc., Beverly, MA.). Thirty μl in each sample with 10 μl loading buffer (10% SDS) were electrophoresed on 20% SDS-polyacrylamide gels containing 1 mg/ml gelatin. After electrophoresis, gels were washed in 2.5% Triton X-100 to remove SDS and allow proteins to renature. Then gels were immersed in incubation buffer containing 1% Triton X-100, 50 mM Tris (pH 7.5), 5 mM $CaCl_2$, and 1 μM $ZnCl_2$ for 24 h at 37°C. The zymograms were stained with 0.1% (w/v) Coomassie Blue R-250 (Sigma) and destained in 40% methanol-10% acetic acid. Identification

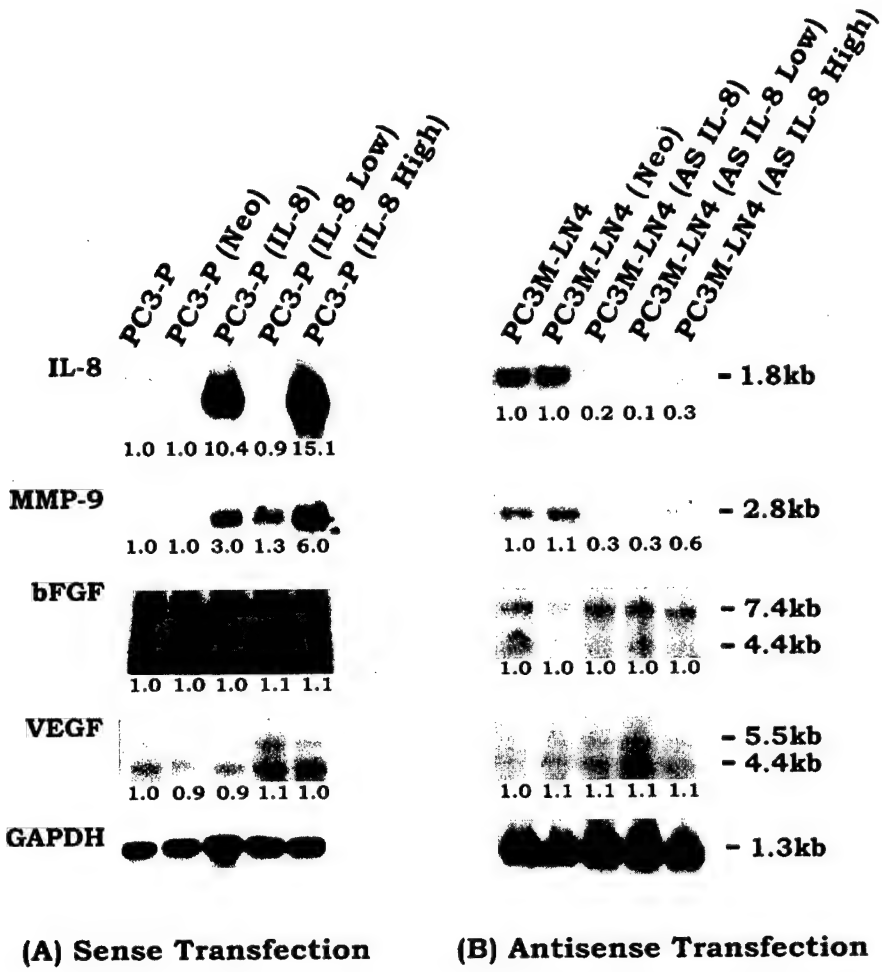

Fig. 1 Northern blot analysis of mRNA for IL-8, bFGF, VEGF, and MMP-9 in the poorly tumorigenic and poorly metastatic human prostate cancer cell line PC-3P, Neo transfectant PC-3P(Neo), and sense IL-8 transfectants PC-3P(IL-8), PC-3P(IL-8 Low), and PC-3P(IL-8 High) (*A*) and in the highly metastatic human prostate cancer cell line PC-3M-LN4, Neo transfectant PC-3M-LN4(Neo), and antisense IL-8 transfectants PC-3M-LN4(AS IL-8), PC-3M-LN4(AS IL-8 Low), and PC-3M-LN4(AS IL-8 High) (*B*). Difference in expression is shown by the ratio of mRNA expression of transfectants to that of parental cells (defined as 1.0). GAPDH served as control for loading. IL-8 expressions were increased 10.4- and 15.1-fold in the PC-3P(IL-8) and PC-3P(IL-8 High) lines, respectively, whereas there was no change in the mRNA expression of bFGF or VEGF. mRNA expression of IL-8 by PC-3M-LN4(AS IL-8) and PC-3M-LN4(AS IL-8 Low) were decreased 5.0- to 10.0-fold, respectively, whereas there was no change in the mRNA expression of bFGF or VEGF. MMP-9 mRNA expressions were increased 3.0- and 6.0-fold in PC-3P(IL-8) and PC-3P(IL-8 High) cells, respectively, and reduced 3.3- and 3.3-fold by PC-3M-LN4(AS IL-8) and PC-3M-LN4(AS IL-8 Low), respectively, after transfection with IL-8 sense or antisense transcripts.

of a transparent band at M_r 92,000 on the Coomassie blue background of the slab gel was considered positive for the presence of the enzymatic activity. The collagenase activity was quantified using densitometry of Image Quant software program (Molecular Dynamics, Sunnyvale, CA).

To determine whether the increase in MMP-9 activity is mediated by IL-8, we incubated parental PC-3P cells in the presence of different doses (0–20 μg/ml) of human rIL-8, and the activity of MMP-9 was determined. We then determined the increased activity of MMP-9 by rIL-8 was inhibited by neutralization by using an anti-IL-8 antibody (100 μg/ml), with a nonspecific IgG (100 μg/ml) as a control.

PCR Analysis. RT-PCR analysis was performed as described previously (47). Briefly, total cellular RNA (1 mg) extracted from various cell lines was transcribed into cDNA using downstreaming primers IL-8 receptors type A and B, respectively (Reverse Transcription System;, Promega). The reverse transcription reaction was performed at 42°C for 50 min. PCR was performed with 40 cycles of denaturation (94°C for 1.5 min), annealing (58°C for 45 s), and extension (72°C for 2.5 min) and 7 min of extension after completion of all cycles. Amplified fragments were analyzed on the 2% gel, and bands of expected sizes were confirmed by sequencing. The primer sequences used were as follows: for IL-8 receptor type A, sense 5-AGT TCT TGG CAC GTC ATC G-3′and antisense 5′-CTT GGA GGT ACC TCA ACA GC-3′; and for IL-8 receptor type B, sense 5′-ACA TTC CTG TGC AAG GTG G-3′ and antisense 5′-CAG GGT GAA TCC GTA GCA GA-3′.

Invasion Assay through Matrigel. Polyinylprolidone-free polycarbonate filters (8 μm pore size; Nucleopore; Becton Dickinson Labware, Franklin Lakes, NJ) were coated with a mixture of basement membrane components (Matrigel, 25 μg/filter) and placed in modified Boyden chambers. The cells (2×10^5) were released from their culture dishes by short exposure to EDTA (1 mmol/l), centrifuged, resuspended in 0.1% BSA-DMEM, and placed in the upper compartment of the Boyden chamber. Fibroblast-conditioned medium in the lower compartment served as a chemoattractant. After incubation for 6 h at 37°C, the cells on the lower surface of the filter were stained with Diff-Quick (American Scientific Products, McGraw Park, IL) and quantified with a cooled CCD Optotronics Tec 470 camera (Optotronics Engineering, Goletha, CA) linked to a computer and digital printer (Sony Corporation, Tokyo, Japan). The results were expressed as the average number of cells in the five highest spots identified within a single ×200 field on the lower surface of the filter (48).

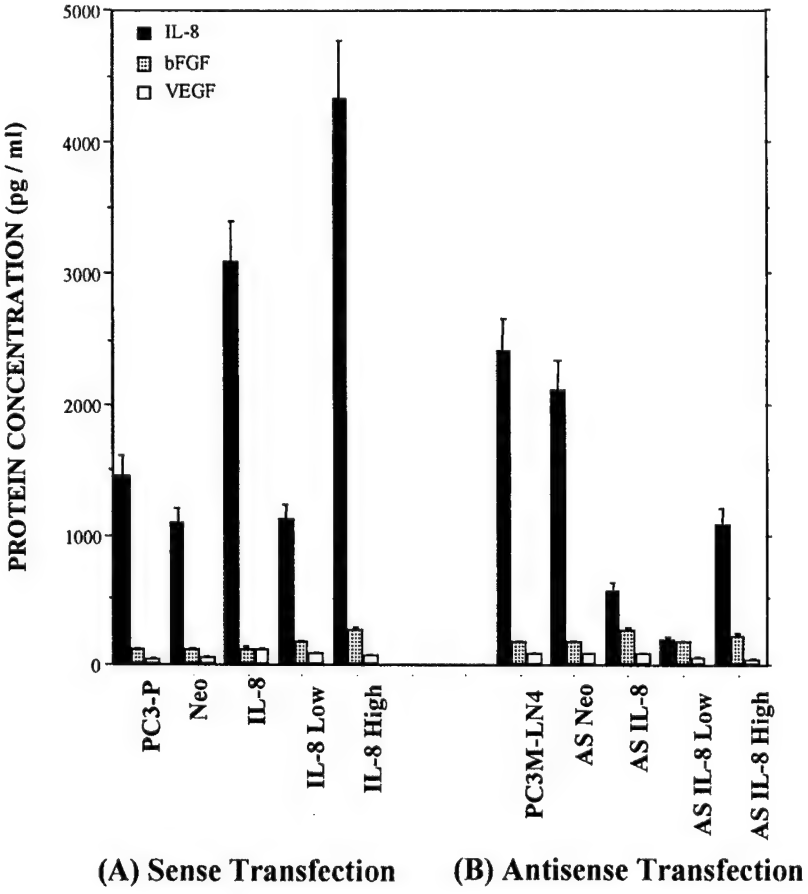

Fig. 2 Protein expression of IL-8, bFGF, and VEGF in PC-3P, Neo transfectant PC-3P(Neo), and sense IL-8 transfectants PC-3P(IL-8), PC-3P(IL-8 Low), and PC-3P(IL-8 High) (*A*) and in PC-3M-LN4, Neo transfectant PC-3M-LN4(Neo), and antisense IL-8 transfectants PC-3M-LN4(AS IL-8), PC-3M-LN4(AS IL-8 Low), and PC-3M-LN4(AS IL-8 High) (*B*) was analyzed by ELISA. Cells (5×10^3/well) were cultured for 48 h in RPMI or CMEM/G418. Cell-free culture supernatant was analyzed for IL-8 and VEGF. Cell lysate was analyzed for bFGF. IL-8 expression was increased 3.0- and 4.0-fold by the PC-3P(IL-8) and PC-3P(IL-8 High) cells, respectively, and decreased 4.0- to 10.0-fold by PC-3M-LN4(AS IL-8) and PC-3M-LN4(AS IL-8 Low), respectively. Changes in protein expression by the transfectant paralleled the changes seen in mRNA expression. bFGF and VEGF protein expressions were unchanged. *Bars,* SD.

Animals. Male athymic BALB/c nude mice were obtained from the Animal Production Area of the National Cancer Institute, Frederick Cancer Research Facility (Frederick, MD). The mice were maintained in a laminar-airflow cabinet under pathogen-free conditions and used at 8–12 weeks of age. All facilities were approved by the American Association for Accreditation of Laboratory Animal Care in accordance with the current regulations and standards of the United States Department of Agriculture, the Department of Health and Human Services, and the NIH.

Orthotopic Implantation of Tumor Cells. Cultured PC-3P, PC-3M-LN4, Neo, sense, and antisense IL-8 transfected cells (60–70% confluent) were prepared for injection as described previously (39, 49). Mice were anesthetized with methoxyflurane. For orthotopic implantation, a lower midline incision was made, and viable tumor cells (2×10^6/40 μl) in HBSS were implanted into the dorsal prostate lobes using a 30-gauge needle with a 1-ml disposable syringe and a calibrated push button-controlled dispensing device (Hamilton Syringe Company, Reno, NV). Formation of a bulla indicated a satisfactory injection. The prostate was returned to the abdominal cavity, and the abdominal wall was closed with a single layer of metal clips. Mice were killed 6 weeks after implantation of tumor cells. The primary tumors were removed and weighed, and the presence of metastases (in the lymph nodes) was determined grossly and microscopically. The prostates were then either quickly frozen in liquid nitrogen for mRNA extraction, fixed in 10% buffered formalin, placed in OCT compound (Miles Laboratories, Elkhart, IN), or mechanically dissociated and put into tissue culture.

ISH Analysis. Specific antisense oligonucleotide DNA probes were designed complementary to the mRNA transcripts based on published reports of the cDNA sequence: IL-8 (CTC CAC AAC CCT CTG CAC CC), 66% guanosine cytosine (GC) content (21); bFGF (CGG GAA GGC GCC GCT GCC GCC), 85.7% GC content (41); VEGF/VPF (TGG TGA TGT TGG ACT CTT CAG TGG GCU), 57.7% GC content (42); and MMP-9 (CCG GTC CAC CTC GCT GGC GCT CCG GU), 80.0% GC content (21). The specificity of the oligonucleotide sequence was initially determined by a Gene Bank European Molecular Biology Library database search with the use of the Genetics Computer Group sequence analysis program (Genetics Computer Group, Madison, WI) based on the FastA algorithm; these sequences showed 100% homology with the target gene and minimal homology with nonspecific mammalian gene sequences. The specificity of each of the sequences was also confirmed by Northern blot analysis (50). A poly $d(T)_{20}$ oligonucleotide was used to verify the integrity and lack of degradation of mRNA in each sample. All DNA probes were synthesized with six biotin molecules (hyperbiotinylated) at the 3′ end via direct coupling with the use of standard phosphoramidite chemical methods (Research Genetics, Huntsville, AL). The

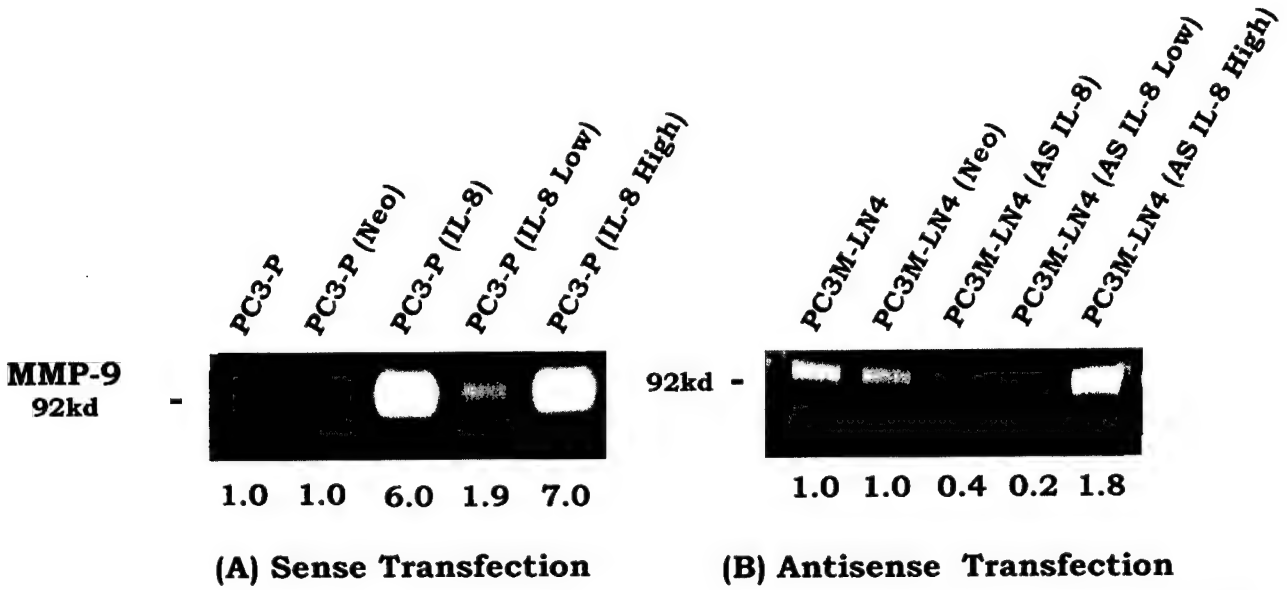

Fig. 3 Gelatinolytic activity of conditioned medium of PC-3P, Neo transfectant PC-3P(Neo), and sense IL-8 transfectants PC-3P(IL-8), PC-3P(IL-8 Low), and PC-3P(IL-8 High) (*A*) and of PC-3M-LN4, Neo transfectant PC-3M-LN4(Neo), and antisense IL-8 transfectants PC-3M-LN4(AS IL-8), PC-3M-LN4(AS IL-8 Low), and PC-3M-LN4(AS IL-8 High) (*B*). CMEM was used as internal control. The difference in expression is expressed as the ratio of gelatinolytic activity of transfectants to that of parental cells (defined as 1.0). The collagenase activity of PC-3P(IL-8) and PC-3P(IL-8 High) cells was increased 6.0- and 7.0-fold, respectively, and that of PC-3M-LN4(AS IL-8) and PC-3M-LN4(AS IL-8 Low) cells was decreased 2.5- to 5.0-fold.

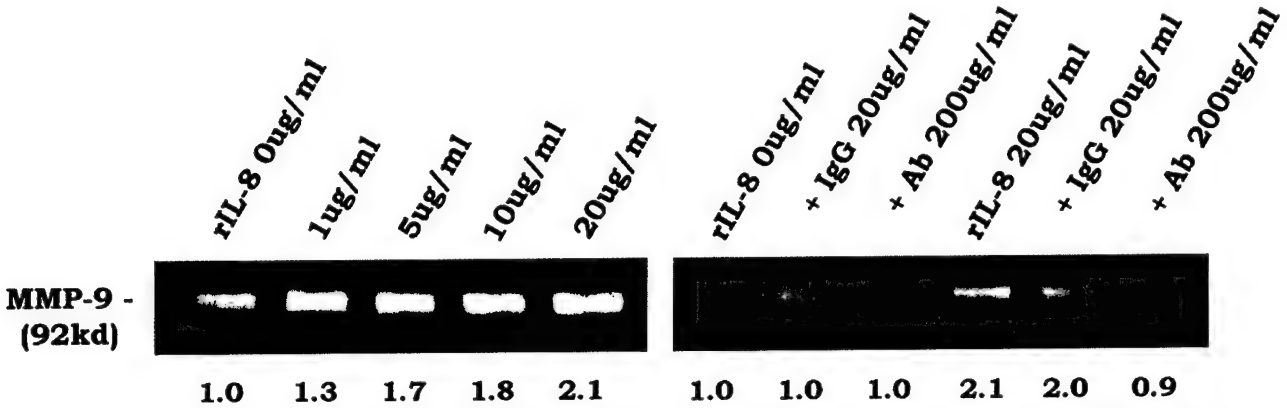

Fig. 4 Regulation of MMP-9 activity by IL-8. We next analyzed whether the increase in MMP-9 activity is mediated by IL-8. Parental PC-3P cells were incubated in the presence of different doses of human rIL-8 (0–20 μg/ml), and the activity of MMP-9 was determined. The results shown at *left* indicate that IL-8 caused an increase in the activity of MMP-9 in a dose-dependent manner. Moreover, the increased activity of MMP-9 by rIL-8 was inhibited by neutralization with anti-IL-8 antibody (100 μg/ml) (*right*).

lyophilized probes were reconstituted to a stock solution at 1 μg/μl in 10 mmol/l Tris (pH 7.6) and 1 mmol/l EDTA. Immediately before use, the stock solution was diluted with probe dilution (Research Genetics, Huntsville, AL).

In situ mRNA hybridization was performed as described previously with minor modifications, (51, 52) using the Microprobe Manual Staining System (Fisher Scientific, Pittsburgh, PA; Ref. 53). Tissue sections (4 μm) of formalin-fixed, paraffin-embedded specimens were mounted on silane-treated ProbeOn slides (Fisher Scientific; Refs. 51 and 52). The slides were placed in the Microprobe slide holder, dewaxed, and rehydrated with Autodewaxer and Autoalcohol (Research Genetics), followed by enzymatic digestion with pepsin. Hybridization of the probe was performed for 45 min at 45°C, and the samples were then washed three times with 2× sodium saline chloride (Research Genetics) for 2 min at 45°C. The samples were incubated with alkaline phosphatase-labeled avidin for 30 min at 45°C, rinsed in 50 mM Tris buffer (pH 7.6), rinsed with alkaline phosphatase enhancer for 1 min, and incubated with a chromogen substrate for 15 min at 45°C. Additional incubation with fresh chromogen substrate was performed if necessary to enhance a weak reaction in this assay; a red staining indicated a

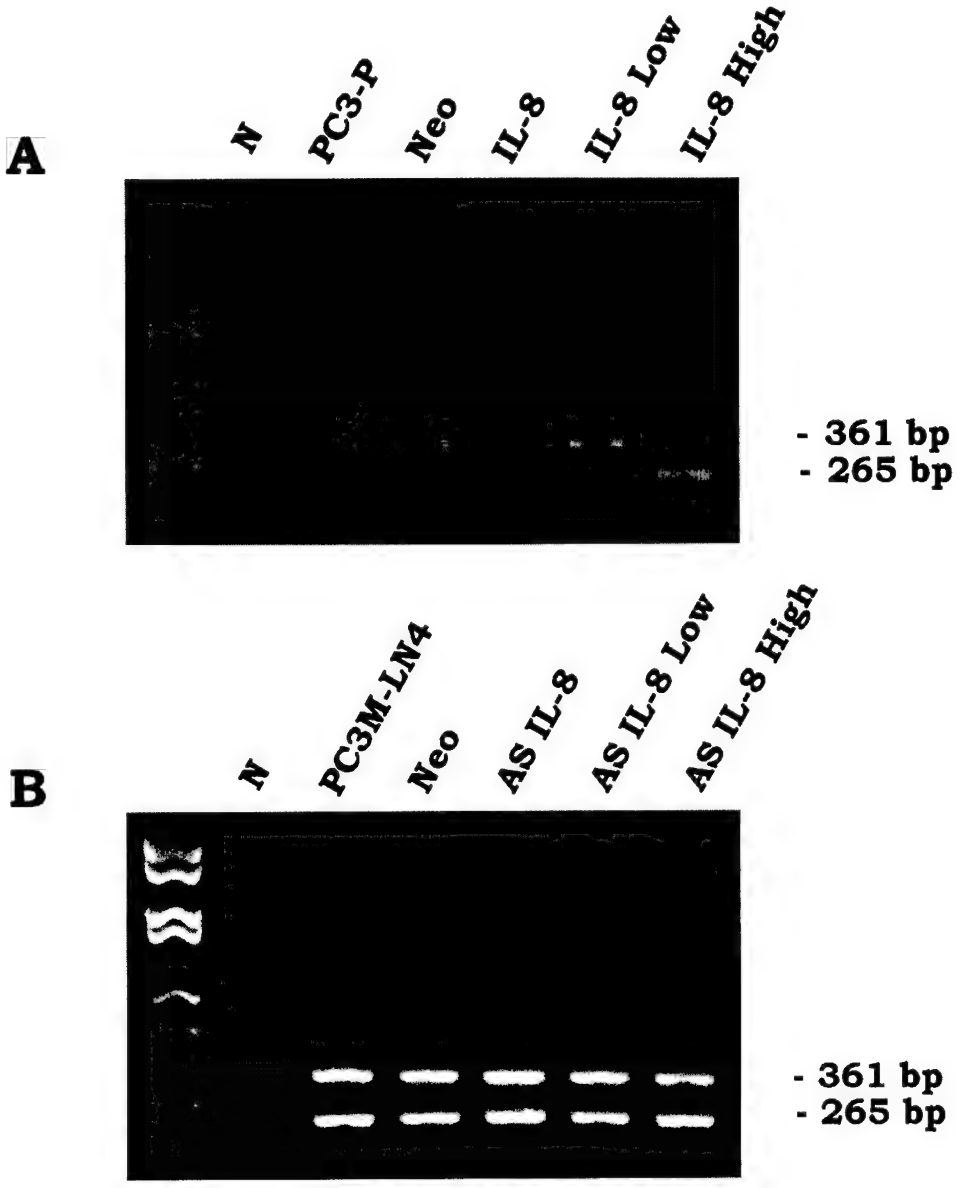

Fig. 5 RT-PCR analysis was performed by primer sequences sense 5′-AGT TCT TGG CAC GTC ATC G-3′and antisense 5′-CTT GGA GGT ACC TCA ACA GC-3′ for IL-8 receptor type A and sense 5′-ACA TTC CTG TGC AAG GTG G-3′ and antisense 5′-CAG GGT GAA TCC GTA GCA GA-3′ for IL-8 receptor type B and performed without reverse transcriptase as a negative control (*N*). RT-PCR analysis revealed that PC-3P, PC-3P(Neo), and sense IL-8 transfectants (IL-8, IL-8 Low, and IL-8 High) (*A*), as well as PC-3M-LN4, PC-3M-LN4(Neo), and antisense IL-8 transfectants (AS IL-8, AS IL-8 Low, and AS IL-8 High) (*B*) express mRNA for both types of IL-8 receptors.

positive reaction. Control for endogenous alkaline phosphatase included treatment of the sample in the absence of the biotinylated probe and the use of chromogen alone.

Quantification of Color Reaction. Stained sections were examined in a Zeiss photomicroscope (Carl Zeiss, Thornwood, NY) equipped with a three-chip, charge-coupled device color camera (model DXC-969 MD; Sony Corp., Tokyo, Japan). The images were analyzed using the Optimas image analysis software (version 4.10; Bioscan, Bothell, WA). The slides were prescreened by one of the investigators to determine the range in staining intensity of the slides to be analyzed. Images covering the range of staining intensities were captured electronically, a color bar (montage) was created, and a threshold value was set in the red, green, and blue mode of the color camera. All subsequent images were quantified based on this threshold. The integrated absorbance of each field was determined based on its equivalence to the mean log inverse gray value multiplied by the area of the field. The samples were not counterstained; therefore, the absorbance was attributable solely to the product of the ISH reaction. Three different fields in each sample were quantified to derive an average value. The intensity of staining was determined by comparison with the integrated absorbance of poly $d(T)_{20}$. The results were presented as the number of cells for each cell line compared with the control, which was set to 100 (45).

IHC. For immunohistochemical analysis, frozen tissue sections (8-μm thick) were fixed with cold acetone. Tissue sections (5-μm thick) of formalin-fixed, paraffin-embedded specimens were deparaffinized in xylene, rehydrated in graded alcohol, and transferred to PBS. The slides were rinsed twice with PBS, antigen retrieval was performed with pepsin for 12 min, and endogenous peroxidase was blocked by the use of 3%

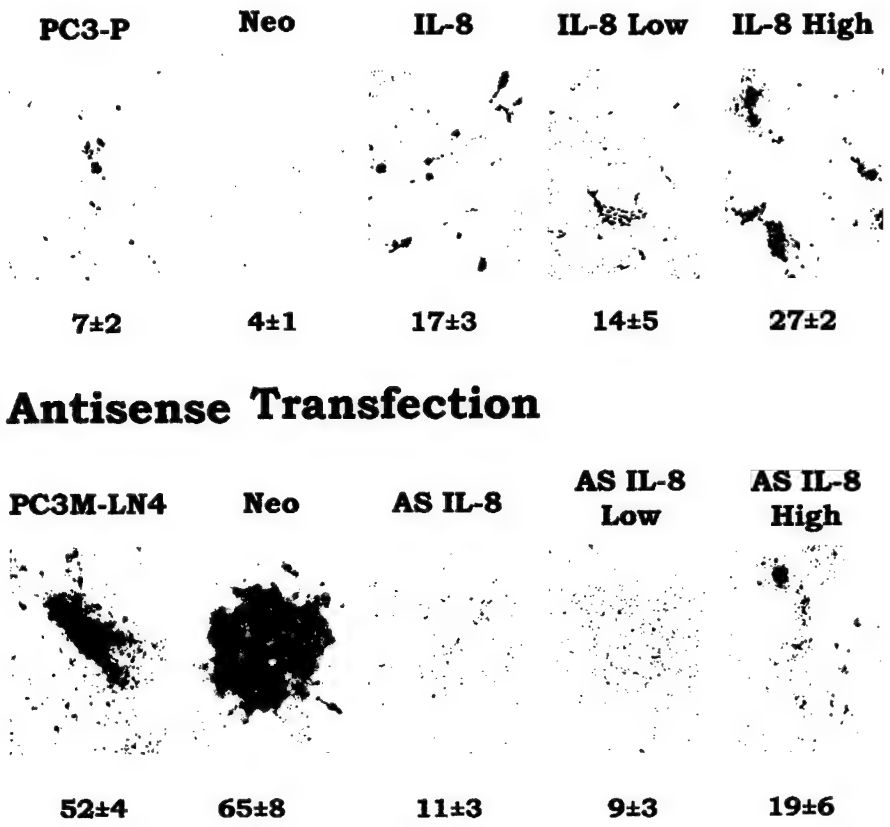

Fig. 6 Migration of cells (2×10^5) of sense transfectants (*A*) and antisense transfectants (*B*) through Matrigel-coated filters into fibroblast-conditioned medium as a source of chemoattractants, expressed as the average number of cells in the five highest spots identified within a single ×200 field on the lower surface of the filter. The number of migrated cells that penetrated through the Matrigel-coated filters increased 3.0- and 4.0-fold for the PC-3P(IL-8) and PC-3P(IL-8 High) cells, respectively ($P < 0.005$), whereas the numbers of cells migrating were markedly reduced in PC-3M-LN4(AS IL-8) and PC-3M-LN4(AS IL-8 Low) cells relative to controls, with 80 and 85% reductions, respectively ($P < 0.005$).

hydrogen peroxide in PBS for 12 min. The samples were washed three times with PBS and incubated for 20 min at room temperature with a protein-blocking solution of PBS (pH 7.5) containing 5% normal horse serum and 1% normal goat serum. Excess blocking solution was drained, and the samples were incubated for 18 h at 4°C with the appropriate dilution (1:100) of rat monoclonal anti-CD31 antibody (PharMingen, San Diego, CA; Ref. 54), a 1:50 dilution of a rabbit polyclonal anti-IL-8 antibody (Biosource International, Camarillo, CA), a 1:500 dilution of rabbit polyclonal anti-bFGF antibody (Sigma Chemical Co., St. Louis, MO), a 1:500 dilution of rabbit polyclonal anti-VEGF/VPF antibody (Santa Cruz Biotechnology, Santa Cruz, CA), or a 1:100 dilution of mouse monoclonal anti-MMP-9 antibody (Oncogene Research Products, Cambridge, MA). The samples were then rinsed four times with PBS and incubated for 60 min at room temperature with the appropriate dilution of the secondary antibody: peroxidase-conjugated anti-rat IgG (H+L) (Jackson ImmunoResearch Laboratory, Inc., West Grove, PA), antirabbit IgG, $F(ab)_2$ fragment (Jackson ImmunoResearch Laboratory, Inc.), or antimouse IgG1 (PharMingen, San Diego, CA). The slides were rinsed with PBS and incubated for 5 min with diaminobenzidine (Research Genetics). The sections were then washed three times with PBS, counterstained with Gill's hematoxylin (Biogenex Laboratories, San Ramon, CA), and again washed three times with PBS. The slides were mounted with Universal Mount mounting medium (Research Genetics).

Quantification of Microvessel Density. Microvessel density was determined by light microscopy after immunostaining frozen sections with anti-CD31 antibodies as described by Weidner *et al.* (55). Clusters of stained endothelial cells distinct from adjacent microvessels, tumor cells, or other stromal cells were counted as one microvessel. The tissue was recorded using a cooled CCD Optotronics Tec 470 camera (Optotronics Engineering, Goletha, CA) linked to a computer and digital printer (Sony Corp.). The density of microvessels was expressed as the average number of the five highest areas identified within a single ×200 field.

Quantification of Intensity of Immunostaining. The intensity of immunostaining of IL-8, bFGF, VEGF, and MMP-9 was quantitated in each sample by an image analyzer using the Optimas software program (Bioscan). Three different areas in each sample were quantified to yield an average measurement. The results were presented as the number of cells for each cell line compared with the control, which was set to 100 (45).

MMP-9 mRNA Half-Life Studies. To determine the effect of IL-8 on MMP-9 mRNA stability, PC-3P, PC-3P(Neo), and PC-3P(IL-8) cells and PC-3M-LN4, PC-3M-LN4(Neo), and

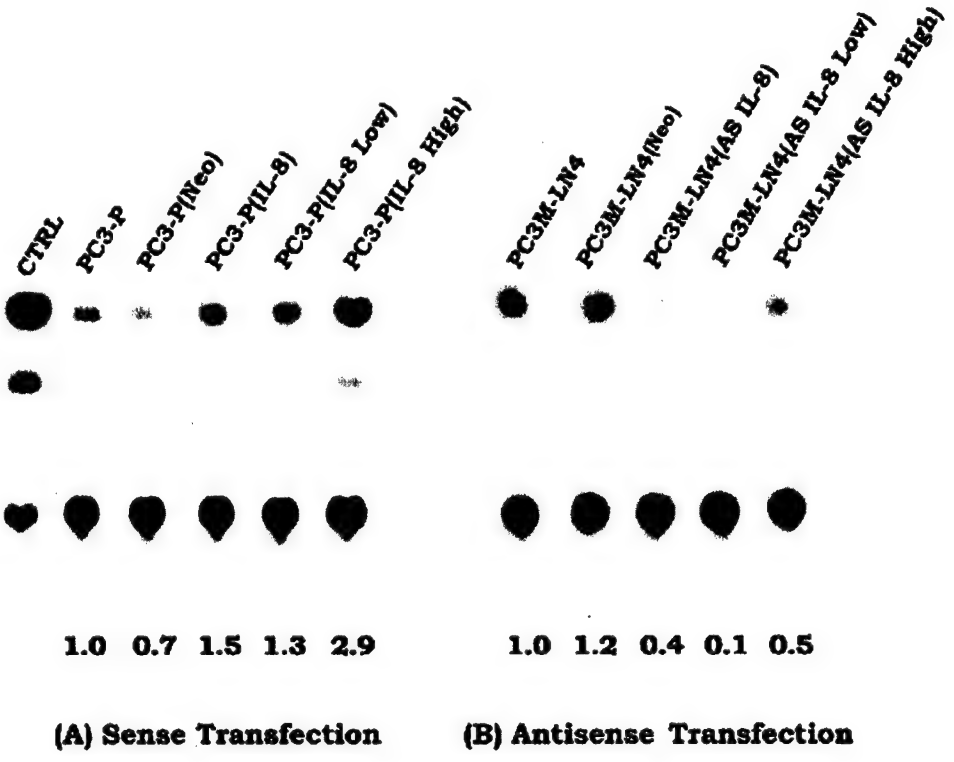

Fig. 7 Effect of IL-8 expression on CAT activity driven by the MMP-9 promoter in sense (*A*) and antisense (*B*) IL-8 transfectants. The CAT activity was evaluated as the ratio of acetylated species to all species. Differences in expression are shown as the ratio of CAT activity of transfectants to that of parental cells (defined as 1.0). CAT activity levels driven by MMP-9 promoter in PC-3P(IL-8) and PC-3P(IL-8 High) cells were increased 1.5- and 2.9-fold, respectively, compared with either PC-3P or PC-3P(Neo) and decreased 2.5- and 10.0-fold by PC-3M-LN4(AS IL-8) and PC-3M-LN4(AS IL-8 Low) cells, respectively, compared with either PC-3M-LN4 or PC-3M-LN4(Neo).

PC-3M-LN4(AS IL-8) cells were incubated for 24 h. Further transcription in the cells was then blocked by the addition of ActD (Calbiochem-Novabiotechnology, Inc., Lake Placid NY; final concentration, 5 μg/ml). Total RNA was extracted from the cells at 0, 1, 2, and 4 h after the addition of ActD, and MMP-9 mRNA expression was determined by Northern blot analysis. MMP-9 mRNA expression of each time point was compared with the control value (total RNA extracted from cells prior to ActD treatment was arbitrarily defined as 100%). The half-life of MMP-9 mRNA was determined by plotting relative MMP-9 mRNA expression levels on a semilogarithmic axis *versus* time (Cricket Software).

CAT Assay. Using the FuGENE 6 protocol (Boehringer Mannheim Corp.), we transfected with the basic CAT expression vector with no promoter/enhancer sequences (pCAT-basic) or a control plasmid with SV40 promoter and enhancer (pCAT-control; Promega Corp., Madison, WI) into PC-3P cells, sense-transfected PC-3P cells, PC-3M-LN4 cells, antisense-transfected PC-3M-LN4 cells, and each Neo transfectant. One copy of the full sequence human 570-bp MMP-9 promoter (a gift of Dr. Seiki Motoharu, University of Tokyo, Tokyo, Japan) was ligated upstream of the basic CAT expression vector. We transfected 5×10^3 cells/well in a six-well tissue culture dish with 2.5 μg of the reporter CAT constructs and 2.5 μg of a β-actin expression plasmid. After 48 h, extracts were prepared from all plates, normalized for β-actin activity, and assayed for CAT activity (56), as Hudson *et al.* (57) described previously. Each assay was repeated twice; there was <10% variation in transfection efficiency. The CAT assay was quantified by densitometry of autoradiographs with the use of the ImageQuant software program (Molecular Dynamics, Sunnyvale, CA) and was evaluated as the ratio of acetylated species to all species.

Statistical Analysis. The Mann-Whitney *U* test analyzed the statistical differences in vessel counts and staining intensity for IL-8, bFGF, VEGF, and MMP-9 of prostate tumors. The incidences of tumor and metastasis were statistically analyzed by χ^2 test. A value of $P < 0.05$ was considered significant.

RESULTS

***In Vitro* Expression of IL-8, bFGF, VEGF, and MMP-9.** Northern blot analysis for IL-8, bFGF, and VEGF steady-state gene expression by PC-3P, PC-3P(IL-8), PC-3P(IL-8 Low), PC-3P(IL-8 High), and PC-3P(Neo) is shown in Fig. 1*A*, and that by PC-3M-LN4, PC-3M-LN4(AS IL-8), PC-3M-LN4(AS IL-8 Low), PC-3M-LN4(AS IL-8 High), and PC-3M-LN4(Neo) is shown in Fig. 1*B*. The level of expression is shown as the ratio of mRNA expression by the transfectants to that by the corresponding parental and Neo transfectant cell lines (which in both cases was equivalent for all three factors). IL-8 mRNA expression levels were increased 10.4- and 15.1-fold higher in PC-3P(IL-8) and PC-3P(IL-8 High), respectively, than in either PC-3P or PC-3P(Neo), whereas there was no change in the mRNA expression of bFGF or VEGF. The mRNA expression levels of IL-8 in PC-3M-LN4(AS IL-8) and in PC-3M-LN4(AS IL-8 Low) were only about one-fifth and one-tenth of those for either PC-3M-LN4 or PC-3M-LN4(Neo), respectively, whereas there was no change in the mRNA expression of bFGF or VEGF. IL-8, bFGF, and VEGF protein production by PC-3P, PC-3M-LN4, and the transfected cell lines was evaluated by

Table 1 Tumorigenicity and production of spontaneous metastases after orthotopic implantation of PC-3P, PC-3P(Neo), and sense IL-8 transfectants and of PC-3M-LN4, PCM-LN4 (AS Neo), and antisense IL-8 transfectant in prostate of nude mice

Cell line	Tumorigenicity		Lymph node metastasis	
	Incidence	Median prostate weight (range) (mg)	Incidence	Median lymph node weight (range) (mg)
Sense transfection				
PC-3P	4/7	55 (24–480)	4/7	20 (16–28)
PC-3P(Neo)	6/9	120 (27–443)	4/9	24 (15–32)
PC-3P(IL-8)	8/8[a]	1,270 (258–1,850)[b]	8/8[a]	93 (36–124)[b]
PC-3P(IL-8 Low)	5/8	155 (25–720)	5/8	38 (25–69)
PC-3P(IL-8 High)	9/9[a]	1,975 (355–2,915)[b]	9/9[a]	131 (55–188)[b]
Antisense transfection				
PC-3M-LN4	5/5	1,921 (250–3,359)	5/5	101 (19–155)
PC-3M-LN4(AS Neo)	5/5	543 (312–713)	5/5	110 (24–122)
PC-3M-LN4(AS IL-8)	2/8[c,d]	(33, 36)[d,e]	0/8[f]	
PC-3M-LN4(AS IL-8 Low)	2/8[c,d]	(31, 39)[d,e]	0/8[f]	
PC-3M-LN4(AS IL-8 High)	6/9	39 (30–525)[f]	0/9[f]	

[a] $P < 0.05$ against PC-3P and PC-3P Neo (χ^2 test).
[b] $P < 0.005$ against PC-3P and PC-3P(Neo) (Mann-Whitney statistical comparison).
[c] $P < 0.05$.
[d] Explants grown in culture; no detectable tumor by immunohistochemistry.
[e] $P < 0.0005$ against PC-3M-LN4 and PC-3M-LN4(As Neo) (Mann-Whitney statistical comparison).
[f] $P < 0.0005$ against PC-3M-LN4 and PC-3M-LN4(As Neo) (χ^2 test).

Table 2 The mRNA expression level, protein expression level, and MVD in prostate tumor with PC-3P, PC-3P(Neo), and sense IL-8 transfectants and with PC-3M-LN4, PC-3M-LN4 (AS Neo), and antisense IL-8 transfectants

Cell line	mRNA expression index[a]				Protein expression index[b]				Microvessel density[c] (per ×200 field)
	IL-8	bFGF	VEGF	MMP-9	IL-8	BFGF	VEGF	MMP-9	
Sense transfection									
PC-3P	100	100	100	100	100	100	100	100	40 ± 9
PC-3P(Neo)	117	98	99	119	108	96	105	117	45 ± 6
PC-3P(IL-8)	288	99	94	295	300	100	100	275	51 ± 12[d]
PC-3P(IL-8 Low)	182	100	96	178	215	96	111	192	80 ± 13
PC-3P(IL-8 High)	371	102	96	349	275	104	105	275	91 ± 18[d]
Antisense transfection									
PC-3M-LN4	100	100	100	100	100	100	100	100	100 ± 20
PC-3M-LN4(AS Neo)	101	101	97	102	100	102	96	96	104 ± 23
PC-3M-LN4(AS IL-8 High)	58	98	94	68	57	102	100	67	47 ± 14[e]

[a] The intensity of the cytoplasmic color reaction was quantified by an image analyzer and compared with maximal intensity of poly d(T) color reaction in each sample. The results were presented as the number of calls for each line with PC-3P and PC-3M-LN4 defined as 100.
[b] The intensity of the cytoplasmic immunostaining was quantified by an image analyzer in three different areas of each sample to yield an average measurement and compared with the intensity of the normal epithelial cells of prostate glands and adjusted to the intensity of the cells of the tumors with parental cell line defined as 100.
[c] MVD was expressed as an average number of five highest areas identified within a single ×200 field.
[d] $P < 0.005$ against PC-3P and PC-3P(Neo).
[e] $P < 0.005$ against PC-3M-LN4 and PC-3M-LN4 and PC-3M-LN4(As Neo) (Mann-Whitney statistical comparison).

ELISA (Fig. 2.). Changes in protein expression by the transfectants paralleled the changes seen in mRNA expression. IL-8 expression levels were 3.0- and 4.0-fold higher in the PC-3P(IL-8) and PC-3P(IL-8 High) cells, respectively, than in the PC-3P parental cell line. PC-3M-LN4(AS IL-8) and PC-3M-LN4(AS IL-8 Low) cell lines were only one-quarter and one-tenth of those in the parental PC-3M-LN4 cells, respectively. bFGF and VEGF protein expression levels were unchanged in all cell lines after transfection.

Metalloproteinase Expression after IL-8 Transfection. Because IL-8 regulates protease activity by human melanoma, we evaluated whether MMP-9 expression was altered in the PC-3P and PC-3M-LN4 cells by transfection with sense or antisense IL-8 transcripts. Fig. 1 shows that MMP-9 mRNA expression levels were 3.0- and 6.0-fold higher in PC-3P(IL-8) and PC-3P(IL-8 High) cells, respectively, compared with their controls, but the values for both PC-3M-LN4(AS IL-8) and PC-3M-LN4(AS IL-8 Low) cells were only one-third of that of their controls. These results demonstrate that IL-8 regulates MMP-9 mRNA expression by the PC-3P and PC-3M-LN4 human prostate cancer cells. Our results are consistent with reports that IL-8 regulates MMP expression by malignant melanoma (31, 32).

Collagenase Activity. To demonstrate that MMP-9 expressed by the transfected cells is biologically active, collagenase activity of the transfected cells was determined by zymog-

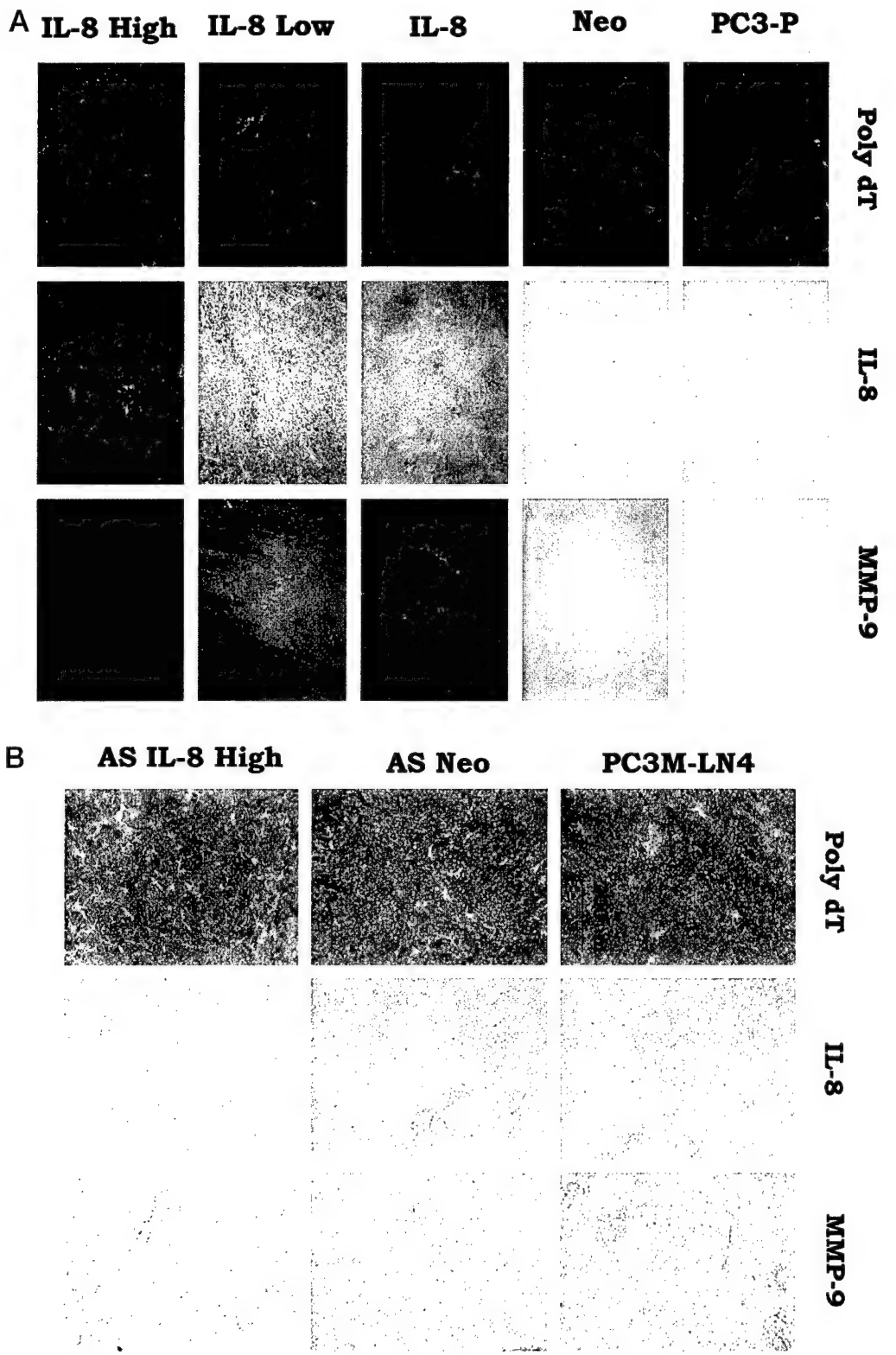

Fig. 8 ISH in PC-3P, Neo transfectant PC-3P(Neo), and sense IL-8 transfectants PC-3P(Neo) and sense IL-8 transfectants PC-3P(IL-8), PC-3P(IL-8 Low), and PC-3P(IL-8 High) (*A*), and in PC-3M-LN4, Neo transfectant PC-3M-LN4(Neo), and antisense IL-8 transfectants PC-3M-LN4(AS IL-8), PC-3M-LN4(AS IL-8 Low), and PC-3M-LN4(AS IL-8 High) (*B*). The intensity of staining was determined by comparison with the integrated absorbance of poly $d(T)_{20}$, which was set to 100. The mRNA expression of IL-8 and MMP-9 was increased 2.5- and 3.0-fold in the tumor of PC-3P(IL-8) and PC-3P(IL-8 High) relative to PC-3P or PC-3P(Neo), respectively. The tumor of PC-3M-LN4(AS IL-8 High) showed a 40% reduction in the mRNA expression of IL-8 and a 30% reduction in the mRNA expression of MMP-9 relative to that of either parental PC-3M-LN4 or PC-3M-LN4(Neo).

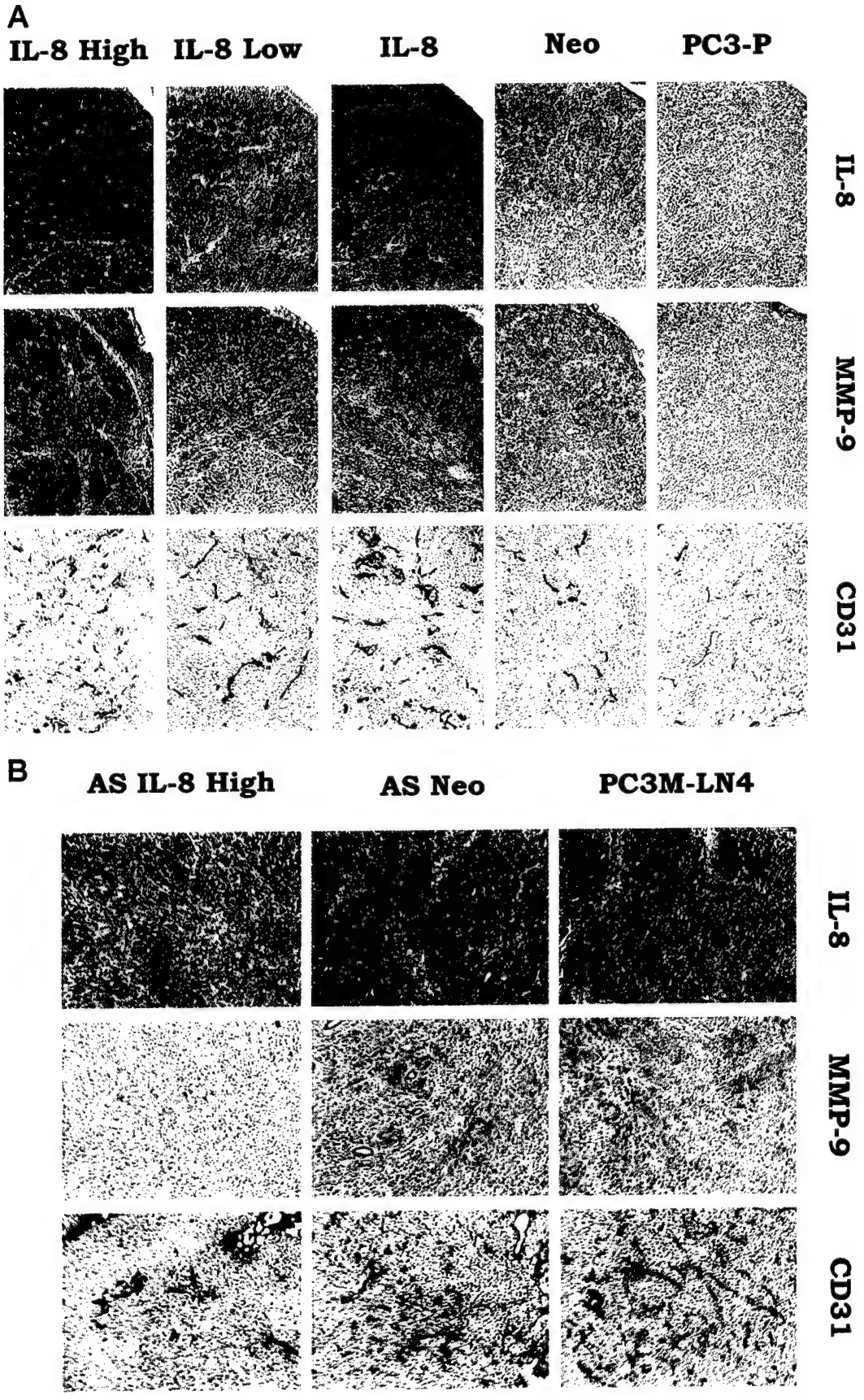
A
IL-8 High
IL-8 Low
IL-8
Neo
PC3-P
IL-8
MMP-9
CD31
B
AS IL-8 High
AS Neo
PC3M-LN4
IL-8
MMP-9
CD31

raphy after normalizing the volume of supernatant for cell number (Fig. 3). By densitometry, the collagenase activity of PC-3P(IL-8) and PC-3P(IL-8 High) cells was increased 6.0- and 7.0-fold, compared with either PC-3P or PC-3P(Neo) (Fig. 3*A*), respectively, whereas that of PC-3M-LN4(AS IL-8) and PC-3M-LN4(AS IL-8 Low) was decreased 2.5- and 5.0-fold compared with either PC-3M-LN4 or PC-3M-LN4(Neo), respectively (Fig. 3*B*).

We next analyzed whether the increase in MMP-9 activity is mediated by IL-8 (Fig. 4). To that end, parental PC-3P cells were incubated in the presence of different doses of human rIL-8, and the activity of MMP-9 was determined by zymography after normalizing the volume of supernatant for cell number. The results shown in Fig. 4*A* indicate that IL-8 caused an increase in the activity of MMP-9. Moreover, the increased activity of MMP-9 by rIL-8 was inhibited by neutralization with anti-IL-8 antibody (Fig. 4*B*).

RT-PCR Analysis. RT-PCR analysis revealed that PC-3P, PC-3P(Neo), and sense IL-8 transfectants (IL-8, IL-8 Low, and IL-8 High; Fig. 5*A*), as well as PC-3M-LN4, PC-3M-LN4(Neo), and antisense IL-8 transfectants (AS IL-8, AS IL-8 Low, and AS IL-8 High; Fig. 5*B*), express mRNA for both IL-8 receptors.

Invasion Assay through Matrigel. We next analyzed whether the expression of MMP-9 and collagenase activity by the IL-8-transfected cells correlated with invasion through the basement membrane. PC-3P(IL-8) and PC-3P(IL-8 High) cells exhibited increased invasion through Matrigel-coated filters, with 3.0- and 4.0-fold increases, compared with either PC-3P or PC-3P(Neo) ($P < 0.005$), respectively (Fig. 6*A*). Invasion by PC-3M-LN4(AS IL-8) and PC-3M-LN4(AS IL-8 Low) was 80 and 85% lower, compared with invasion by PC-3M-LN4 or PC-3M-LN4(Neo) ($P < 0.005$), respectively (Fig. 6*B*).

CAT Activity. The full-sequence MMP-9 promoter was linked upstream of the CAT reporter gene and transfected into PC-3P, PC-3M-LN4, sense IL-8 transfected, antisense IL-8 transfected, and the Neo-transfected cells to examine the effect of IL-8 expression on MMP-9 transcription. Forty-eight h after transfection, cell extracts were prepared, and equivalent amounts of extracts exhibiting the same β-actin activity were tested for CAT activity. CAT activity driven by MMP-9 promoter in PC-3P(IL-8) and PC-3P(IL-8 High) was increased 1.5- and 2.9-fold (Fig. 7*A*) compared with either PC-3P or PC-3P(Neo), respectively, and decreased 2.5- and 10.0-fold by PC-3M-LN4(AS IL-8) and PC-3M-LN4(AS IL-8 Low) (Fig. 7*B*) compared with either PC-3M-LN4 or PC-3M-LN4(Neo), respectively. CAT activity driven by the SV40 promoter was the same in both cell populations and served as an additional internal control for transfection efficiency. Next, the stability of MMP-9 mRNA was investigated by examining its half-life. The half-life of MMP-9 mRNA of PC-3P(IL-8) was similar to that of PC-3P or PC-3P(Neo), and that of PC-3M-LN4(AS IL-8) was similar to that of PC-3M-LN4 or PC-3M-LN4(Neo) (data not shown).

Tumorigenicity and Production of Metastasis. To evaluate whether IL-8 expression regulates tumorigenicity and metastasis of androgen-independent prostate cancer, we implanted PC-3P, PC-3M-LN4, Neo-transfected, and the IL-8 sense- and antisense-transfected cells into the prostate of athymic nude mice and evaluated tumor growth and metastasis 6 weeks later (Table 1). The PC-3P(IL-8) and PC-3P(IL-8 High) tumors were larger than the PC-3P and PC-3P(Neo) tumors [mean weight (range; *P*): 1270 mg (258–1850 mg; $P < 0.005$) and 1975 mg (355–2915 mg; $P < 0.005$) *versus* 55 mg (24–480 mg) and 120 mg (27–443 mg)]. Moreover, the incidences of spontaneous lymph node metastasis, as well as tumor burden within the metastatic lymph nodes, were significantly greater for the PC-3P(IL-8) and PC-3P(IL-8 High) cell lines than for the PC-3P and PC-3P(Neo) [incidences: 8 of 8, 9 of 9, 4 of 7, 4 of 9, respectively ($P < 0.05$); mean lymph node weight (range): 93 mg (36–124 mg), 131 mg (55–188 mg), 20 mg (16–28 mg), and 24 mg (15–32 mg), respectively; $P < 0.005$]. Conversely, the tumorigenicity of PC-3M-LN4 was significantly inhibited when IL-8 expression was reduced by antisense IL-8 transfection. Only two of eight mice implanted with PC-3M-LN4(AS IL-8) (tumor weights, 33 and 36 mg) and PC-3M-LN4(AS IL-8 Low) (tumor weights, 31 and 39 mg) developed tumors at 6 weeks ($P < 0.01$) compared with the mice implanted with PC-3M-LN4 and PC-3M-LN4(Neo). These tumors were not apparent histologically but grew out as tissue explants in culture. Tumorigenicity was also inhibited in PC-3M-LN4(AS IL-8 High), but this difference did not reach statistical significance. There was a significant reduction in spontaneous lymph node metastases at 6 weeks in mice implanted with PC-3M-LN4(AS IL-8), PC-3M-LN4(AS IL-8 Low), or PC-3M-LN4(AS IL-8 High) (no mice developed metastasis) compared with mice implanted either PC-3M-LN4 or PC-3M-LN4(Neo) (all mice developed metastasis; $P < 0.0005$). Therefore, IL-8 expression by PC-3P and PC-3M-LN4 regulates both tumorigenicity and metastasis in androgen-independent prostate cancer.

Fig. 9 IHC and MVD in PC-3P, Neo transfectant PC-3P(Neo), sense IL-8 transfectants PC-3P(Neo) and sense IL-8 transfectants PC-3P(IL-8), PC-3P(IL-8 Low), and PC-3P(IL-8 High) (*A*) and in PC-3M-LN4, Neo transfectant PC-3M-LN4(Neo), and antisense IL-8 transfectants PC-3M-LN4(AS IL-8), PC-3M-LN4(AS IL-8 Low), and PC-3M-LN4(AS IL-8 High) (*B*). Three different areas in each sample were quantified to obtain an average measurement of intensity of immunostaining. The density of microvessels was expressed as the average of the five highest area identified within a single ×200 field. The protein expressions of IL-8 and MMP-9 were increased 2.5- and 3.0-fold in the tumor of PC-3P(IL-8) relative to that of either parental PC-3P or PC-3P(Neo), respectively. The tumor of PC-3M-LN4(AS IL-8 High) showed a 40% reduction in the protein expression of IL-8 and a 30% reduction in the protein expression of MMP-9 relative to that of either PC-3M-LN4 or PC-3M-LN4(Neo). The number of $CD31^+$ microvessels counted per ×200 field in prostate tumors of PC-3P(IL-8) cells was increased from 40 ± 9 or 45 ± 6 in the tumors of parental PC-3P or PC-3P(Neo) to 80 ± 13 and 91 ± 18 in that of PC-3P(IL-8) and PC-3P(IL-8 High) cells, respectively ($P < 0.005$). The number of $CD31^+$ microvessels was reduced from 100 ± 20 or 104 ± 23 in the tumors of parental PC-3M-LN4 or PC-3M-LN4(Neo), respectively, to 47 ± 14 in that of PC-3M-LN4(AS IL-8 High) cells ($P < 0.005$).

***In Vivo* Expression of IL-8, bFGF, VEGF, and MMP-9.** IL-8, bFGF, VEGF, and MMP-9 mRNA and protein were evaluated by ISH (Table 2; Fig. 8) and IHC (Table 2; Fig. 9), respectively. The mRNA and protein expressions of IL-8 and MMP-9 were increased 2.5- and 3.0-fold in the PC-3P(IL-8) and PC-3P(IL-8 High) tumors, respectively, relative to either PC-3P or PC-3P(Neo). The PC-3M-LN4(AS IL-8 High) tumors showed a 42% reduction in the mRNA and protein expression of IL-8 and a 33% reduction in the mRNA and protein expression of MMP-9 relative to either PC-3M-LN4 or PC-3M-LN4(Neo) tumors. There was no change in the mRNA and protein expression of bFGF or VEGF in the IL-8-transfected tumors.

Tumor Angiogenesis. Tumor-induced neovascularization (as indicated by MVD) was determined by IHC using anti-CD31 antibodies (Table 2; Fig. 9). The numbers of $CD31^+$ microvessels counted per ×200 field were 40 ± 9 and 45 ± 6 in PC-3P and PC-3P(Neo), respectively, compared with 80 ± 13 and 91 ± 18 in PC-3P(IL-8) and PC-3P(IL-8 High), respectively ($P < 0.005$). Conversely, antisense IL-8 transfection of PC-3M-LN4 significantly decreased MVD from 100 ± 20 and 104 ± 23 in the PC-3M-LN4 and PC-3M-LN4(Neo) tumors, respectively, to 47 ± 14 in the PC-3M-LN4(AS IL-8 High) tumors ($P < 0.005$; Table 2; Fig. 9). Because the PC-3M-LN4(IL-8) and PC-3M-LN4(AS IL-8 Low) cells grew only as explants in tissue culture, we could not evaluate MVD. These studies indicate that tumor-induced neovascularization correlates directly with IL-8 expression, tumorigenicity, and metastasis.

DISCUSSION

Prostate cancer growth and metastasis depend upon the ability of the cancer to induce its own blood supply (18, 21, 23). This process of angiogenesis depends on the outcome between stimulatory and inhibitory regulation by the tumor and its microenvironment (14–16). Human prostate cancer express a number of angiogenesis factors including VEGF (17, 18, 58), bFGF (19, 20), and IL-8 (18, 21, 22, 33). The metastatic potential of the LNCaP prostate cancer cell line correlates with VEGF (58), and that of the PC-3 lineage with bFGF and IL-8 expression (19, 21). Recently, Moore *et al.* (33) provided direct evidence that IL-8 regulates the growth of PC-3. They reported that neutralizing antibodies to IL-8 reduced the angiogenic activity of PC-3 homogenates and inhibited tumor growth after ectopic implantation in SCID mice, suggesting that the growth inhibition seen after treatment with IL-8 neutralizing antibodies is secondary to inhibition of tumor-induced angiogenesis. The present study provides direct evidence for the role of IL-8 in regulating tumor-induced neovascularization and subsequent growth of human prostate cancer implanted within the prostate of athymic nude mice. Our results are similar to those reported by Luca *et al.* (32), who enforced the expression of IL-8 in the SB-2 melanoma cell line by sense transfection and demonstrated that IL-8 regulated tumorigenicity in human melanoma.

We enforced IL-8 expression by transfecting the poorly tumorigenic and poorly metastatic human prostate cancer cell line PC-3P (which expresses relatively low levels of IL-8) with the sense IL-8 construct and were able to establish several cell lines that overexpress IL-8 relative to the original PC-3P cell line. These sense IL-8-transfected cells demonstrated enhanced tumor growth and metastasis compared with the PC-3P or PC-3P(Neo) cells and demonstrated enhanced tumor-induced neovascularization, growth within the prostate, and spontaneous metastasis to the lymph nodes. Conversely, after antisense IL-8 transfection, we were able to reduce IL-8 expression by the highly tumorigenic and metastatic PC-3M-LN4 cell line (which expresses relatively high levels of IL-8) and to inhibit tumor-induced neovascularization, growth within the prostate, and metastasis. Because neither bFGF nor VEGF expression was altered by IL-8 transfection, we conclude that these effects are independent of the activity of these angiogenesis factors. Because IL-8 transfection did not affect *in vitro* proliferation of PC-3P or PC-3M-LN4, the effects on growth and metastasis are independent of proliferation, although the cells do have both type A (CXCR1; Refs. 59 and 60) and type B (CXCR2; Refs. 59 and 60) of the IL-8 receptors. Therefore, our results provide evidence for the involvement of IL-8 in the induction of *in vivo* angiogenesis and in the subsequent growth and metastasis of prostate cancer. These results are similar to previous reports in which transfection with VEGF or bFGF increased MVD and enhanced tumor growth and metastasis of melanoma and breast cancer (61–63). However, because of the differences in tumor size between control and IL-8 sense and antisense transfectants, the difference in tumor-induced angiogenesis and in metastatic potential may reflect tumor size.

The metastatic potential of prostate cancer depends upon the expression of several metastasis-related genes, such as *IL-8,* that regulate endothelial cell proliferation and capillary morphogenesis (28), and other genes, such as *MMP-9,* that regulate the degradation of the extracellular matrix (35, 64). The local production of MMP-9 or other proteases, such as plasminogen activator, by prostate cancer cells or stroma facilitates the local degradation of the extracellular matrix and results in tumor invasion and subsequent metastasis (35, 64–66). The proteolytic effect of MMPs facilitates the migration of endothelial cells through the altered extracellular matrix toward the source of the angiogenic stimulus; in this manner, MMPs are an integral component of the angiogenesis pathway. The highly metastatic PC-3M-LN4 expresses high levels of MMP-9 compared with the poorly metastatic PC-3P cell line. Recently, Luca *et al.* (32) reported that IL-8 regulates MMP-2 activity by malignant melanoma cells. They transfected the melanoma cell line SB-2 with the sense IL-8 transcript and up-regulated MMP-2 expression and collagenase activity. They considered this up-regulation of collagenase activity to be an important mechanism that explained the associated increase in metastatic ability demonstrated by the sense-transfected SB-2 cells. Similarly, we found that the activity of both MMP-9 by human prostate cancer cells directly correlated with their expression of IL-8. Moreover, when we altered the expression of IL-8 by sense or antisense transfection, we observed a corresponding change in MMP-9 expression and activity both *in vitro* and *in vivo*. The MMP-9 induced by sense transfection was biologically active, because it increased collagenase activity and increased cellular invasion through Matrigel. When MMP-9 activity was reduced after antisense transfection, both collagenase activity and invasion through Matrigel decreased. The altered local growth of the antisense-transfected tumors may reflect a relative growth inhibition secondary to the inability to induce a robust microcircu-

lation, whereas the loss of metastatic potential may be attributable to both a decrease in the tumor-induced neovascularization by IL-8 and a reduction in invasion attributable to the reduction in MMP-9 activity. Conversely, increased IL-8 expression by the sense IL-8-transfected prostate cancer cells may explain their enhanced tumorigenicity, whereas both increased IL-8 and MMP expression may contribute to their increased metastatic potential. Because these experiments were conducted in athymic nude mice, they do not address the well-established role of IL-8 in tumor immunity (25).

MMP-9 expression is regulated by both transcriptional and posttranscriptional events. Whereas bFGF and VEGF regulate the transcription of MMP-9 through activation of Ets-1 and Ets-2 binding sites in the promoter (67, 68), transforming growth factor-β1 up-regulates MMP-9 by increasing mRNA stability (37). IL-8 probably regulates MMP-9 expression at the level of transcription. We evaluated MMP-9 mRNA stability and the level of gene transcription of MMP-9 in IL-8 transfectants and control cells. Although the expression of MMP-9 mRNA varied among the IL-8 transfectants and controls, the stability of MMP-9 mRNA was not changed by transfection with sense or antisense IL-8. However, CAT activity driven by the MMP-9 promoter was up-regulated in IL-8 sense transfectants and down-regulated after antisense transfection. bFGF regulates MMP-9 expression in human bladder cancer. Because bFGF levels were not affected by IL-8 transfection, the regulation of MMP-9 transcription in PC-3P and PC-3M-LN4 cells is independent of bFGF and likely regulated by IL-8. These results are in keeping with the report of Luca *et al.* (32), who found that IL-8 regulated *MMP-2* gene transcription.

In summary, our present study demonstrates that IL-8 regulates angiogenesis, tumorigenesis, MMP-9 expression, and metastasis by androgen-independent human prostate cancer. This effect may be mediated, in part, by the regulation of the expression and activity of MMP-9.

REFERENCES

1. Greenlee, R. T., Murray, T., Bolden, S., and Wingo, P. A. Cancer statistics, 2000. CA Cancer J. Clin., *50:* 7–33, 2000.

2. Thompson, I. M., and Zeidman, E. J. Current urological practice: routine urological examination and early detection of carcinoma of the prostate. J. Urol., 326–330, 1992.

3. Powell, I. J., Heilbrun, L., Littrup, P. L., Franklin, A., Parzuchowski, J., Gelfand, D., and Sakr, W. Outcome of African American men screened for prostate cancer: the Detroit Education and Early Detection Study. J. Urol., *158:* 146–149, 1997.

4. Catalona, W. J., Smith, D. S., Ratliff, T. L., and Basler, J. W. Detection of organ-confined prostate cancer is increased through prostate-specific antigen-based screening [see comments]. J. Am. Med. Assoc., *270:* 948–954, 1993.

5. Catalona, W. J., Richie, J. P., Ahmann, F. R., Hudson, M. A., Scardino, P. T., Flanigan, R. C., deKernion, J. B., Ratliff, T. L., Kavoussi, L. R., Dalkin, B. L., *et al.* Comparison of digital rectal examination and serum prostate specific antigen in the early detection of prostate cancer: results of a multicenter clinical trial of 6,630 men [see comments]. J. Urol., *151:* 1283–1290, 1994.

6. Kreis, W. Current chemotherapy and future directions in research for the treatment of advanced hormone-refractory prostate cancer. Cancer Investig., *13:* 296–312, 1995.

7. Crissman, J. D. Tumor-host interactions as prognostic factors in the histologic assessment of carcinomas. Pathol. Annu., *1:* 29–52, 1986.

8. Dickson, R. B. Regulation of tumor-host interactions in breast cancer. J. Steroid Biochem. Mol. Biol., *41:* 389–400, 1992.

9. Fidler, I. J. Origin and biology of cancer metastasis. Cytometry, *10:* 673–680, 1989.

10. Fidler, I. J. Critical factors in the biology of human cancer metastasis: twenty-eighth G. H. A. Clowes memorial award lecture. Cancer Res., *50:* 6130–6138, 1990.

11. Fidler, I. J. Critical determinants of melanoma metastasis. J. Investig. Dermatol. Symp. Proc., *1:* 203–208, 1996.

12. Fidler, I. J., Kumar, R., Bielenberg, D. R., and Ellis, L. M. Molecular determinants of angiogenesis in cancer metastasis. Cancer J. Sci. Am., S58–S66, 1998.

13. Kumar, R., and Fidler, I. J. Angiogenic molecules and cancer metastasis. In Vivo, *12:* 27–34, 1998.

14. Folkman, J. Tumor angiogenesis. Adv. Cancer Res., *43:* 175–203, 1985.

15. Folkman, J. How is blood vessel growth regulated in normal and neoplastic tissue? G. H. A. Clowes memorial award lecture. Cancer Res., *46:* 467–473, 1986.

16. Folkman, J. What is the evidence that tumors are angiogenesis dependent? J. Natl. Cancer Inst., *82:* 4–6, 1990.

17. Jackson, M. W., Bentel, J. M., and Tilley, W. D. Vascular endothelial growth factor (VEGF) expression in prostate cancer and benign prostatic hyperplasia [see comments]. J. Urol., *157:* 2323–2328, 1997.

18. Ferrer, F. A., Miller, L. J., Andrawis, R. I., Kurtzman, S. H., Albertsen, P. C., Laudone, V. P., Kreutzer, D. L. Angiogenesis and prostate cancer: in vivo and in vitro expression of angiogenesis factors by prostate cancer cells. Urology, *51:* 161–167, 1998.

19. Nakamoto, T., Chang, C. S., Li, A. K., Chodak, G. W. Basic fibroblast growth factor in human prostate cancer cells. Cancer Res., *52:* 571–577, 1992.

20. Cronauer, M. V., Hittmair, A., Eder, I. E., Hobisch, A., Culig, Z., Ramoner, R., Zhang, J., Bartsch, G., Reissigl, A., Radmayr, C., Thurnher, M., Klocker, H. Basic fibroblast growth factor levels in cancer cells and in sera of patients suffering from proliferative disorders of the prostate. Prostate, *31:* 223–233, 1997.

21. Greene, G. F., Kitadai, Y., Pettaway, C. A., von Eschenbach, A., Bucana, C. D., Fidler, I. J. Correlation of metastasis-related gene expression with metastatic potential in human prostate carcinoma cells implanted in nude mice using an in situ messenger RNA hybridization technique. Am. J. Pathol., *150:* 1571–1582, 1997.

22. Veltri, R. W., Miller, M. C., Zhao, G., Ng, A., Marley, G. M., Wright, F. L., Jr., Vessella, F. L., Ralph, D. Interleukin-8 serum levels in patients with benign prostatic hyperplasia and prostate cancer. Urology, *53:* 139–147, 1999.

23. Weidner, N., Carroll, P. R., Flax, J., Blumenfeld, W., Folkman, J. Tumor angiogenesis correlates with metastasis in invasive prostate carcinoma. Am. J. Pathol., *143:* 401–409, 1993.

24. Matsushima, K., Morishita, K., Yoshimura, T., Lavu, S., Kobayashi, Y., Lew, W., Appella, E., Kung, H. F., Leonard, E. J., Oppenheim, J. J. Molecular cloning of a human monocyte-derived neutrophil chemotactic factor (MDNCF) and the induction of MDNCF mRNA by interleukin 1 and tumor necrosis factor. J. Exp. Med., *167:* 1883–1893, 1988.

25. Matsushima, K., Baldwin, E. T., Mukaida, N. Interleukin-8 and MCAF: novel leukocyte recruitment and activating cytokines. Chem. Immunol., *51:* 236–265, 1992.

26. Wang, J. M., Taraboletti, G., Matsushima, K., Van, D. J., Mantovani, A. Induction of haptotactic migration of melanoma cells by neutrophil activating protein/interleukin-8. Biochem. Biophys. Res. Commun., *169:* 165–170, 1990.

27. Krueger, G., Jorgensen, C., Miller, C., Schroeder, J., Sticherling, M., Christopher, E. Effect of IL-8 on epidermal proliferation. J. Invest. Dermatol., *94:* 545, 1990.

28. Kumar, R., Yoneda, J., Bucana, C. D., Fidler, I. J. Regulation of distinct steps of angiogenesis by different angiogenic molecules. Int. J. Oncol., *12:* 749–757, 1998.

29. Smith, D. R., Polverini, P. J., Kunkel, S. L., Orringer, M. B., Whyte, R. I., Burdick, M. D., Wilke, C. A., Strieter, R. M. Inhibition of interleukin 8 attenuates angiogenesis in bronchogenic carcinoma. J. Exp. Med., *179:* 1409–1415, 1994.

30. Arenberg, D. A., Kunkel, S. L., Polverini, P. J., Glass, M., Burdick, M. D, Strieter, R. M. Inhibition of interleukin-8 reduces tumorigenesis of human non-small cell lung cancer in SCID mice. J. Clin. Invest., *97:* 2792–2802, 1996.

31. Singh, R. K., Gutman, M., Radinsky, R., Bucana, C. D., Fidler, I. J. Expression of interleukin 8 correlates with the metastatic potential of human melanoma cells in nude mice. Cancer Res., *54:* 3242–3247, 1994.

32. Luca, M., Huang, S., Gershenwald, J. E., Singh, R. K., Reich, R., Bar-Eli, M. Expression of interleukin-8 by human melanoma cells up-regulates MMP-2 activity and increases tumor growth and metastasis. Am. J. Pathol., *151:* 1105–1113, 1997.

33. Moore, B. B., Arenberg, D. A., Stoy, K., Morgan, T., Addison, C. L., Morris, S. B., Glass, M., Wilke, C., Xue, Y. Y., Sitterding, S., Kunkel, S. L., Burdick, M. D., Strieter, R. M. Distinct CXC chemokines mediate tumorigenicity of prostate cancer cells. Am. J. Pathol., *154(5):* 1503–1512, 1999.

34. Stearns, M. E. In situ hybridization studies of metalloproteinases 2 and 9 and TIMP-1 and TIMP-2 expression in human prostate cancer. Clin. Exp. Metastasis., *15:* 246–258, 1997.

35. Hamdy, F. C., Fadlon, E. J., Cottam, D., Lawry, J., Thurrell, W., Silcocks, P. B., Anderson, J. D., Williams, J. L., Rees, R. C. Matrix metalloproteinase 9 expression in primary human prostatic adenocarcinoma and benign prostatic hyperplasia. Br. J. Cancer, *69:* 177–182, 1994.

36. Moses, M. A., Wiederschain, D., Loughlin, K. R., Zurakowski, D., Lamb, C. C., Freeman, M. R. Increased incidence of matrix metalloproteinases in urine of cancer patients. Cancer Res., *1:* 1395–1399, 1998.

37. Still, K., Robson, C. N., Autzen, P., Robinson, M. C., Hamdy, F. C. Localization and quantification of mRNA for matrix metalloproteinase-2 (MMP-2) and tissue inhibitor of matrix metalloproteinase-2 (TIMP-2) in human benign and malignant tissue. Prostate, *42:* 18–25, 2000.

38. Sehgal, I., Thompson, T. C. Novel regulation of type IV collagenase (matrix metalloproteinase-9 and –2) activities by transforming growth factor-β1 in human prostate cancer cell lines. Mol. Biol. Cell, *10:* 407–416, 1999.

39. Pettaway, C. A., Pathak, S., Greene, G., Ramirez, E., Wilson, M. R., Killion, J. J., and Fidler, I. J. Selection of highly metastatic variants of different human prostatic carcinomas using orthotopic implantation in nude Mice. Clin. Cancer Res., *2:* 1627–1636, 1996.

40. Kozlowski, J. M., Fidler, I. J., Campbell, D., Zuo-liang, X., Kaighn, M. E., and Hart, I. R. Metastatic behavior of human tumor cell lines grown in the nude mouse. Cancer Res., *44:* 3522–3529, 1984.

41. Rogelj, S., Weinberg, R. A., Fanning, P., and Klagsbrun, M. Basic fibroblast growth factor fused to a signal peptide transforms cells. Nature (Lond.), *331:* 173–175, 1988.

42. Berse, B., Brown, L. F., Van de Water, L., Dvorak, H. F., and Senger, D. R. Vascular permeability factor (vascular endothelial growth factor) gene is expressed differentially in normal tissues, macrophages, and tumors. Mol. Biol. Cell, *3:* 211–220, 1992.

43. Fort, P., Marty, L., Piechaczyk, M., Dani, C., Jeanteur, P., and Blanchard, J. M. Various rat adult tissues express only one major mRNA species from the glyceraldehyde-3-phosphate dehydrogenase multigenic family. Nucleic Acids Res., *13:* 1431–1442, 1985.

44. Feinberg, A. P., and Vogelstein, B. A technique for radiolabeling DNA restriction endonuclease fragments to high specific activity. Anal. Biochem., *132:* 6–13, 1983.

45. Perrotte, P., Matsumoto, T., Inoue, K., Kuniyasu, H., Eve, B. Y., Hicklin, D. J., Radinsky, R., and Dinney, C. P. Anti-epidermal growth factor receptor antibody C225 inhibits angiogenesis in human transitional cell carcinoma growing orthotopically in nude mice. Clin. Cancer Res., *5:* 257–265, 1999.

46. Nakajima, M., Lotan, D., Baig, M. M., Carralero, R. M., Wood, W. R., Hendrix, M. J., and Lotan, R. Inhibition by retinoic acid of type IV collagenolysis and invasion through reconstituted basement membrane by metastatic rat mammary adenocarcinoma cells. Cancer Res., *49:* 1698–1706, 1989.

47. Wei, Q., Guan, Y., Cheng, L., Radinsky, R., Bar, E. M., Tsan, R., Li, L., and Legerski, R. J. Expression of five selected human mismatch repair genes simultaneously detected in normal and cancer cell lines by a nonradioactive multiplex reverse transcription-polymerase chain reaction. Pathobiology, *65:* 293–300, 1997.

48. Repesh, L. A. A new *in vitro* assay for quantitating tumor cell invasion. Invasion Metastasis, *9:* 192–208, 1989.

49. Stephenson, R. A., Dinney, C. P., Gohji, K., Ordonez, N. G., Killion, J. J., and Fidler, I. J. Metastatic model for human prostate cancer using orthotopic implantation in nude mice. J. Natl. Cancer Inst., *84:* 951–957, 1992.

50. Kitadai, Y., Bucana, C. D., Ellis, L. M., Anzai, H., Tahara, E., and Fidler, I. J. *In situ* mRNA hybridization technique for analysis of metastasis-related genes in human colon carcinoma cells. Am J. Pathol., *147:* 1238–1247, 1995.

51. Bucana, C. D., Radinsky, R., Dong, Z., Sanchez, R., Brigati, D. J., and Fidler, I. J. A rapid colorimetric *in situ* mRNA hybridization technique using hyperbiotinylated oligonucleotide probes for analysis of mdr1 in mouse colon carcinoma cells. J. Histochem. Cytochem., *41:* 499–506, 1993.

52. Radinsky, R., Bucana, C. D., Ellis, L. M., Sanchez, R., Cleary, K. R., Brigati, D. J., and Fidler, I. J. A rapid colorimetric *in situ* messenger RNA hybridization technique for analysis of epidermal growth factor receptor in paraffin-embedded surgical specimens of human colon carcinomas. Cancer Res., *53:* 937–943, 1993.

53. Reed, J. A., Manahan, L. J., Park, C. S., and Brigati, D. J. Complete one-hour immunocytochemistry based on capillary action. Biotechniques, *13:* 434–443, 1992.

54. Vecchi, A., Garlanda, C., Lampugnani, M. G., Resnati, M., Matteucci, C., Stoppacciaro, A., Schnurch, H., Risau, W., Ruco, L., Mantovani, A., *et al.* Monoclonal antibodies specific for endothelial cells of mouse blood vessels. Their application in the identification of adult and embryonic endothelium. Eur. J. Cell Biol., *63:* 247–254, 1994.

55. Weidner, N., Semple, J. P., Welch, W. R., and Folkman, J. Tumor angiogenesis and metastasis–correlation in invasive breast carcinoma. N. Engl. J. Med., *324:* 1–8, 1991.

56. Gorman, C. M., Moffat, L. F., and Howard, B. H. Recombinant genomes which express chloramphenicol acetyltransferase in mammalian cells. Mol. Cell. Biol., *2:* 1044–1051, 1982.

57. Hudson, J. M., Frade, R., and Bar, E. M. Wild-type p53 regulates its own transcription in a cell-type specific manner. DNA Cell Biol., *14:* 759–766, 1995.

58. Balbay, M. D., Pettaway, C. A., Kuniyasu, H., Inoue, K., Ramirez, E., Li, E., Fidler, I. J., and Dinney, C. P. Highly metastatic human prostate cancer growing within the prostate of athymic mice overexpresses vascular endothelial growth factor. Clin. Cancer Res., *5:* 783–789, 1999.

59. Holmes, W. E., Lee, J., Kuang, W. J., Rice, G. C., and Wood, W. I. Structure and functional expression of a human interleukin-8 receptor. Science (Washington DC), *253:* 1278–1280, 1991.

60. Murphy, P. M., and Tiffany, H. L. Cloning of complementary DNA encoding a functional human interleukin-8 receptor. Science (Washington DC), *253:* 1280–1283, 1991.

61. Singh, R., Reich, R., Radinsky, R., Berry, K., Dave, B., and Fidler, I. Expression of basic fibroblast growth factor is necessary but insufficient for production of metastasis. Int. J. Oncol., *10:* 23–31, 1996.

62. Claffey, K. P., Brown, L. F., del Aguila, L. F., Tognazzi, K., Yeo, K. T., Manseau, E. J., and Dvorak, H. F. Expression of vascular permeability factor/vascular endothelial growth factor by melanoma cells increases tumor growth, angiogenesis, and experimental metastasis. Cancer Res., *56:* 172–181, 1996.

63. McLeskey, S. W., Tobias, C. A., Vezza, P. R., Filie, A. C., Kern, F. G., and Hanfelt, J. Tumor growth of FGF or VEGF transfected

MCF-7 breast carcinoma cells correlates with density of specific microvessels independent of the transfected angiogenic factor. Am. J. Pathol., *153:* 1993–2006, 1998.

64. Sehgal, G., Hua, J., Bernhard, E. J., Sehgal, I., Thompson, T. C., and Muschel, R. J. Requirement for matrix metalloproteinase-9 (gelatinase B) expression in metastasis by murine prostate carcinoma. Am. J. Pathol., *152:* 591–596, 1998.

65. Festuccia, C., Dolo, V., Guerra, F., Violini, S., Muzi, P., Pavan, A., and Bologna, M. Plasminogen activator system modulates invasive capacity and proliferation in prostatic tumor cells. Clin. Exp. Metastasis, *16:* 513–528, 1998.

66. Stearns, M. E., and Stearns, M. Immunohistochemical studies of activated matrix metalloproteinase-2 (MMP-2a) expression in human prostate cancer. Oncol. Res., *8:* 63–67, 1996.

67. Sato, Y. Transcription factor ETS-1 as a molecular target for angiogenesis inhibition. Hum. Cell, *11:* 207–214, 1998.

68. Watabe, T., Yoshida, K., Shindoh, M., Kaya, M., Fujikawa, K., Sato, H., Seiki, M., Ishii, S., and Fujinaga, K. The Ets-1 and Ets-2 transcription factors activate the promoters for invasion-associated urokinase and collagenase genes in response to epidermal growth factor. Int. J. Cancer, *77:* 128–137, 1998.

Relative Expression of Type IV Collagenase, E-cadherin, and Vascular Endothelial Growth Factor/Vascular Permeability Factor in Prostatectomy Specimens Distinguishes Organ-confined from Pathologically Advanced Prostate Cancers[1]

Hiroki Kuniyasu, Patricia Troncoso, Dennis Johnston, Corazon D. Bucana, Eiichi Tahara, Isaiah J. Fidler, and Curtis A. Pettaway[2]

Departments of Cancer Biology [H. K., C. D. B., I. J. F., C. A. P.], Pathology, [P. T.], Biomathematics [D. J.], and Urology [C. A. P.], The University of Texas M. D. Anderson Cancer Center, Houston, Texas 77030-4095, and First Department of Pathology, Hiroshima University School of Medicine, Hiroshima, Japan [E. T.]

ABSTRACT

The tumor grade (Gleason score) in the biopsy and pretherapy prostate-specific antigen level do not accurately predict disease outcome of individual patients' prostate cancer. We used a rapid colorimetric *in situ* hybridization technique to evaluate the expression level of E-cadherin (which affects cell cohesion); matrix metalloproteinases (MMPs) types 2 and 9 (which affect invasion); and vascular endothelial growth factor/vascular permeability factor (which affects angiogenesis) in archival prostatectomy specimens from 40 patients. Intratumoral heterogeneity for gene expression (edge *versus* center *versus* perineural area) was more pronounced in advanced cancers than in those that were organ confined. Regardless of Gleason score, the highest expression level for E-cadherin was found in the center or perineural area of the tumors, whereas the highest expression levels for MMP-2 and MMP-9 were associated with the invasive edge. The relationship between advancing pathological stage and expression of all four metastasis-related genes was highly significant. Decreased expression of E-cadherin and increased expression of MMP-2, MMP-9, and vascular endothelial growth factor/vascular permeability factor were associated with the Gleason score of the tumors. Irrespective of serum prostate-specific antigen level or Gleason score, the ratio between expression of MMPs and E-cadherin at the invasive edge of tumors exhibited the strongest association with nonorgan-confined prostate cancer. These data suggest that the relative expression of metastasis-related genes in radical prostatectomy specimens can distinguish between organ-confined and advanced prostate cancers and provides the rationale for a prospective study correlating gene expression in pretherapy core biopsies with outcome.

INTRODUCTION

Prostate cancer is the most common cancer and the second leading cause of cancer death in men in the United States (1). Despite earlier diagnosis and presumably smaller tumor volumes, 35–50% of patients with clinically organ-confined prostate cancer will be shown to have extraprostatic disease subsequent to radical prostatectomy (2–4). The strongest predictive factors for advanced disease are the Gleason score, serum PSA,[3] and clinical stage (5). Of the three, Gleason score and pretherapy PSA levels are the most important.

The Gleason grading system in biopsy or prostatectomy specimens is a measure of biological aggressiveness and correlates well with final pathological stage and the prognosis of prostate cancer patients (5–9). Serum PSA is strongly associated with tumor volume and several other factors and also correlates with stage (10–12). Both serum PSA and Gleason score provide significant prognostic information as individual variables when their values are at the very high (PSA level >20 ng/ml; Gleason score ≥8) or low ends (PSA level <4 ng/ml; Gleason score 2–4) of the spectrum (13, 14). However, most patients present with intermediate PSA levels and Gleason scores (5, 9). Recently, several groups have combined clinical stage, serum PSA level, and Gleason score to generate "nomograms" that predict for pathological stage or prognosis (5, 9, 15). Although these efforts allow a "ballpark" estimate of prognosis to be made with readily available clinical data, they do not predict with accuracy disease outcome of individual patient's prostate cancer.

Recent advances in the understanding of the molecular regulation of cancer metastasis and the design of molecular

Received 12/7/99; revised 3/23/00; accepted 3/28/00.

The costs of publication of this article were defrayed in part by the payment of page charges. This article must therefore be hereby marked *advertisement* in accordance with 18 U.S.C. Section 1734 solely to indicate this fact.

[1] This work was supported in part by Cancer Center Support Core Grant CA16672, Grant 030813 from the Robert Wood Johnson Foundation (to C. A. P.), Grant R35-CA42107 from the National Cancer Institute, NIH (to I. J. F.) and United States Department of Defense Grant DAMD-17-98-1-8479.

[2] To whom requests for reprints should be addressed, at Department of Urology-110, The University of Texas M. D. Anderson Cancer Center, 1515 Holcombe Boulevard, Houston, TX 77030. Phone: (713) 792-3250; Fax: (713) 794-4824; E-mail: cpettawa@mdanderson.org.

[3] The abbreviations used are: PSA, prostate-specific antigen; ISH, *in situ* hybridization; VEGF/VPF, vascular endothelial growth factor/vascular permeability factor; MMP, matrix metalloproteinase; TNM, Tumor-Node-Metastasis; NGF, nerve growth factor.

diagnostic tools have provided new procedures with which to predict the malignant potential of individual human cancers (16). The outcome of metastasis is determined by multiple interactions between metastatic tumor cells and host factors (16, 17). To produce clinically relevant metastases, tumor cells must complete all steps in the metastatic cascade (18, 19). Thus, the failure to produce a metastasis can be attributable to different single or multiple deficiencies (19). We have developed a rapid colorimetric ISH technique to evaluate gene expression in formalin-fixed, paraffin-embedded surgical specimens of human tumors (20–25). We used this technique to study the expression level of several genes that regulate particular steps of metastasis in human prostate cancer cells implanted into the prostate of nude mice (26). Highly metastatic cells expressed higher mRNA levels of type IV collagenase (which affects invasion; Refs. 27–29); basic fibroblast growth factor and interleukin 8 (which affect angiogenesis; Refs. 30–32); and the multidrug resistance gene (33, 34) compared with cells of lower metastatic potential (27). No difference in the epidermal growth factor receptor expression (which affects growth; Ref. 35) was found between the cells, but the expression of E-cadherin (which affects cell cohesion; Refs. 36 and 37) was decreased in the metastatic cells (27). VEGF/VPF, which affects tumor angiogenesis (38–41), has also been found to be overexpressed in prostate cancer in comparison with normal epithelium or benign prostatic hyperplasia (42, 43). We found that VEGF/VPF levels correlated with microvessel density and metastatic potential of human prostate cancer cells growing in the prostate of nude mice (44). Similarly, treatment with anti-VEGF monoclonal antibody was shown to inhibit the growth of DU 145 human prostate cancer cells in nude mice (45).

Several studies have evaluated the expression of E-cadherin (46–51), type IV collagenase (29, 52, 53), and microvessel density (surrogate marker of angiogenesis; Refs. 55–62) in human cancers as single prognostic factors. Most of these correlative studies reached the inevitable conclusion that the expression of a given gene is necessary but insufficient to account for the multistep process of metastasis (19). Because each of the discrete steps in the pathogenesis of metastasis is regulated by one or several independent genes, the identification of cells with metastatic potential in heterogeneous primary human prostate cancer requires multiparametric-multivariate analysis of gene expression (19–25).

The present study analyzed expression of metastasis-related genes in 40 archival prostatectomy specimens (59 tumors). We show that increased expression of collagenase type IV (MMP-2 and MMP-9), VEGF/VPF, and decreased expression of E-cadherin are associated with increasing Gleason score. The ratio of MMP-2 and MMP-9 to E-cadherin, however, exhibited the strongest association with advanced prostate cancer.

MATERIALS AND METHODS

Surgical Specimens and Patient Characteristics. Forty formalin-fixed, paraffin-embedded, archival radical prostatectomy specimens from patients treated at the University of Texas M. D. Anderson Cancer Center were examined. Fifty-nine tumors from the 40 cases were included (15 cases with multiple tumors). The cases were selected at random, and no patients received any therapy prior to prostatectomy. Methods for handling specimens, including gross examination, sample processing, and assignment of Gleason score and pathological stage have been published previously (11). The specimens were classified by the TNM system (63), where pT_2 cancer is organ-confined, pT_{3a} cancer exhibits extraprostatic extension, and pT_{3b} cancers invade the seminal vesicles. N+ cases exhibit regional metastasis to the lymph nodes irrespective of primary T stage. In our study, the primary tumor in all node-positive cases was pT_{3a} or pT_{3b}. Tumors were graded according to the Gleason system (6). In cases with multiple tumors, the Gleason score and TNM stage of each tumor was noted. When multiple tumors were present in a case with lymph node metastasis, we arbitrarily denoted the tumor of the highest histological grade in the prostate as the tumor from which the dissemination occurred. Clinical stage in the 40 patients was assigned by retrospective chart review with 38 of 40 patients having clinically confined prostate cancer ($T \leq 2$) by digital rectal exam and transrectal ultrasound and 2 of 40 patients with suspected extraprostatic extension (T3). Preoperative serum PSA levels in the 40 patients were determined in the laboratory of The University of Texas M. D. Anderson Cancer center using the Tosoh AIA assay.

Histopathology. Thin sections (4 μm) from the prostatectomy specimens were stained with H&E and evaluated histopathologically for further correlation with the ISH findings. We examined the expression of metastasis-related genes in serial sections of individual tumors and normal epithelium by mRNA ISH. Previous reports analyzing the expression of metastasis-related genes in surgical specimens of human gastric carcinomas (24), human colon carcinomas (21–23), and human pancreatic carcinomas (25) concluded that the expression level of collagenase type IV and E-cadherin varied between the edge and center of the lesions. For this reason, we examined the expression level of E-cadherin, MMP-9, MMP-2, and VEGF/VPF at the invasive edge (toward the prostate's periphery) and the center of the cancers. In addition, in 21 tumors, we studied the expression of metastasis-related genes in tumor foci invading nerves (perineural invasion), because this has been associated previously with locally advanced prostate cancer (64). Within a specimen, tumors of different Gleason scores and pathological stage were studied. Within individual tumor foci, areas of the tumor with different Gleason grades were selected for analysis. When the Gleason score was uniform, we studied multiple random areas.

Oligonucleotide Probes. Specific antisense oligonucleotide DNA probes were designed complementary to the mRNA transcripts of four metastasis-related genes, based on published reports of the cDNA sequences (65–68). The specificity of the oligonucleotide sequences was initially determined by a GenEMBL database search using the FastA algorithm (69), which showed 100% homology with the target gene and minimal homology with nonspecific mammalian gene sequences. The sequences and working dilution of the probes are as follows: MMP-9, 5′-CCG GTC CAC CTC GCT GGC GCT CCG GA-3′ (1:200); MMP-2, 5′-GGC CAC ATC TGG GTT GCG GC-3′ (1:200); E-cadherin, mixture of 5′-TGG AGC GGG CTG GAG TCT GAA CTG-3′ (1:200) and 5′-GAC GCC GGC GGC CCC TTC ACA GTC-3′ (1:200); and VEGF/VPF, 5′-TGG TGA TGT TGG ACT CCT CAG TGG GC-3′ (1:200). A $d(T)_{20}$

Table 1 Intratumoral heterogeneity of prostate cancer

Intratumoral location	No. of tumors	Expression[b]				
		E-cadherin	MMP-9	MMP-2	VEGF/VPF	MMP:E-cadherin ratio[c]
Organ-confined tumors (pT_2)[a]						
Edge	34	73 ± 4[b]	157 ± 14	149 ± 63	111 ± 38	2.2 ± 0.1[c]
		(42–98)[b]	(97–324)	(34–322)	(67–220)	(1.2–5.5)[c]
Center	34	80 ± 11	120 ± 27	131 ± 45	118 ± 31	1.6 ± 0.4
		(55–100)	(84–211)	(36–280)	(76–203)	(1.1–3.3)
Perineural invasion	7	100 ± 60	107 ± 75	94 ± 29	102 ± 22	1.1 ± 0.5
		(57–113)	(29–215)	(57–148)	(68–143)	(0.7–2.1)
P[d]	E *vs.* C	NS[e]	0.005	NS	NS	0.001
	E *vs.* N	0.009	0.035	0.041	NS	0.001
	C *vs.* N	0.073	NS	NS	NS	NS
Advanced tumors (pT_{3a}, pT_{3b}, $pT_{3a-b}N_1$)[a]						
Edge	25	39 ± 13	312 ± 121	346 ± 141	197 ± 71	8.9 ± 2
		(20–70)	(162–600)	(100–611)	(67–359)	(5.0–13.2)
Center	25	49 ± 13	243 ± 119	245 ± 120	220 ± 91	5.3 ± 2
		(27–79)	(127–500)	(78–524)	(67–424)	(2.3–10.5)
Perineural invasion	14	50 ± 10	199 ± 73	214 ± 74	168 ± 71	4.2 ± 1
		(32–70)	(100–338)	(135–320)	(58–323)	(2.6–6.2)
P[d]	E*vs.*C	0.032	NS	0.013	NS	<0.001
	E*vs.*N	0.032	0.010	0.005	NS	<0.001
	C*vs.*N	NS	NS	NS	NS	NS

[a] TNM classification (63).

[b] The numbers are expression intensities compared with normal epithelium of prostate glands (expression at normal glands, 100). The data are shown as mean ± SD (range).

[c] Mean of calculated MMP:E-cadherin expression ratios. The data shown are mean ± SD (range).

[d] Examined by Tukey HSD multiple range test. E, edge; C, center; N, neural.

[e] NS, no significant difference.

oligonucleotide was used to verify the integrity of mRNA in each sample (70). All DNA probes were synthesized with six biotin molecules (hyperbiotinylated) at the 3′ end via direct coupling using standard phosphormidine chemistry (Research Genetics, Huntsville, AL; Refs. 70 and 71). The lyophilized probes were reconstituted to a 1 μg/μl stock solution in 10 mM Tris-HCl (pH 7.6) and 1 mM EDTA. The stock solution was diluted with Probe Diluent (Research Genetics) immediately before use.

ISH. ISH was performed as described previously (72, 73) with a minor modification. The Microprobe manual staining system (Fisher Scientific, Pittsburgh, PA) was used to stain tissue sections mounted on Silane-coated ProbeOn slides (Fisher Scientific). The slides were placed in the Microprobe slide holder, dewaxed, and dehydrated with Autodewaxer and Autoalcohol (Research Genetics), followed by enzymatic digestion with pepsin (73). Hybridization of the probe was carried out for 60 min at 45°C, and the samples were then washed three times with 2× SSC for 2 min at 45°C. The samples were incubated with alkaline phosphatase-labeled avidin for 30 min at 45°C, briefly rinsed in 50 mM Tris buffer (pH 7.6), rinsed with alkaline phosphatase enhancer (Biomeda Corp., Foster City, CA) for 1 min, and finally incubated with the chromogen substrate Fast-Red (Research Genetics) for 30 min at 45°C. A positive reaction in this assay stained red.

ISH Control Experiments. Controls for endogenous alkaline phosphatase activity included treatment of the samples in the absence of the biotinylated probe and use of chromogen in the absence of any oligonucleotide probes. In addition, to analyze the specificity of the hybridization signal, the following controls were performed: RNase pretreatment of tissue sections, a biotin-labeled sense probe, and competition assays with unlabeled antisense probe. A markedly decreased or absent signal was obtained under all of these conditions.

Image Analysis. To quantify intensity of the reaction, stained sections were examined in a Zeiss photomicroscope (Carl Zeiss, Inc., Thornwood, NY) equipped with a three-clip charged coupled device color camera (model DXC-960 MD; Sony Corp., Tokyo, Japan). The images were analyzed using the Optimas image analysis software (version 5.2; Bothell, WA). The slides were prescreened to determine the range in staining intensity of the slides to be analyzed. Images covering the range of staining intensities were captured electronically, a color bar (montage) was created, and a threshold value was set in the red, green, and blue mode of the color camera. All subsequent images were quantified based on this threshold. The integrated absorbance of the selected fields was determined based on their equivalence to the mean log inverse gray scale value multiplied by the area of the field. The samples were not counterstained; therefore, the absorbance was attributable solely to the product of the ISH reaction.

For each tumor focus analyzed, we measured the expression of metastasis-associated genes at the invasive edge (edge facing the outer surface of the prostate), at the center of the tumor and, in selected cases (21 separate tumor foci), in areas of perineural tumor invasion (located at the edge of the tumor facing the outer surface of the prostate). The areas to be measured were selected and identified with ink on the corresponding H&E stained section as follows: (*a*) normal glands of peripheral or transition zone distant from the tumor; (*b*) at least five

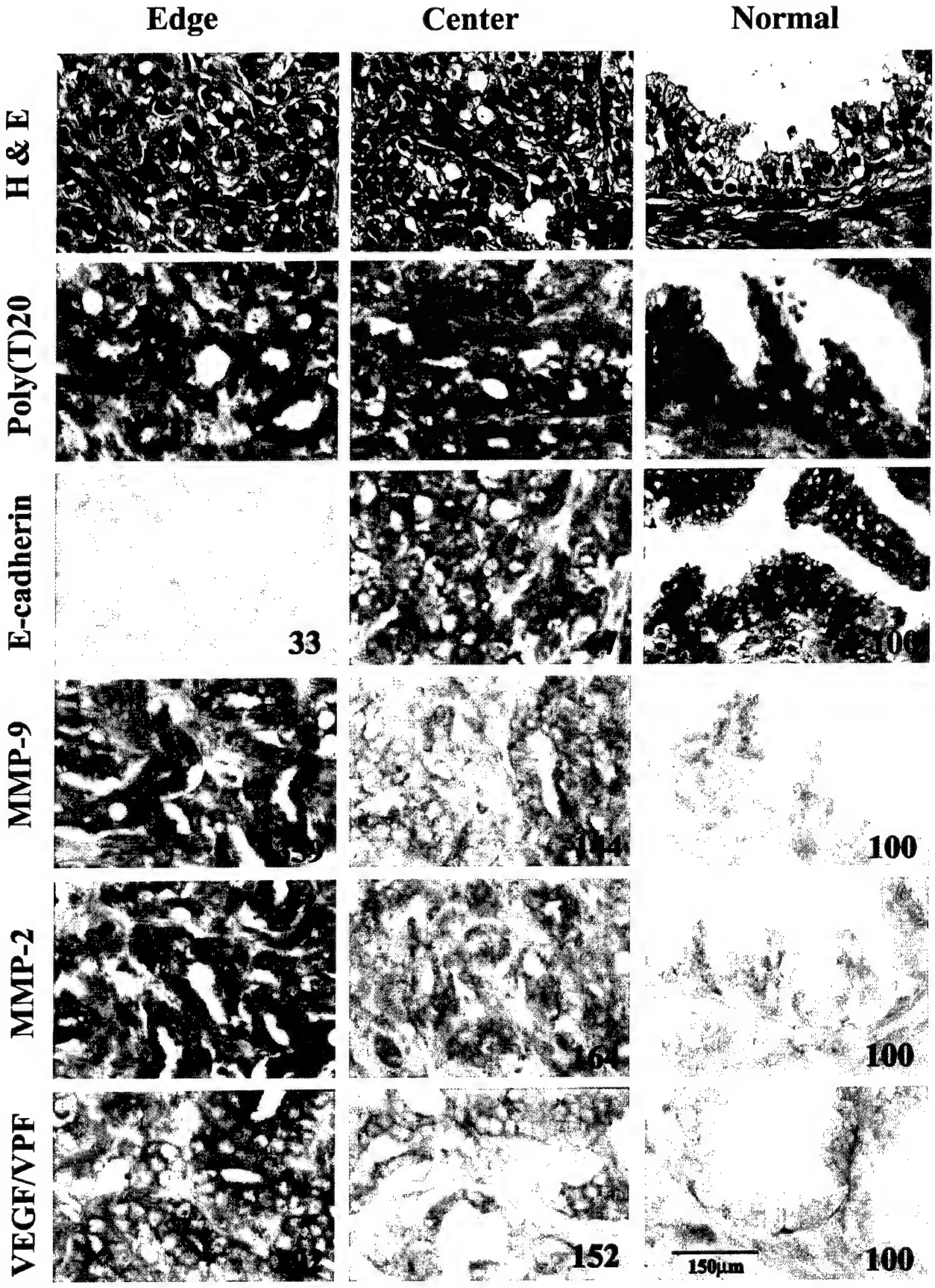
Edge
Center
Normal
H & E
Poly(T)20
E-cadherin
MMP-9
MMP-2
VEGF/VPF
33
100
100
100
152
100
150μm

separate fields (approximately one field every 2 mm) irrespective of the Gleason score from the invasive edge (toward the periphery of the prostate) of the tumor; (*c*) Two to four separate fields, including at least one representative field of each of the different Gleason grades present from the center of the tumor; and (*d*) areas of perineural tumor invasion. Within each 1-mm^2 field, we analyzed at least 10 cells (range, 10–20) with adequate cytoplasm, permitting measurement of staining intensity. Areas of nuclear staining and necrotic cells were avoided. Whenever possible, measurements for each probe were performed in the same tumor cell cluster/cells. This was particularly important for the values of MMP-9 and MMP-2 and E-cadherin; therefore, the corresponding ratio reflected values for the same cells. For each tumor, multiple data points were recorded. The values assigned to a given tumor for E-cadherin and MMP-2 and MMP-9 expression were those of the "representative field" providing the highest MMP:E-cadherin ratio. The VEGF/VPF value assigned reflected the highest value among the measured fields.

Controls for Image Analysis. To minimize experimental variations in staining intensities, normalization of mRNA expression levels was performed. The levels of E-cadherin, MMP-2, MMP-9, and VEGF/VPF for each field were normalized by subtracting background staining and then dividing by the expression level of the poly $d(T)_{20}$ probe (mRNA integrity) for the same area. To allow for a comparison of samples run on different days, the staining intensity of each probe was further normalized for the mRNA expression level in histologically normal prostate glands on the same slide.

Statistical Analysis. The mean of the assigned expression levels (± SD, range) for E-cadherin, MMP-2, MMP-9, VEGF/VPF, and the MMP:E-cadherin ratio for the 59 tumors was stratified according to pathological stage, Gleason score (6, 60), and location of the measured area. To assess the statistical significance of differences in mean expression levels, ANOVA (with the Tukey honestly significant difference multiple comparison post-hoc test) was performed (74). $P \leq 0.05$ was considered a significant difference. The MMP:E-cadherin ratio was used to express the invasive profile of a tumor and was calculated using the following formula: (MMP-2 + MMP-9)/2 ÷ E-cadherin expression level. To determine the significance of the mRNA expression levels for the above genes that were representative of the whole radical prostatectomy specimen, a separate analysis was performed using only the mRNA expression levels of the tumor focus of the highest Gleason score or pathological stage in the specimen (dominant tumor). For these 40 cases, mRNA expression as well as the preoperative serum PSA levels were related to the final pathological stage. In addition, logistic regression analysis was used on the same data set to define the most important variables predicting organ-confined *versus* nonorgan-confined (*i.e.*, more advanced) prostate cancer (SPSS, Inc., Chicago, IL; Ref. 74).

RESULTS

Intratumoral Heterogeneity of the Expression of Metastasis-related Genes. The integrity of mRNA in each sample was first verified using a poly $d(T)_{20}$ probe (22–25). All samples had an intense reaction, indicating that the mRNA was preserved. Normalization of mRNA expression intensities for poly $d(T)_{20}$ probe intensity and also for normal prostate glands on the same slide allowed for a comparison of expression intensities of multiple samples analogous to loading controls (*i.e.*, glyceraldehyde-3-phosphate dehydrogenase) used for Northern blot analysis.

Intratumoral heterogeneity for gene expression was observed for E-cadherin, MMP-2, and MMP-9. Pathologically advanced (pT_{3a-b}, N_0- N+) cancers exhibited a greater degree of intratumoral heterogeneity than organ-confined cancers (pT_2; Table 1; Fig. 1). Specifically, E-cadherin expression was highest at the center and lowest at the edge of the tumors [significant difference, edge *versus* perineural (organ-confined tumors) $P = 0.009$; edge *versus* center, or perineural area (advanced tumors) $P = 0.032$]. In contrast, the expression of type IV collagenase (MMP-2 and MMP-9) was significantly elevated at the edge as compared with the central or perineural areas for both organ-confined and advanced cancers. Because down-regulation of E-cadherin and up-regulation of MMP-2 and MMP-9 were found at the tumor edge, the MMP:E-cadherin ratio was also highest at the edge of 52 of the 59 tumors (88%). In seven cases (12%), however, the ratio was highest in the center of the tumor. Overall, intratumoral heterogeneity of gene expression with respect to the MMP:E-cadherin ratio was highly significant for both organ-confined ($P = 0.001$) and advanced ($P < 0.001$) cancers. This was not the case, however, for VEGF/VPF because the expression varied throughout the tumors and did not differ significantly among the edge, center, or perineural areas (Table 1).

Perineural invasion is characteristic of aggressive cancers, such as pancreatic carcinoma (25), and is also thought to be a poor prognostic feature in prostate cancer (64). Although most of the areas of perineural invasion were found on the edge of tumors, the expression of E-cadherin and type IV collagenase genes in these tumor cells was essentially identical to that of tumor cells in the center of lesions (Table 1).

Intertumoral Heterogeneity for Expression of Metastasis-related Genes. Next, we related the expression level of metastasis-related genes to the tumor pathological stage (Table 2). The expression levels of VEGF/VPF, E-cadherin, MMP-2, and MMP-9 significantly differed ($P = 0.015-<0.001$) between organ-confined (pT_2) and advanced cancers (pT_{3a}, pT_{3b}, and $pT_{3a-b}N+$). Advanced tumors expressed lower E-cadherin but higher VEGF/VPF, MMP-2, and MMP-9 than organ-confined tumors. The calculated MMP:E-cadherin ratio at the tumor edge also showed clear differences between organ-confined and ad-

Fig. 1 Intratumoral heterogeneity for expression of metastasis-related genes. ISH analysis of E-cadherin, MMP-2, MMP-9, and VEGF/VPF expression in normal tissue and prostate cancer (Gleason score 7) exhibiting extraprostatic extension (pT_{3a}). Hybridization with the poly $d(T)_{20}$ probe confirmed mRNA integrity. A positive reaction in this assay stains red. The numbers for E-cadherin, MMP-9, MMP-2, and VEGF/VPF indicate expression intensities as compared with the epithelium of normal glands, which were assigned a value of 100.

Table 2 Relationship between the expression of metastasis-related genes and pathological stage

Pathological stage[a]	No. of tumors	Expression[b] VEGF/VPF	MMP-9	MMP-2	E-cadherin	MMP:E-cadherin ratio[c]
pT_2	34	113 ± 40[b] (77–220)[b]	154 ± 56 (97–324)	151 ± 66 (34–322)	73 ± 14 (42–93)	2.2 ± 0.9 (1.2–5.5)
pT_{3a}	13	181 ± 69 (123–454)	327 ± 131 (143–584)	318 ± 125 (123–550)	40 ± 11 (20–59)	8.5 ± 1.9 (6.4–12.2)
pT_{3b}	5	208 ± 74 (196–533)	216 ± 57 (154–297)	283 ± 77 (164–378)	31 ± 7 (22–39)	8.2 ± 1.1 (7.4–9.8)
$pT_{3a-b}N+$	7	195 ± 63 (194–755)	330 ± 85 (213–449)	438 ± 110 (280–573)	35 ± 7 (24–47)	11 ± 1 (9.4–12.6)
P[d]						
pT_2 *vs.* pT_{3a}		0.001	<0.001	<0.001	<0.001	<0.001
pT_2 *vs.* pT_{3b}		0.021	NS[e]	0.015	<0.001	<0.001
pT_2 *vs.* $pT_{3a-b}N+$		0.002	<0.001	<0.001	<0.001	<0.001
pT_{3a} *vs.* pT_{3b}		NS	NS	NS	NS	NS
pT_{3a} *vs.* $pT_{3a\ b}N+$		NS	<0.001	0.026	NS	<0.001
pT_{3b} *vs.* $pT_{3a-b}N+$		NS	NS	0.021	NS	0.002

[a] TNM classification (63).
[b] The numbers are expression intensities compared with normal epithelium of prostate glands (expression at normal glands, 100). The data are shown as mean ± SD (range).
[c] Mean of calculated MMP:E-cadherin expression ratios. The data shown are mean ± SD (range).
[d] Examined by Tukey HSD multiple range test.
[e] NS, no significant difference.

Table 3 Relationship between the expression of metastasis-related genes and Gleason score

Gleason score[a]	No. of tumors	Expression[b] VEGF/VPF	MMP-9	MMP-2	E-cadherin	MMP:E-cadherin ratio[c]
5, 6	18	107 ± 36[b] (77–203)[b]	146 ± 52 (100–324)	150 ± 75 (34–322)	72 ± 169 (42–93)	2.1 ± 0.7[c] (1.2–3.4)[c]
7	25	157 ± 70 (93–454)	218 ± 118 (97–500)	230 ± 143 (77–573)	61 ± 20 (20–90)	4.7 ± 3.6 (1.3–12.0)
8–10	16	168 ± 65 (123–755)	302 ± 102 (170–584)	333 ± 109 (126–539)	36 ± 8.5 (22–57)	9.2 ± 2 (5.5–12.6)
P[d]						
5–6 *vs.* 7		0.029	NS[e]	NS	NS	0.006
5–6 *vs.* 8–10		0.015	<0.001	<0.001	<0.001	<0.001
7 *vs.* 8–10		NS	0.025	0.021	<0.001	<0.001

[a] According to Gleason *et al.* (6, 7).
[b] The numbers are expression intensities compared with normal epithelium of prostate glands (expression at normal glands, 100). The data are shown as mean ± SD (range).
[c] Mean of calculated MMP:E-cadherin expression ratios. The data shown are mean ± SD (range).
[d] Examined by Tukey HSD multiple range test.
[e] NS, no significant difference.

vanced cancers ($P < 0.001$). The MMP:E-cadherin expression ratio even separated tumors with extraprostatic extension alone (pT_{3a} and pT_{3b}, N_0) from tumors with lymph node metastasis (pT_{3a-b}, N+; $P = 0.002$ to <0.001).

The expression of metastasis-related genes was next compared with the Gleason score of the tumors (Table 3). The expression levels of VEGF/VPF, E-cadherin, MMP-2, and MMP-9 differed significantly between tumors with a Gleason score of 5–6 (well differentiated) and those with a Gleason score of 8–10 (poorly differentiated). The high grade, poorly differentiated tumors expressed a lower level of E-cadherin mRNA ($P < 0.001$), a higher level of MMP-2 mRNA ($P < 0.001$), a higher level of MMP-9 mRNA ($P < 0.001$), and a higher level of VEGF/VPF mRNA ($P = 0.015$) than Gleason score 5–6 tumors. The MMP:E-cadherin ratio was also significantly higher in high-grade tumors (Gleason score 8–10) than in low-grade tumors (Gleason score 5 and 6; $P < 0.001$). Tumors with a Gleason score of 7 (intermediate in aggressiveness) exhibited intermediate levels of expression. Only VEGF/VPF expression and the MMP:E-cadherin ratio were different between Gleason 5–6 and Gleason 7 cancers as a group.

Of interest, the Gleason score 7 tumors were heterogeneous and included 15 (60%) organ-confined tumors and 10 (40%) tumors that were associated with extension into extraprostatic tissue (7 cases), seminal vesicles (2 cases), or lymph node metastasis (1 case). This difference in tumor aggressiveness prompted us to categorize the analysis of the Gleason score 7 tumors to pathologically organ-confined or advanced disease (Table 4; Fig. 2). The difference in expression levels of VEGF/VPF, E-cadherin, MMP-2, and MMP-9, and the MMP:E-

Table 4 Comparison between organ-confined and advanced Gleason 7 tumors

Pathological stage[a]	No. of tumors	Expression[b] VEGF/VPF	MMP-9	MMP-2	E-cadherin	MMP:E-cadherin ratio[c]
Organ confined	15	120 ± 47[b] (93–220)[b]	159 ± 58 (97–298)	146 ± 49 (77–263)	75 ± 9 (61–90)	2.1 ± 0.6 (1.3–3.8)
Advanced	10	214 ± 61 (177–454)	306 ± 134 (143–500)	356 ± 148 (123–573)	40 ± 11 (20–59)	8.7 ± 2.2 (6.4–12.0)
P[d]		<0.001	0.001	<0.001	<0.001	<0.001

[a] TNM classification: Organ confined (pT_2); Advanced (pT_{3a}, $n = 7$; pT_{3b}, $n = 2$; $pT_{3a}N+$, $n = 1$; Ref. 63).

[b] The numbers are expression intensities compared with normal epithelium of prostate glands (expression at normal glands, 100). The data are shown as mean ± SD (range).

[c] Mean of MMP:E-cadherin expression ratios. The data shown are mean ± SD (range).

[d] Examined by two-sided t test.

cadherin ratio between Gleason 7 tumors that were organ confined or advanced was highly significant (Table 4, $P < 0.001$). In fact, organ-confined Gleason score 7 tumors exhibited a pattern of gene expression that was similar to Gleason score 5–6 cancers (Tables 3 and 4), whereas the pattern of gene expression of advanced Gleason score 7 tumors was identical to high-grade tumors (Tables 3 and 4). Thus, an assessment of metastasis-related genes was very informative in cancers with similar histology.

Shown in Table 5 are the mRNA expression levels of VEGF/VPF, MMP-9, MMP-2, and E-cadherin as well as the MMP:E-cadherin ratios for the dominant tumor in the radical prostatectomy specimen. Also shown are the mean serum PSA levels stratified by pathological stage. Significant overlap in serum PSA between the various pathological stages precluded separation with the exception of organ-confined cancer from seminal vesicle involvement. On the other hand, the expression levels of VEGF/VPF, MMP-9, MMP-2, and E-cadherin correctly separated the patients with extraprostatic extension and lymph node metastasis from those with pathologically organ-confined disease. Furthermore, the MMP:E-cadherin ratio separated patients into three different groups: (*a*) organ-confined cancer (pT_2); (*b*) those with extraprostatic extension ($pT_{3a\text{-}b}$); and (*c*) those with lymph node metastasis ($pT_{3a\text{-}b}$, N+; Table 5). The specific gene expression was clinically significant because 38 of 40 patients underwent a prostatectomy for clinically confined prostate cancer ($\leq T_2$). In reality, the cancer was pathologically confined (pT_2) in 18 (45%) patients, and the MMP:E-cadherin ratio identified all 18 cases at a cutoff value of <6. This conclusion is illustrated in Fig. 3.

Because all measured variables, including Gleason score, were highly associated with the pathological stage of disease, we performed both univariate and multivariate regression analyses on the 40 cases to determine which factors were most informative for predicting organ-confined prostate cancer. The data summarized in Table 6 conclude that all of the variables studied, except serum PSA level, were highly associated with organ-confined prostate cancer. However, the MMP:E-cadherin ratio provided the highest log-likelihood score (Table 6). Subsequent to a multivariate regression analysis, once the MMP:E-cadherin ratio was taken into account, all other variables were irrelevant in distinguishing organ-confined from non-organ-confined (advanced) prostate cancer.

DISCUSSION

The purpose of the present study was 3-fold: (*a*) to define the feasibility of determining metastasis-related gene expression using an ISH technique in archival radical prostatectomy specimens; (*b*) to ascertain the distribution of gene expression in a cancer known for its histological heterogeneity; and (*c*) to determine whether the expression of metastasis-related genes correlates with aggressive behavior in individual patients as assessed by the tumor pathological stage. The present results show that the ISH technique is feasible and that normalization of gene expression for mRNA integrity [poly $d(T)_{20}$] as well as for expression in the normal epithelium allows for quantitation as well as for comparisons between samples that were performed on different days.

As with other neoplasms, human prostate carcinomas consist of multiple subpopulations of tumor cells interspersed with host fibroblasts, epithelial cells, endothelial cells, and leukocytes (56, 57, 64). Because metastases originate from a small subpopulation of preexisting tumor cells (16, 75, 76), the identification of these cells requires a sensitive technique that preserves zonal heterogeneity. Northern blot analysis represents the average level of mRNA of all of the cells in a sample and thus cannot identify a small subpopulation of cells in a heterogeneous tumor (22, 23). Moreover, in many human tumors, the expression of E-cadherin, collagenase type IV, and other genes varies between the center and the edge of the tumor (21–25). Our present data agree with these findings and show that the difference in expression levels was more marked in advanced prostate cancers, suggesting a causal relationship between invasion and low expression of E-cadherin (37, 46, 49) and high expression of MMPs (25, 28, 52, 53).

E-cadherin, a cell surface glycoprotein involved in calcium-dependent homotypic cell-to-cell adhesion, is responsible for the organization, maintenance, and morphogenesis of epithelial tissues (36, 77). Reduced levels of E-cadherin are associated with decreases in cellular and tissue differentiation and a resulting higher histological grade in various epithelial neoplasms (37, 46, 49, 77). The transfection of an E-cadherin-encoding cDNA into invasive cancer cells has been shown to inhibit their motility and invasiveness (80, 81), and immunohistochemical studies in patient specimens demonstrate that re-

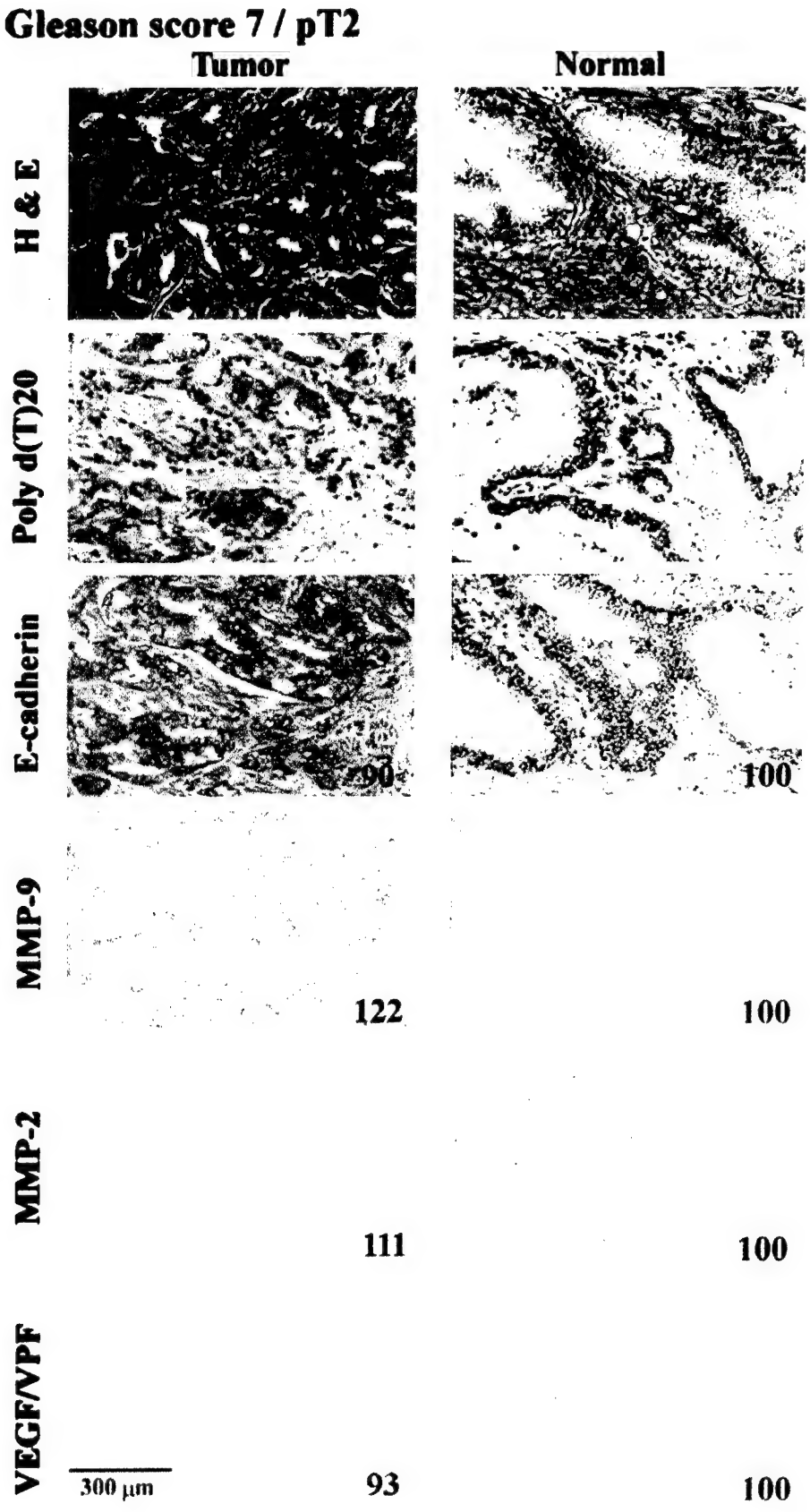

Fig. 2 *A,* ISH analysis of E-cadherin, type IV collagenase (at the edge of the tumor), and VEGF/VPF (at the center of the tumor) mRNA of an organ-confined (pT_2) tumor. H&E staining shows that the tumor has a Gleason score 7. Hybridization with the poly $d(T)_{20}$ probe confirmed mRNA integrity. A positive reaction in this assay stains red. The numbers for E-cadherin, MMP-9, MMP-2, and VEGF/VPF indicate expression intensities as compared with the epithelium of normal glands, which were assigned a value of 100. The expression intensity values for E-cadherin, MMP-9, MMP-2, and VEGF/VPF were 90, 122, 111, and 93, respectively. The MMP:E-cadherin ratio [(122 + 111) ÷ 2/90] = 1.3. *B,* ISH analysis of E-cadherin, type IV collagenase (at the edge of the tumor), and VEGF/VPF (at the center of the tumor) mRNA of a tumor exhibiting extraprostatic extension (pT_{3a}). H&E staining shows that the tumor has a Gleason score 7. Hybridization with the poly $d(T)_{20}$ probe confirmed mRNA integrity. The numbers for E-cadherin, MMP-9, MMP-2, and VEGF/VPF indicate expression intensities as compared with the epithelium of normal glands, which were assigned a value of 100. The expression intensity values for E-cadherin, MMP-9, MMP-2, and VEGF/VPF were 33, 359, 368, and 192, respectively. The MMP:E-cadherin ratio [(359 + 368) ÷ 2/33] = 11.0.

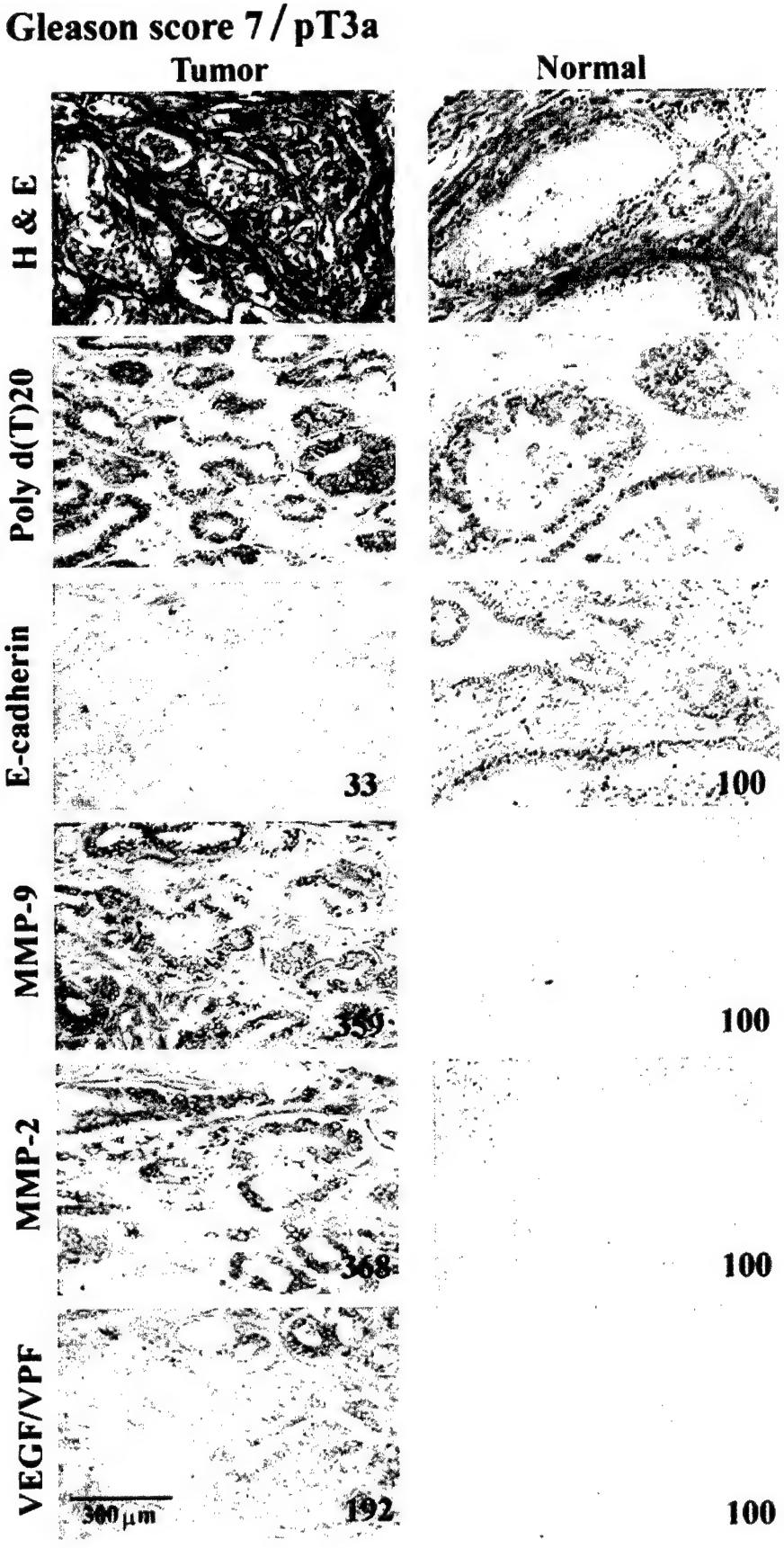

Fig. 2 Continued.

Table 5 Relationship between expression of metastasis-related genes, PSA, and pathological stage in the prostatectomy specimen

Pathological stage[a]	No. of cases	Serum PSA level	Expression[b] VEGF/VPF	MMP-9	MMP-2	E-cadherin	MMP:E-cadherin ratio[c]
pT_2	18	8 ± 6 (2.5–27)	111 ± 43 (72–220)	174 ± 67 (97–324)	152 ± 75 (34–322)	72 ± 13 (47–93)	2.4 ± 1 (1.2–5.5)
pT_{3a}	12	10 ± 6.5 (2–21)	181 ± 72 (67–308)	318 ± 133 (143–584)	323 ± 129 (123–550)	41 ± 11 (20–59)	8.2 ± 1.8 (6.4–12.4)
pT_{3b}	5	18 ± 5 (11–24)	208 ± 74 (153–292)	216 ± 57 (154–297)	284 ± 77 (164–378)	31 ± 7 (22–39)	8.2 ± 1 (7.4–9.8)
$pT_{3a-b}N_1$	5	5 ± 1 (3–6.6)	217 ± 58 (151–281)	351 ± 83 (270–449)	465 ± 104 (321–573)	37 ± 8 (24–47)	11.2 ± 0.9 (10.2–12.6)
P[d]							
pT_2 *vs.* pT_{3a}		NS[e]	0.017	0.001	<0.001	<0.001	<0.001
pT_2 *vs.* pT_{3b}		0.009	NS	NS	NS	<0.001	<0.001
pT_2 *vs.* $p_{3a-b}N_1$		NS	0.006	0.003	<0.001	<0.001	<0.001
pT_{3a} *vs.* pT_{3b}		NS	NS	NS	NS	NS	NS
pT_{3a} *vs.* $pT_{3a-b}N_1$		NS	NS	NS	0.047	NS	<0.001
pT_{3b} *vs.* $pT_{3a-b}N_1$		0.005	NS	NS	0.029	NS	0.005

[a] TNM classification (63).
[b] The numbers are expression intensities compared with normal epithelium of prostate glands (expression at normal glands, 100). The data are shown as mean ± SD (range).
[c] Mean of calculated MMP:E-cadherin expression ratios. The data shown are mean ± SD (range).
[d] Examined by Tukey HSD multiple range test.
[e] NS, no significant difference.

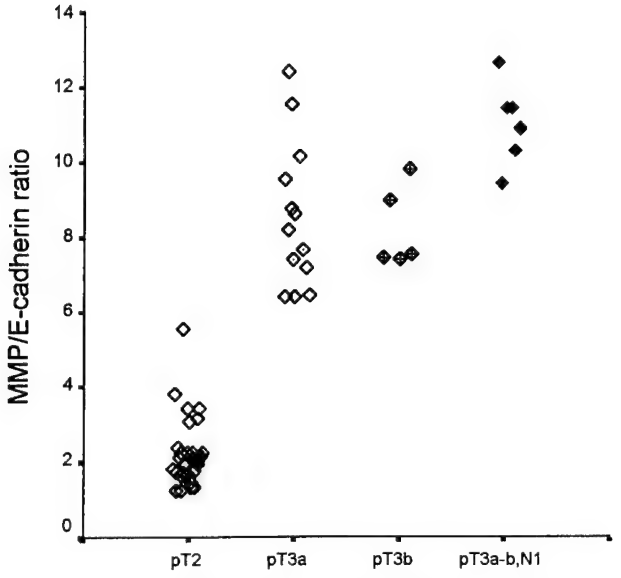

Fig. 3 MMP:E-cadherin ratios of organ-confined (pT_2) *versus* advanced (pT_{3a}, pT_{3b}, pT_{3a-b}, N+) prostate cancers. The MMP:E-cadherin ratio was calculated by the following equation: (MMP-2 + MMP-9)/2 ÷ E-cadherin.

Table 6 Prediction of organ-confined prostate cancer subsequent to radical prostatectomy by logistic regression analysis

	Log-likelihood	*P*
Serum PSA[a]	0.4	0.5
Gleason score[b]	15.1	0.005
VEGF/VPF[a]	12.6	0.0004
MMP-9[a]	13.4	0.0002
MMP-2[a]	16.5	<0.0001
E-cadherin[a]	24.0	<0.0001
MMP:E-cadherin ratio[a,c]	29.0	<0.0001

[a] Assessed as continuous variables.
[b] Assessed as categorical variable: Gleason score <7, 7, or >7.
[c] MMP:E-cadherin ratio is the sole variable necessary to predict organ-confined prostate cancer using multivariate regression analysis.

duced expression of E-cadherin predicts for advanced disease and poor prognosis (37, 46–51).

The production of type IV collagenase (gelatinase, MMP) in metastatic tumor cells also correlates with the invasive capacity of human cancer cells (26–28, 52, 53, 65, 80). The MMPs degrade the basement membrane and extracellular matrix and hence facilitate invasion of the stroma. In prostate cancer, increased levels of type IV collagenase have been associated with increasing Gleason score (28). Moreover, the balance of the expression of type IV collagenase and one family of inhibitors (tissue inhibitor of metalloproteinase-1 and tissue inhibitor to metalloproteinase-2) correlates with the invasive and metastatic capacity of human prostate cancer (53). The present data confirm these findings because the concurrent relationship of expression of type IV collagenase to E-cadherin in radical prostatectomy specimens was a measure of the invasive phenotype.

Tumor foci surrounding nerves (perineural invasion) exhibited a pattern of metastasis-related gene expression similar to that of the center of tumors, where we noted lower levels of type IV collagenase and higher levels of E-cadherin. This was somewhat surprising because perineural invasion in radical prostatectomy and prostate biopsy specimens has been reported to be associated with extraprostatic extension of the tumor (37, 81, 82). However, in several recent studies where a multivariate statistical analysis was performed, perineural invasion did not predict extraprostatic extension when serum PSA level, Gleason score, or ultrasound contact length were accounted for (81–83). Similarly, perineural invasion does not predict survival in pros-

tate cancer (81). Whether the affinity of prostate cancer cells for growth around nerves is mediated via paracrine growth factors produced by nerve or nerve-associated cells is unknown. Candidate growth factors include NGF, NGF-like protein, and neural cell adhesion molecules (84–86). NGF has been shown to inhibit apoptosis in non-neuronal cells, and in one study perineural prostate cells in the perineural space exhibited a lower apoptotic rate than prostate cancer cells in nonperineural areas (87). Alternatively, perineural migration may represent the path of least resistance for prostate cancer spread, implying that such cells may not have enhanced invasive capacity (88). Indeed, recent data showed that *in vitro* treatment of human prostate cancer cells (PC-3 and DU-145) with NGF led to re-expression of the *KAI1* metastasis suppressor gene, decreased telomerase activity, reduced cell growth, and reduced invasive capacity and that treatment of nude mice with NGF inhibited s.c. tumors (89).

Intratumoral heterogeneity for gene expression was not observed for all metastasis-related genes. Tumors of higher pathological stage exhibited higher VEGF/VPF expression levels than tumors of low pathological stage. Regardless of stage, VEGF/VPF levels were similar within different areas of a given tumor, agreeing with a published study using immunohistochemical staining of human prostate cancer tissue with a polyclonal anti-VEGF antiserum (39). VEGF/VPF-induced neovascularization plays a prominent role in tumor progression. Elevated levels of VEGF/VPF have been noted in glioblastomas, breast, ovarian, gastrointestinal, and prostate carcinomas (reviewed in Refs. 41 and 42). A causal relationship between cancer progression, neovascularity, and expression of VEGF/VPF has been shown in several animal models in which VEGF/VPF was overexpressed from full-length cDNA (90), VEGF/VPF mRNA (antisense mRNA transfection) was down-regulated (91), or neutralizing VEGF/VPF antibodies were used (45). Studies are in progress to ascertain the relationship of VEGF/VPF expression levels within individual tumors to the microvessel density of the same area.

The finding that the expression levels of E-cadherin, MMP-2, MMP-9, and VEGF/VPF correlated with tumor stage supports the roles of angiogenesis, cell cohesion, and invasion in the metastatic cascade. Furthermore, the relationship among all four genes correlated with the tumor Gleason score, another clinically used histological prognostic marker (5–9, 13–15). In our own data set as well as others, Gleason ≤ 6 prostate cancers were often organ confined (7, 8), whereas Gleason ≥ 8 cancers were associated with extraprostatic disease and hence poor prognosis. Histopathological examination of prostate cancers with a Gleason score of 7 revealed both organ-confined and advanced cancers. The present study using ISH for metastasis-related genes clearly distinguished between the Gleason score 7 cancers that were or were not organ-confined (Table 4). This was even true when Gleason score 7 cases were categorized as to the dominant pattern being Gleason 3 + 4 = 7 or Gleason 4 + 3 = 7 (data not shown).

The level of PSA in the serum is often used in the prognosis and clinical management of prostate cancer (5, 9–10, 13). In our study, however, the level of serum PSA did not distinguish between the patients with organ-confined cancer and many patients with advanced disease. In contrast, the expression ratio between the tumor-invasive profile, *i.e.,* the MMP:E-cadherin ratio, was particularly informative in that it separated organ-confined from advanced prostate cancers with virtually no overlap (at a cutoff of <6; Fig. 3) and could do so independently of the tumor Gleason score, serum PSA, and VEGF/VPF expression levels. Moreover, an extremely high MMP:E-cadherin ratio (>10) was often associated with lymph node metastasis.

In summary, we used an ISH technique to examine the concurrent expression of metastasis-related genes in formalin-fixed, paraffin-embedded radical prostatectomy specimens. Decreasing expression of E-cadherin and increasing expression of VEGF/VPF, MMP-2, and MMP-9 characterized pathologically advanced prostate cancers as well as those of high histological grade (Gleason score ≥ 8). The MMP:E-cadherin ratio, however, exhibited the greatest ability to distinguish organ-confined cancer. To determine the ultimate prognostic value of such measurements (considering the intratumoral heterogeneity of metastasis-related gene expression in the present study), the correlation between gene expression in pretreatment biopsies of prostate cancer and subsequent radical prostatectomy specimens in a large series of patients with long-term follow-up is under way.

ACKNOWLEDGMENTS

We thank Walter Pagel for critical editorial comments and Deborah Horton and Lola López for expert assistance in the preparation of the manuscript.

REFERENCES

1. Landis, S. H., Murray, T., and Bolden-Wingo, P. A. Cancer statistics 1999. Cancer (Phila.), *49:* 8–31, 1999.

2. Soh, S., Kattan, M. W., Berkman, S., Wheeler, T. M., and Scardino, P. T. Has there been a recent shift in the pathological features and prognosis of patients treated with radical prostatectomy? J. Urol., *157:* 2212–2218, 1997.

3. Xia, Z., Jacobsen, S. J., Bergstralh, E. J., Chute, C. G., Katusic, S. K., and Leiber, M. M. Secular changes in radical prostatectomy utilization rates in Olmsted County, Minnesota, 1980 to 1995. J. Urol., *159:* 904–908, 1998.

4. Smith, D. S., Humphrey, P. A., and Catalona, W. J. The early detection of prostate carcinoma with prostate-specific antigen: the Washington University experience. Cancer (Phila.), *80:* 1852–1856, 1997.

5. Partin, A. W., Kattan, M. W., Subong, E. N. P., Walsh, P. C., Wojno, K. J., Oesterling, J. E., Scardino, P. T., and Pearson, J. D. The use of prostate-specific antigen, clinical stage, and Gleason score to predict pathological stage in men with localized prostate cancer: a multi-institutional update. J. Am. Med. Assoc., *277:* 1445–1451, 1997.

6. Gleason, D. F., Mellinger, G. T., and The Veterans Administrative Cooperative Urologic Research Group. Histologic grading and clinical staging of prostatic carcinoma. *In:* M. Tannenbaum (ed.), Urologic Pathology: The Prostate, pp. 171–198. Philadelphia: Lea & Febiger, 1998.

7. Epstein, J. I., Partin, A. W., Sauageot, J., and Walsh, P. C. Prediction of progression following radical prostatectomy: a multivariate analysis of 721 men with long-term follow-up. Am. J. Surg. Pathol., *20:* 286–292, 1996.

8. Wheeler, T. M., Dillioglugil, O., Kattan, M. W., Arakawa, A., Soh, S., Suyama, K., Ohori, M., and Scardino, P. T. Clinical and pathological significance of the level and extent of capsular invasion in clinical stage T1–2 prostate cancer. Hum. Pathol., *29:* 856–862, 1998.

9. D'Amico, A. V., Whittington, R., Malkowicz, S. B., Fondurulia, J., Chen, M., Tomaszewski, J. E., and Wein, A. The combination of preoperative prostate-specific antigen and postoperative pathological

findings to predict prostate specific antigen outcome in clinically localized prostate cancer. J. Urol., *160:* 2096–2101, 1998.

10. Oesterling, J. E. Prostate-specific antigen: a critical assessment of the most useful tumor marker for adenocarcinoma of the prostate. J. Urol., *145:* 907–913, 1991.

11. Babaian, R. J., Troncoso, P., Steelhammer, L. C., Loreta-Trull, J., and Ramirez, E. I. Tumor volume and prostate-specific antigen: implications for early detection and defining a window of curability. J. Urol., *154:* 1808–1812, 1995.

12. Young, C. Y. F., Montgomery, B. T., Andrews, P. E., Qiu, S., Bilhartz, D. L., and Tindall, D. J. Hormonal regulation of prostate-specific antigen messenger RNA in human prostatic adenocarcinoma cell line LNCaP. Cancer Res., *51:* 3748–3752, 1991.

13. Zagars, G. K., and Pollack, A. Radiation therapy for T1 and T2 prostate cancer: prostate-specific antigen and disease outcome. Urology, *45:* 476–483, 1995.

14. Partin, A. W., Pound, C. R., Clemens, J. Q., Epstein, J. I., and Walsh, P. C. Serum PSA after anatomic radical prostatectomy: the Johns Hopkins experience after 10 years. Urol. Clin. North Am., *20:* 713–725, 1993.

15. Kattan, M. W., Eastham, J. A., Stapleton, A. M. F., Wheeler, T. M., and Scardino, P. T. A preoperative monogram for disease recurrence following radical prostatectomy for prostate cancer. J. Natl. Cancer Inst., *90:* 766–771, 1998.

16. Fidler, I. J. Critical factors in the biology of human cancer metastasis: twenty-eighth G. H. A. Clowes Memorial Award lecture. Cancer Res., *50:* 6130–6138, 1990.

17. Fidler, I. J. Modulation of the organ microenvironment for the treatment of cancer metastasis (Commentary). J. Natl. Cancer Inst., *87:* 1588–1592, 1995.

18. Aukerman, S. L., Price, J. E., and Fidler, I. J. Different deficiencies in the prevention of tumorigenic-low-metastatic murine K-1735 melanoma cells from producing metastasis. J. Natl. Cancer Inst., *77:* 915–924, 1986.

19. Fidler, I. J, and Radinsky, R. Genetic control of cancer metastasis. J. Natl. Cancer Inst., *82:* 166–168, 1990.

20. Bucana, C. D., Radinsky, R., Dong, Z., Sanchez, R., Brigati, D. J., and Fidler, I. J. A rapid colorimetric *in situ* mRNA hybridization technique using hyperbiotinylated oligonucleotide probes for analysis of *mdr*-1 in mouse colon carcinoma cells. J. Histochem. Cytochem., *41:* 499–506, 1993.

21. Kitadai, Y., Bucana, C. D., Ellis, L. M., Anzai, H., Tahara, E., and Fidler, I. J. *In situ* hybridization technique for analysis of metastasis-related genes in human colon carcinoma cells. Am. J. Pathol., *147:* 1238–1247, 1995.

22. Kitadai, Y., Ellis, L. M., Takahashi, Y., Bucana, C. D., Anzai, H., Tahara, E., and Fidler, I. J. Multiparametric *in situ* messenger RNA hybridization analysis to detect metastasis-related genes in surgical specimens of human colon carcinomas. Clin. Cancer Res., *1:* 1095–1102, 1995.

23. Kitadai, Y., Ellis, L. M., Tucker, S. L., Greene, G. F., Bucana, C. D., Cleary, K. R., Takahashi, Y., Tahara, E., and Fidler, I. J. Multiparametric *in situ* mRNA hybridization analysis to predict disease recurrence in patients with colon carcinoma. Am. J. Pathol., *149:* 1541–1551, 1996.

24. Anzai, H., Kitadai, Y., Bucana, C. D., Sanchez, R., Omoto, R., and Fidler, I. J. Intratumoral heterogeneity and inverse correlation between expression of E-cadherin and collagenase type IV in human gastric carcinomas. Differentiation, *60:* 119–127, 1996.

25. Kuniyasu, H., Ellis, L. M., Evans, D. B., Abbruzzese, J. L., Fenoglio, C. J., Bucana, C. D., Cleary, K. R., Tahara, E., and Fidler, I. J. Relative expression of E-cadherin and type IV collagenase genes predicts disease outcome in patients with resectable pancreatic carcinoma. Clin. Cancer Res., *5:* 25–33, 1999.

26. Pettaway, C. A., Pathak, S., Greene, G., Ramirez, E., Wilson, M. R., Killion, J. J., and Fidler, I. J. Selection of highly metastatic variants of different human prostatic carcinomas utilizing orthotopic implantation in nude mice. Clin. Cancer Res., *2:* 1627–1636, 1996.

27. Greene, G. F., Kitadai, Y., Pettaway, C. A., von Eschenbach, A. C., and Fidler, I. J. *In situ* mRNA hybridization technique for analysis of metastasis-related genes in human prostate carcinoma cells. Am. J. Pathol., *150:* 1571–1582, 1997.

28. Stearns, M. E., and Wang, M. Regulation of kinase expression and type IV collagenase secretion in invasive human prostate PC-3 tumor sublines. Cancer Res., *51:* 5866–5875, 1991.

29. Stearns, M., and Stearns, M. E. Evidence for increased activated metalloproteinase-2 (MMP-2): expression associated with human prostate cancer progression. Oncol. Res., *8:* 69–75, 1996.

30. Singh, R. K., Bucana, C. D., Gutman, M., Fan, D., Wilson, M. R., and Fidler, I. J. The influence of the organ microenvironment on the expression of basic fibroblast growth factor in human renal cell carcinoma cells. Am. J. Pathol., *145:* 365–374, 1994.

31. Nakamoto, T., Chang, C., Li, A., and Chodak, G. W. Basic fibroblast growth factor in human prostate cancer cells. Cancer Res., *52:* 571–577, 1992.

32. Singh, R. K., Gutman, M., Radinsky, R., Bucana, C. D., and Fidler, I. J. Expression of interleukin-8 correlates with the metastatic potential of human melanoma cells in nude mice. Cancer Res., *54:* 3242–3247, 1994.

33. Weinstein, R. S., Jakate, S. M., Dominguez, J. M., Lebovitz, M. D., Koukoulis, G. K., Kuzak, J. R., Klusens, L. F., Grogan, T. M., Saclarides, T. J., Robinson, I. B., and Coon, J. S. Relationship of the expression of the multidrug resistance gene product (P-glycoprotein) in human colon carcinoma to local tumor aggressiveness and lymph node metastasis. Cancer Res., *1:* 2720–2726, 1991.

34. Theyer, G., Schirmbock, M., Thalhammer, T., Sherwood, E. R., Baumgartner, G., and Hamilton, G. Role of the MDR-1 encoded multiple drug resistance phenotype in prostate cancer cell lines. J. Urol., *150:* 1544–1547, 1993.

35. Radinsky, R., Risin, S., Fan, D., Dong, Z., Bielenberg, D., Bucana, C. D., and Fidler, I. J. Level and function of epidermal growth factor receptor predict the metastatic potential of human colon carcinoma cells. Clin. Cancer Res., *1:* 19–31, 1995.

36. Takeichi, M. Cadherins: a molecular family important in selective cell-cell adhesion. Annu. Rev. Biochem., *59:* 237–252, 1990.

37. Mayer, B., Johnson, J. P., Leitl, F., Jauch, K. W., Heiss, M. M., Schildberg, F. W., Birchmeier, W., and Funke, I. E-cadherin expression in primary and metastatic gastric cancer: downregulation correlates with cellular dedifferentiation and glandular disintegration. Cancer Res., *53:* 1690–1695, 1993.

38. Brown, L. F., Berse, B., Jackmon, R. W., Tognazzi, K., Manseau, E. J., Senger, D. R., and Dvorak, H. F. Expression of vascular permeability factor (vascular endothelial growth factor) and its receptors in adenocarcinoma of the gastrointestinal tract. Cancer Res., *53:* 4727–3475, 1993.

39. Takahashi, Y., Kitadai, Y., Bucana, C. D., Cleary, K., and Ellis, L. M. Expression of vascular endothelial growth factor and its receptor, KDR, correlates with vascularity, metastasis, and proliferation of human colon cancer. Cancer Res., *55:* 3964–3968, 1995.

40. Alon, T., Hemo, I., Itin, A., Peter, J., Stone, J., and Keshet, E. Vascular endothelial growth factor acts as a survival factor for newly formed retinal vessels and has implications for retinopathy of prematurity. Nat. Med., *1:* 1024–1028, 1995.

41. Senger, D. R., Van De Water, L., Brown, L. F., Nagy, J. A., Yeo, K., Yeo, T., Berse, B., Jackman, R. W., Dvorak, A. M., and Dvorak, H. F. Vascular permeability factor (VPF/VEGF) in tumor biology. Cancer Metastasis Rev., *12:* 303–324, 1993.

42. Jackson, M. W., Bentel, J. M., and Tilley, W. D. Vascular endothelial growth factor (VEGF) expression in prostate cancer and benign prostatic hyperplasia. J. Urol., *157:* 2323–2328, 1997.

43. Ferrer, F. A., Miller, L. J., Andrawis, R. I., Kurtzman, S. H., Albertsen, P. C., Laudone, V. P., and Kreutzer, D. L. Human prostate cancer: *in situ* and *in vitro* expression of VEGF by human prostate cancer cells. J. Urol., *157:* 2329–2333, 1997.

44. Balbay, M. D., Pettaway, C. A., Kuniyasu, H., Inoue, K., Ramirez, E., Li, E., Fidler, I. J., and Dinney, C. P. N. Highly metastatic human

prostate cancer growing within the prostate of athymic mice overexpresses vascular endothelial growth factor. Clin. Cancer Res., *5:* 783–789, 1999.

45. Borgstrom, P., Bourdon, M. A., Hillan, K. J., Sriramarao, P., and Ferrara, N. Neutralizing antivascular endothelial growth factor antibody completely inhibits angiogenesis and growth of human prostate carcinoma micro tumors *in vivo*. Prostate, *35:* 1–10, 1998.

46. Schipper, J. H., Frixen, U. H., Behrens, J., Unger, A., Jahnke, K., and Birchmeier, W. E-Cadherin expression in squamous carcinomas of the head and neck: inverse correlation with tumor dedifferentiation and lymph node metastasis. Cancer Res., *51:* 6328–6337, 1991.

47. Oka, H., Shiozaki, H., Kobayashi, H., Inoue, M., Tahara, H., Kobayashi, T., Takatsuka, Y., Matsuyoshi, N., Hirano, S., Takeichi, M., and Mori, T. Expression of E-cadherin cell adhesion molecule in human breast cancer tissues and its relationship to metastasis. Cancer Res., *53:* 1696–1701, 1993.

48. Mattijssen, V., Peters, H. M., Schalkwijk, L., Manni, J. J., Van't Hof Grootenboer, B., de Mulder, P. H., and Ruiter, D. J. E-cadherin expression in head and neck squamous-cell carcinoma is associated with clinical outcome. Int. J. Cancer, *55:* 580–585, 1993.

49. Umbas, R., Schalken, J. A., Alders, T. W., Carter, B. S., Karthas, H. F. M., Schaafsma, H. E., Debruyne, F. M. J., and Isaac, W. B. Expression of the cellular adhesion molecule E-cadherin is reduced or absent in high-grade prostate cancer. Cancer Res., *52:* 5104–5109, 1992.

50. Umbas, R., Isaacs, W. B., Bringuier, P. P., Schraafsma, H. E., Karthaus, H. F. M., Oosterhof, G. O. N., Debruyne, F. M. J., and Schalken, J. A. Decreased E-cadherin expression is associated with poor prognosis in patients with prostate cancer. Cancer Res., *54:* 3929–3933, 1994.

51. Richmond, P. J. M., Karayiannakis, A. J., Nagafuchi, A., Kaisary, A. V., and Pignatelli, M. Aberrant E-cadherin and α-catenin expression in prostate cancer: correlation with patient survival. Cancer Res., *57:* 3189–3193, 1997.

52. D'Errico, A., Garbisa, S., Liotta, L. A., Castronovo, V., Stetler-Stevenson, W. G., and Grigioni, W. F. Augmentation of type IV collagenase, laminin receptor, and Ki67 proliferation antigen associated with human colon, gastric, and breast carcinoma progression. Mod. Pathol., *4:* 239–246, 1991.

53. Wood, M., Fudge, K., Mohler, L., Frost, A. R., Garcia, F., Wang, M., and Stearns M. E. *In situ* hybridization studies of metalloproteinase 2 and 9 and TIMP-1 and TIMP-2 expression in human prostate cancer. Clin. Exp. Metastasis, *15:* 246–258, 1996.

54. Weidner, N., Folkman, J., Pozza, F., Bevilaqua, P., Allred, E., Mili, S., and Gasparini, G. Tumor angiogenesis: a new significant and independent prognostic indicator in early stage breast carcinoma. J. Natl. Cancer Inst., *84:* 1875–1887, 1992.

55. Gasparini, G., and Harris, A. L. Clinical importance of the determination of tumor angiogenesis in breast carcinoma: much more than a new prognostic tool. J. Clin. Oncol., *13:* 765–782, 1995.

56. Brawer, M. K., Deering, R. E., Brown, M., Preston, S. D., and Bigler, S. A. Predictors of pathologic stage in prostatic carcinoma: the role of neovascularity. Cancer (Phila.), *73:* 678–687, 1994.

57. Bostwick, D. G., Wheeler, T. M., Blute, M., Barrett, D. M., MacLennan, G. T., Sebo, T. J., Scardino, P. T., Humphrey, P. A., Hudson, M. A., Fradet, Y., Miller, G. J., Crawford, E. D., Blumenstein, B. A., Mahran, H. E., and Miles, B. J. Optimized microvessel density analysis improves prediction of cancer stage from prostate needle biopsies. Urology, *48:* 47–57, 1996.

58. Silberman, M. A., Partin, A. W., Velti, R. W., and Epstein, J. I. Tumor angiogenesis correlates with progression after radical prostatectomy but not with pathologic stage in Gleason sum 5 to 7 adenocarcinoma of the prostate. Cancer (Phila.), *79:* 772–779, 1997.

59. Weidner, N., Carroll, P. R., Flax, J., Flumenfield, W., and Folkman, J. Tumor angiogenesis correlates with metastasis in invasive prostate carcinoma. Am. J. Pathol., *143:* 401–409, 1993.

60. Graham, C. H., Rivers, J., Kerbel, R. S., Stankiewicz, K. S., and White, W. L. Extent of vascularization as a prognostic indicator in thin (<0.76 mm) malignant melanomas. Am. J. Pathol., *145:* 510–514, 1994.

61. Hollingsworth, H. C., Kohn, E. C., Steinberg, S. M., Rothenberg, M. L., and Meriono, M. J. Tumor angiogenesis in advanced stage ovarian carcinoma. Am. J. Pathol., *147:* 33–41, 1995.

62. Maeda, K., Chung, Y-S., Takatsuka, S., Ogawa, Y., Onoda, N., Sawada, T., Kato, Y., Nitta, A., Arimoto, Y., and Kondo, Y. Tumour angiogenesis and tumour cell proliferation as prognostic indicators in gastric carcinomas. Br. J. Cancer, *72:* 319–323, 1995.

63. Fleming, I. D., Cooper, J. S., Henson, D. E., Hutter, R. V. P., Kennedy, B. J., Murphy, G. P., O'Sullivan, B., Sobin, L. H., and Yarbro, J. W. AJCC Cancer Staging Manual, Ed. 5, pp. 121–126. Philadelphia: Lippincott-Raven, 1997.

64. Bastacky, S. I., Walsh, P. C., and Epstein, J. I. Relationship between perineural invasion on needle biopsy and radical prostatectomy capsular penetration in clinical stage B adenocarcinoma of the prostate. Am. J. Surg. Pathol., *17:* 336–341, 1993.

65. Collier, I. E., Wilheim, S. M., Eisen, A. Z., Marmer, B. L., Grant, G. A., Selzter, J. L., Kronberger, A., He, C., Bauer, E. A., and Goldberg, G. I. H-*ras* oncogene-transformed human bronchial epithelial cells (TBE-1) secrete a single metalloproteinase capable of degrading basement membrane collagen. J. Biol. Chem., *263:* 6579–6587, 1988.

66. Bussenmakers, M. J. G., van Bokhoven, A., Mees, S. G. M., Kemler, R., and Schalken, J. A. Molecular cloning and characterization of the human E-cadherin cDNA. Mol. Biol. Rep., *17:* 123–128, 1993.

67. Tischer, E., Mitchell, R., Hartman, T., Silva, M., Gospodarowicz, D., Fiddes, J. C., and Abraham, J. A. The human gene for vascular endothelial growth factor. Multiple protein forms are encoded through alternative exon splicing. J. Biol. Chem., *266:* 11947–11954, 1991.

68. Leung, D. W., Cachianes, G., Kuang, W. J., Goeddel, D. V., and Ferrara, N. Vascular endothelial growth factor is a secreted angiogenic mitogen. Science (Washington DC), *246:* 1306–1309, 1989.

69. Pearson, W. R., and Lipman, D. J. Improved tools for biological sequence comparison. Proc. Natl. Acad. Sci. USA, *85:* 2444–2448, 1988.

70. Park, C-S., Manahan, L. J., and Brigati, D. J. Automated molecular pathology: one hour *in situ* DNA hybridization. J. Histotechnol., *14:* 219–229, 1991.

71. Caruthers, M. H., Beaucage, S. L., Efcavitch, J. W., Fisher, E. F., Goldman, R. A., De Haseth, P. L., Mandechi, W., Matteucci, M. D., Rosendahl, M. S., and Stabinsky, Y. Chemical synthesis and biological studies on mutated gene-control region. Cold Spring Harbor Symp. Quant. Biol., *47:* 411–418, 1982.

72. Radinsky, R., Bucana, C. D., Ellis, L. M., Sanchez, R., Cleary, K. R., Brigati, D. J., and Fidler, I. J. A rapid colorimetric *in situ* messenger RNA hybridization technique for analysis of epidermal growth factor receptor in paraffin-embedded surgical specimens of human colon carcinomas. Cancer Res., *53:* 937–943, 1993.

73. Reed, J. A., Manahan, L. J., Park, C. S., and Brigati, D. J. Complete one-hour immunocytochemistry based on capillary action. Biotechniques, *13:* 434–443, 1992.

74. Zar, J. Biostatistics Analysis, Ed. 3. Upper Saddle River, NJ: 1996.

75. Fidler, I. J. Metastasis: quantitative analysis of distribution and fate of tumor emboli labeled with ^{125}I-5-iodo-2′-deoxyuridine. J. Natl. Cancer Inst., *45:* 773–782, 1970.

76. Fidler, I. J, and Kripke, M. L. Metastasis results from preexisting variant cells within a malignant tumor. Science (Washington DC), *197:* 893–895, 1997.

77. Shimoyama, Y., Hirohashi, S., Hirano, S., Noguchi, M., Shimasato, Y., Takeichi, M., and Abe, O. Cadherin cell adhesion molecules in human epithelial tissues and carcinomas. Cancer Res., *49:* 2128–2133, 1989.

78. Frixen, U. H., Beherens, J., Sachs, M., Eberle, G., Voss, B., Warda, A., Loechner, D., and Birchmeier, W. E-Cadherin-mediated cell-cell

adhesion prevents invasiveness of human carcinoma cells. J. Cell Biol., *113:* 173–185, 1991.

79. Vleminckx, K., Vakaet, L., Jr., Mareel, M., Fiers, W., and VanRoy, F. Genetic manipulation of E-cadherin expression by epithelial tumor cells reveals an invasion suppressor role. Cell, *66:* 107–119, 1991.

80. Liotta, L. A. Tumor invasion and metastasis–role of the extracellular matrix: Rhoads memorial award lecture. Cancer Res., *46:* 1–7, 1986.

81. Van voden Outen, D., Hop, W. C. J., Kranse, R., and Schroder, F. H. Tumor control according to pathological variables in patients treated by radical prostatectomy for clinically localized carcinoma of the prostate. Br. J. Urol., *79:* 203–211, 1997.

82. Ukimura, O., Troncoso, P. T., Ramirez, E. I., and Babaian, R. J. Prostate cancer staging: correlation between ultrasound determined tumor contact length and pathologically confirmed extraprostatic extension. J. Urol., *159:* 1251–1269, 1998.

83. Egan, A. J. M., and Bostwick, D. G. Prediction of extraprostatic extension of prostate cancer based on needle biopsy findings: perineural invasion lacks significance on multivariate analysis. Am. J. Surg. Pathol., *21:* 1496–500, 1997.

84. Djakiew, D., Pflug, B. R., Delsite, R., Onada, M., Lynch, J. H., Arand, G., and Thompson, E. W. Chemotaxis and chemokinesis of human prostate tumor cell lines in response to human prostate stromal cell secretory proteins containing a nerve growth factor-like protein. Cancer Res., *53:* 1416–420, 1993.

85. Seki, H., Tanaka, J., Sato, Y., Kato, Y., Umezawa, A., and Koyama, K. Neural cell adhesion molecule (NCAM) and perineural invasion in bile duct cancer. J. Surg. Oncol., *53:* 78–83, 1993.

86. Geldof, A. A., De Kleijn, M. A. T., Rao, B. R., and Newling, D. W. W. Nerve growth factor stimulates *in vitro* invasive capacity of DU145 human prostatic cancer cells. J. Cancer Res. Clin. Oncol., *123:* 107–112, 1997.

87. Yang, G., Wheeler, T. M., Kattan, M. W., Scardino, P. T., and Thompson, T. C. Perineural invasion of prostate carcinoma cells is associated with reduced apoptotic index. Cancer (Phila.), *78:* 1267–1271, 1996.

88. Villers, A., McNeal, J. E., Redwine, E. A., Freiha, F. S., and Stamey, T. A. The role of perineural space invasion in the local spread of prostatic adenocarcinoma. J. Urol., *142:* 763–768, 1989.

89. Sigala, S., Isabella, F., Botticini, D., Paez-Pereda, P., Missale, C., Bonmassar, E., and Spano, P. Suppression of telomerase, reexpression of KAI1, and abrogation of tumorigenicity by nerve growth factor in prostate cancer cell lines. Clin. Cancer Res., *5:* 1211–1218, 1999.

90. Claffey, K. P., Brown, L. F., del Aguila, L. F., Tognazzi, K., Yeo, K. T., Manseau, E. J., and Dvorak, H. F. Expression of vascular permeability factor/vascular endothelial growth factor by melanoma cells increases tumor growth, angiogenesis, and experimental metastasis. Cancer Res., *56:* 172–181, 1996.

91. Saleh, M., Stacker, S. A., and Wilks, A. F. Inhibition of growth of C6 glioma cells *in vivo* by expression of antisense vascular endothelial growth factor sequence. Cancer Res., *56:* 393–398, 1996.